# ELUCIDATION OF THE ROLE OF FAT10 IN TUMORIGENESIS


## STEVEN SETIAWAN THENG

*(Dipl.Ing., Hamburg University of Applied Sciences)*


**A THESIS SUBMITTED FOR THE DEGREE OF**

**DOCTOR OF PHILOSOPHY**


**NUS GRADUATE SCHOOL FOR**

**INTEGRATIVE SCIENCES AND ENGINEERING**

**NATIONAL UNIVERSITY OF SINGAPORE**


**2013**

# Declaration

**I hereby declare that the thesis is my original work and it has been written by me in its entirety. I have duly acknowledged all the sources of information, which have been used in this thesis.**

**This thesis has also not been submitted for any degree in any university previously.**

**Steven Setiawan Theng**

**28 March 2013**

# *Acknowledgements*

*First and foremost, I would like to express my sincere gratitude to my supervisor Associate Professor Caroline Lee for her endless support, guidance, and invaluable insights throughout my postgraduate studies as well as for providing me with opportunity and resources to complete my project. Four and a half years-stint under her guidance has helped me to become a mature student and scientist.*

*My genuine thanks to my TAC members Dr. Thilo Hagen and Associate Professor Paula Lam for their encouragement, direction for my thesis, and also their constructive comments and questions during my PhD study. Thank you for inspiring me with your knowledge and passion in research.*

*Thanks also to National Cancer Singapore for hosting and providing me with resources during my PhD. To the cancer patients, thank you for your pillar of support and inspiring story of your life, you are the reasons why I am still persevering in my research and Phd study.*

*My sincere thanks also goes to our collaborators A/Prof.Song Jianxing and Wang Wei for their help in NMR study.*

*Special thanks to my fellow lab mates Champ, Cheryl, Soo Ting, and Maulana for your help in one or another ways of my research and colleagues in NCC Huiting, Huisun, and Peiyun, which have become my dear friends.*

*I would like to express my deepest thanks to my parents for their unwavering support and encouragement. I would not have contemplated this road if not you, who instilled me with your valuable advice, knowledge, and patience during my difficult times in pursuing my PhD study. This thesis would not be possible without your abundance of love and supports.*

*Last but not least I would like to thanks my attachment students (Lester, Junhao, and Jiekai) that have enriched my life and your supports during my PhD study.*

*Above all, I would like to thank God for your abundant of grace and loves throughout this journey of my life.*

## Table of Contents

# Summary

FAT10 (human leukocyte antigen **F**-**a**ssociated **t**ranscript **10**) is an 18kDA protein, which consists of 165 amino acid residues. It belongs to the ubiquitin-like modifier (UBL) family of proteins and encompasses two ubiquitin-like domains in tandem array. The sequence similarity between FAT10 and ubiquitin at its N- and C-terminal regions are 29% and 36%, respectively. Since Ubiquitin is known to be involved in tumorigenesis, we hypothesized that FAT10 as an ubiquitin-like protein also played a role in tumorigenesis, since FAT10 has been reported to be overexpressed in several cancers, including colorectal cancer. Moreover, FAT10 upregulation was previously associated with colorectal cancer progression. However, it remains unclear whether FAT10 plays a causal role in driving the malignancy of colorectal cancer, and if so, what the mechanisms involved were. Therefore, this study aimed to address the role of FAT10 in promoting the malignancy of colorectal cancer cells as well as to uncover the mechanism underlying FAT10's role in driving tumorigenesis. In this thesis, we showed that FAT10 overexpression in a colorectal cancer cell line HCT116 facilitated cell proliferation compared to wild type- (WT) HCT116 as well as FAT10 stable knockdown- (FATi) HCT116 cells. Additionally, FAT10-overexpressing HCT116 cells showed enhanced invasion *in vitro* as well as anchorage-independent growth in soft agar. Importantly, FAT10 overexpression in HCT116 promoted tumor growth *in vivo* based on xenograft mouse model. Having shown FAT10's ability in supporting cell and tumor growth of colorectal cancer HCT116, we further investigated the role of FAT10 in non-tumorigenic cells. We have shown that not only was FAT10 overexpression able to enhance the malignant transformation of

cancer cells; it also conferred malignant transformation in the non-tumorigenic immortalized human neonatal hepatocytes (NeHepLxHT). Collectively, our results demonstrated the pro-malignancy functions of FAT10 in inducing cell proliferation, invasion and tumor growth in both colorectal cancer cells as well as non-tumorigenic immortalized hepatocytes.

Previously, FAT10 was reported to interact with mitotic spindle checkpoint Mad2, which resulted in the reduction of Mad2 localization at the kinetochore during pro-metaphase and subsequent acceleration of mitosis duration, which led to aneuploidy. Aneuploidy, a hallmark of cancer cells, as well as aberrant functions of mitotic spindle checkpoint are both associated with tumorigenesis. In order to delineate the mechanism of FAT10 in tumorigenesis, we utilized nuclear magnetic resonance (NMR) technique to analyze the specific binding sites for Mad2 in FAT10 protein. Through NMR we found two FAT10-Mad2 interaction sites on FAT10 protein. Using fusion-PCR-mutagenesis method we mutated the specific amino acid residues in FAT10 protein obtained from the NMR protein-protein interaction study and we subsequently generated stable HCT116 cell lines overexpressing wild type FAT10 as well as FAT10 mutants with abolished Mad2-binding function. Our findings confirmed that mutating both Mad2 binding sites on FAT10 abrogated FAT10 and MAD2 binding, based on co-immunoprecipitation and *in situ* proximity ligation assay (PLA), whereas mutation at either one of the Mad2-binding sites did not abolish the FAT10-Mad2 binding. Remarkably, this resulted in a decrease in the number of aneuploid cells and malignant cell behaviors *in vitro*, such as cell proliferation, survival, invasion and migration were observed. Importantly, the disruption of FAT10 and MAD2 interaction led to tumor regression *in vivo.* Thus far, we were able to confirm FAT10's role in

aneuploidy and tumorigenesis. Our results suggest that Mad2-binding is an important mechanism by which FAT10 exerts its effect on cell malignancy. Therefore, based on our collective data, we have demonstrated that FAT10 exerts its pro-malignancy effects through disruption of mitotic spindle checkpoint via interaction with Mad2.

In conclusion, we have, for the first time, demonstrated that FAT10 plays an important role in tumorigenesis and cell malignancy, consistent with the reports of FAT10 overexpression in human tumor samples. We have elucidated the specific Mad2 interaction sites on FAT10 protein and have also demonstrated that disruption of FAT10 and Mad2 binding significantly resulted in tumor regression in the *in vivo* xenograft model and reduced cell proliferation, migration, invasion and anchorage-independent growth *in vitro*. Our findings have unraveled FAT10 as a crucial determinant of malignant cellular behaviors as well as its potential role as a therapeutic target in inflammation-associated cancer.

# List of Tables

# List of Figures

## List of Publications

S.S. Theng, G. Yun, J. Zhuo, W.B. Teo, J. Ren, C.G. Lee. FAT10, an Ubiquitin-like Protein, Confers Malignant Properties in Non-tumorigenic and Tumorigenic Cells. (Submitted to *Carcinogenesis*)

S.S. Theng, G. Yun, J. Zhuo, J.Song, C.G. Lee. Disruption of FAT10 and MAD2 binding as a potential cancer therapeutic target. (In preparation for submission after patent protection)

## Patent

S.S. Theng, G. Yun, J. Zhuo, J.Song, C.G. Lee. Molecular tools, compounds and methods related to the disruption of FAT10 and MAD2 binding. (Submitted).

# Chapter1 Introduction

According to World Health Organization (WHO) cancer is the leading cause of death globally with an estimated 7.6 million deaths or around 13% of all deaths in 2008 (http://www.who.int/mediacentre/factsheets/fs297/en/). WHO has estimated that 84 million people will die in the next 10 years if no action is taken against cancer (http://whqlibdoc.who.int/publications/2007/9241547111_eng.pdf). However, the cure for cancer based on the current treatments available are still far from satisfactory (DeVita and Rosenberg 2012, Markowitz et al 2002). Therefore, more specific and targeted cancer research focused on understanding the mechanism of tumorigenesis, prevention, diagnosis and treatment need to be improved in order to tackle this serious disease. As third leading cancer related deaths (http://globocan.iarc.fr/factsheet.asp), discovering genes that contribute to the basic phenotypes of colorectal cancer (CRC) such as chromosomal instability, invasiveness and its metastatic spread has been carried out under intense research investigation (Hanahan and Weinberg 2011, Markowitz et al 2002, Markowitz and Bertagnolli 2009). Currently, surgery with resection of the affected segment is the most common treatment for colorectal cancer (Marin et al 2012) and clinical outcomes among the patients diagnosed at the same tumor stage are also variable (Galandiuk et al 1992). Hence, finding a new therapeutic target, which potentially causes the malignancy in colorectal cancer or biomarkers for diagnosis of CRC is needed.

## 1.1 Colorectal cancer

Worldwide, colorectal cancer is statistically reported to be the third leading cause of cancer-related deaths, with an annual occurrence of 1.2 million cases and mortality rate of more than 500,000 cases and its prevalence is constantly

increasing (http://globocan.iarc.fr/factsheet.asp) (Jemal et al 2010b). CRC is one of the most common cancers in the world, including Singapore (Figure 1.1). The mortality caused by CRC, much like any other solid tumors, is arise not from the primary tumor itself, but rather from its metastatic spread (Rajput et al 2008). Metastasis is a complex biological process, which involves multistep process such as changes in the extracellular matrix, which supports and increases cell invasion, motility, cellular extravasation, and also the ability of cells in initiating and maintaining growth at a distant site (Steeg 2003). Benign adenomatous polyp is the onset of this disease, which then develops into an advanced adenoma with high-grade dysplasia and then finally progresses to an invasive cancer. Invasive cancers, which are contained within colon's wall, are curable. However, those that are spread to regional lymph nodes or distant sites are more difficult to be cured and have a poor 5-year survival rate (Herszenyi and Tulassay 2010, Jemal et al 2010a, Jemal et al 2010b). Thus, understanding the molecular mechanism for CRC is needed to control this disease.

CRC is developed over a multistep of colon neoplasia that extends over several years (Markowitz et al 2002) The risk factors of CRC include family or personal history of CRC or polyps, aging, inflammatory bowel disease, hereditary syndromes such as polyposis or nonpolyposis CRC, diabetes, smoking, and obesity (Amersi et al 2005, Knekt et al 1998, Markowitz et al 2002, Sandler 1996). Only about 20% of colorectal cancer has a familial basis (Rustgi 2007), some are associated with well-defined syndrome like hereditary non-polyposis colorectal cancer (HNPCC). Nevertheless, the biggest reason of colorectal cancer (CRC) has been linked to environmental causes, such as food-borne mutagens, specific

intestinal pathogens, and chronic intestinal inflammation, which cause this disease (Cannon-Albright et al 1988, Kinzler and Vogelstein 1996, Terzic et al 2010).


**Figure 1.1. New CRC reported cases in 2009 in representative countries worldwide.** The graph presented above are based on 2009 WHO database of CRC disease estimates (http://www-dep.iarc.fr/WHOdb/graph7.asp)

## 1.2 Hallmarks of cancers

Genomic instability, which creates the genetic diversity, as well as inflammation, has long been proposed as the underlying cause of cancer development that leads to the several hallmarks of human cancers. These six well – known hallmarks or phenotypes of human tumors, which acquired during its multistep development, consist of sustaining proliferative signaling, evasion of growth suppressors, resisting cell death, enabling replicative immortality, induction of angiogenesis, and activation of invasion and metastasis (Figure 1.2) (Hanahan and Weinberg 2000, Hanahan and Weinberg 2011).

In order to understand more about the biology of cancer, these six hallmarks of cancers play distinctive and complementary capabilities to prove the solid foundation of cancer development.

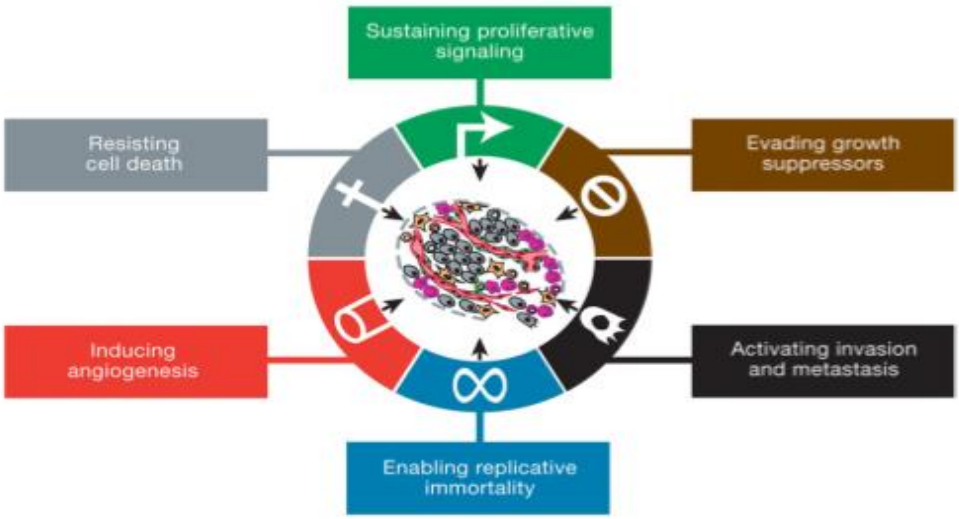


**Figure 1.2. The hallmarks of cancers.** This figure depicts the six well-studied hallmarks of human cancers. Lots of research was done toward understanding the mechanism underpinnings of each hallmark. Adapted from Hanahan and Weinberg, 2011, *Cell*, 144 (5): 646-74.

### 1.2.1 Aneuploidy and cancers

An aberrant change in chromosome number or structure that is not exact multiple of haploid karyotype is known as aneuploidy and it is a type of chromosome abnormality. This condition is a common characteristic of solid tumor and it has long been proposed to contribute or even drive tumorigenesis (Kops et al 2005b, Torres et al 2008). In fact, approximately 90% of solid human tumors and about 75% of hematopoietic cancers were found to have aneuploidy (Weaver and Cleveland 2008). Errors in chromosome segregation or the occurrence of pre-mature anaphase during cell division are usually the reason of aneuploidy. The fact that it could promote aberrant mitotic division gives the evidence that it could also promote carcinogenesis, as aneuploidy is a characteristic of human cancers (Gordon et al 2012).

Mitotic checkpoint or also known as spindle assembly checkpoint (SAC) play a major role in controlling the cell cycle process during mitosis. A tight control of cell cycle process by SAC acts as a prevention of chromosome misseggregation and its accompanying aneuploidy (Murray 2011, Weaver et al 2008). Mitotic progressions from metaphase to anaphase and sister-chromatid segregation are controlled by anaphase promoting complex (APC/C), an E3 ubiquitin ligase, its co-activator CDC20, as well as a group of spindle checkpoint proteins, which include Bub1, BubR1 (MAD3), Bub3, CENPE, MPS1, Mad1, Mad2, p31, ROD, Zwilch, and ZW10 (De Antoni et al 2005, Kops et al 2005b, Musacchio and Salmon 2007) (Table 1.1).

| Protein | Characteristics | Binding partners | Function in checkpoint | References |
|---|---|---|---|---|
| BUB1 | 122 kDa; serine/threonine kinase | BUB3 | Inhibits CDC20 by phosphorylation | (Tang et al 2004) |
| BUBR1 | 120 kDa; serine/threonine kinase | CENPE, BUB3, CDC20 | Part of APC/C inhibitory complex. Directly binds to CDC20 and inhibits APC/C activity | (Fang 2002, Lampson and Kapoor 2005, Sudakin et al 2001, Tang et al 2001)2 |
| BUB3 | 37 kDa; structure determined: 7-bladed propeller of WD40 repeats | BUB1, BUBR1 | Part of APC/C inhibitory complex. Localizes BUB1 and BUBR1 to kinetochores | (Logarinho et al 2008, Taylor et al 1998)3 |
| MAD1 | 83 kDa; coiled coil | MAD2 | Directly recruits MAD2 to unattached kinetochore | (Ryan et al 2012)3 |
| MAD2 | 23 kDa; structure determined | MAD1, CDC20, CMT2/p31$^{comet}$ | Part of APC/C inhibitory complex. Directly binds to CDC20 and inhibits APC/C activity | (Fang et al 1998, Schuyler et al 2012, Yang et al 2008)3 |
| CMT2/p31$^{comet}$ | 31 kDa; none identified | MAD2 | Inhibits mitotic checkpoint signalling by antagonizing MAD2 | (Westhorpe et al 2011, Yang et al 2007)3 |
| MPS1 | 97 kDa; dual-specificity kinase | Unknown | Unknown | (Morin et al 2012)3 |
| CENPE | 312 kDa; plus-end directed microtubule motor | BUBR1 | Activates BUBR1 at the unattached kinetochore | (Yang et al 2010a, Yao et al 2000)3 |
| ZW10 | 89 kDa; none identified | ROD, Zwilch | Part of complex that recruits the MAD1–MAD2 heterodimer to unattached kinetochores | (Kops et al 2005a)3 |
| ROD | 251 kDa; none identified | ZW10, Zwilch | Part of complex that recruits the MAD1–MAD2 heterodimer to unattached kinetochores | (Buffin et al 2005, Karess 2005)3 |
| Zwilch | 67 kDa; none identified | ROD, ZW10 | Part of complex that recruits the MAD1–MAD2 heterodimer to unattached kinetochores | (Karess 2005)3 |

**Table 1.1 List of Mitotic checkpoint proteins**.

As shown in Figure 1.3, in the process of mitosis in normal cells, SAC will bind to kinetochore (Musacchio and Salmon 2007), when spindle checkpoint detects errors in cell division, such as unattached kinethochore or lack of chromosome tension. It will give a "stop anaphase signal" to prevent the premature advance to anaphase, while it attempts to correct the mistakes (Khodjakov and Rieder 2009). The "stop signal" is consist of complexes of Bub3, BubR1, and Mad2 (Sullivan and Morgan 2007). These signals will then be transferred into the mitotic cytosol, where it will binds to APC/C co-activator CDC20 and inactivates the APC/C and CDC20 complex (APC/C –CDC20). Inactivation of APC/C-CDC20 complex inhibits the binding to securin and cyclin B1, whereby it will prevents the advance to anaphase until the kinetochores are properly attached (Cleveland et al 2003, Peters 2002). As the chromosomes are correctly attached to microtubules, through their kinetochores and place under tension by spindle forces, Several SAC like MAD2, BubR1, BUB3, and MPS1 are rapidly released from the correctly attached kinetochore and the "stop anaphase signal" will be suspended and the inhibition of SAC to APC/C-CDC20 complex will also be acquitted (Howell et al 2004, Shah et al 2004). The activation of APC/C-CDC20 complex will then catalytically mediate the degradation of securin and cyclin B1, which leads to the activation of separase, which in mammalian cells its inhibition is associated with binding to securin and cyclinB1/Cdk1- mediated phosporylation. Further, separase cleaves the cohesin links that hold together the sister chromatid by cleavage of the chosein subunit Scc1 and initiates anaphase (Peters 2002, Taylor et al 2004, Weaver and Cleveland 2006). A tight control in metaphase to

**A.**

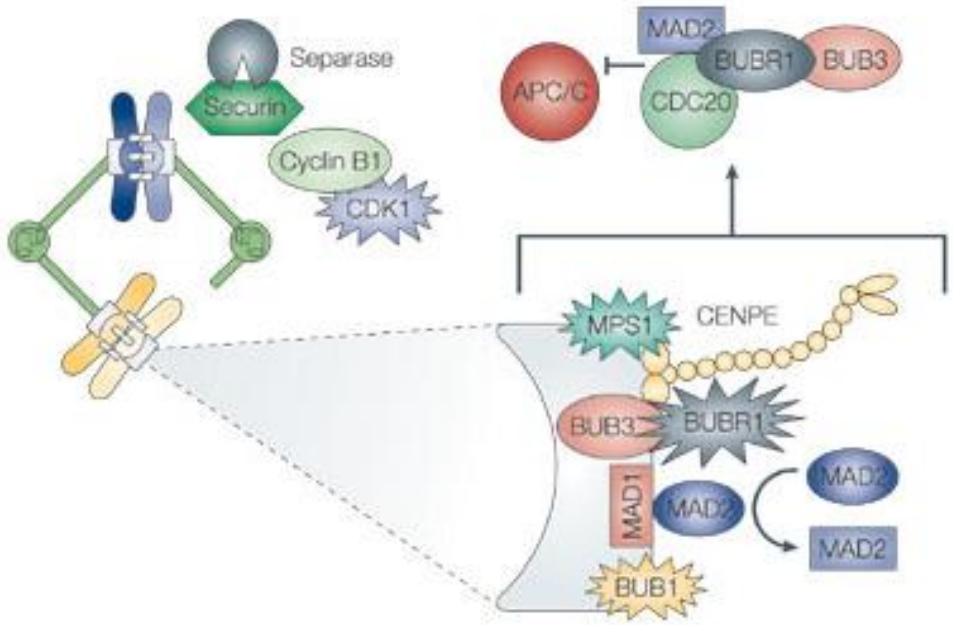


**B.**

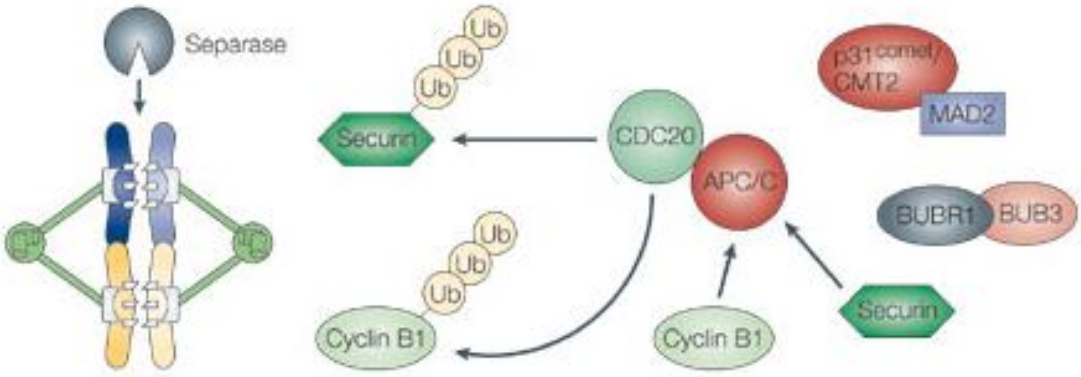


**Figure 1.3. The mitotic checkpoint signaling in mammalian cells.** A. During pro-metaphase, recruitment of MAD1, MAD2, MPS1, BUB1, BUB3, BUBR1, and CENPE to unattached kinetochore. This will inhibit APC/C-CDC20 to bind to Securin and prevent anaphase initiation. B). During anaphase, MAD2 is removed from kinetochore and active APC/C-CDC20 will bind to Securin and Separase will cleave Cohesins, which hold sister chromatid together and results in chromosome segregation. Reprinted by permission from Nature Publishing Group. (Kops et al 2005b)

anaphase progression ensures sister chromosomes to be evenly distributed and segregated into daughter cells (Kucej and Zou 2010, Pines 2006).

Normal cells have an intact and robust mitotic checkpoint function, in which one or more unattached kinetochores are sufficient to inhibit all cellular APC/C activity and thereby block the premature anaphase (Rieder et al 1994). However, in the cancer cells the function of mitotic checkpoint might not be sufficient to control the mitotic progression. As a result if there are any chromosomes misalignment during metaphase, these cells are unable to generate sufficient inhibitory signal and resulted in premature progression into anaphase and chromosome misseggregation, which leads to aneuploidy (Kops et al 2005b). This malfunction in mitotic checkpoint proteins to give an efficient signal is one of the main factors that cause aneuploidy in cancer cells, and many studies have reported the lack or deficiency of these mitotic checkpoint proteins in human cancers (Hanks et al 2004, Rao et al 2005, Schuyler et al 2012, Schvartzman et al 2010). Mice that carried out a heterozygous deficient checkpoint such as Mad2 (Michel et al 2004, Michel et al 2001), BubR1(Baker et al 2012, Rao et al 2005), and Bub3 (Baker et al 2006) have been reported to increase aneuploidy, which is one of the hallmarks of cancers.

For nearly a century, genetic alterations such as insertion, mutations, and deletion of genomic DNA is always seen as the major cause of cancer (Hanahan and Weinberg 2011). Rigorous efforts and studies have been done to prove on gene mutation hypothesis. However, so far, it is failed to identify the cancer-specific mutation that could transform normal cells to become malignant cells, as well as to answer why that the occurrence of cancer only happens many months or even decades after mutation by carcinogens and why almost 90% of solid tumors

are aneuploid (Weaver and Cleveland 2008), despite conventional mutation does not depend on karyotype alteration. In contrast, aneuploidy hypothesis seems to provide a better understanding and explanation about the cancer-specific phenotypes (Birchler and Veitia 2007, Duesberg and Rasnick 2000, Li et al 2000). Comparison with the conventional evolution of new species, aneuploidy can predict the long latent periods and the clonality based on these following two-stage mechanism: stage one, a carcinogen (or mutant gene) develops aneuploidy; stage two, aneuploidy destabilizes the karyotype and hence, initiates an autocatalytic karyotype evolution generating preneoplastic and eventually neoplastic karyotypes. Since the odds are very low that an abnormal karyotype will surpass the viability of a normal diploid cell, the evolution of a neoplastic cell species is slow and thus clonal. Moreover, aneuploidy based on the complexity of cancer-specific phenotypes, such as abnormal cellular and nuclear morphology, metabolism, growth, invasiveness, and metastasis, is more in accordance with the alterations of the dosage of thousands of regulation and structural genes than with gene mutations (Li et al 2000).

Strong evidences shows for high frequency of aneuploidy in cancer. Aneuploidy is claimed to be the second common form of genetic abnormality found in human cancers (Weaver and Cleveland 2006). Recently with the advancement in cytogenetic analysis, a comprehensive study from *Beroukhim et al.* is able to identify genomic regions that undergo frequent alterations in terms of somatic copy number alterations (SCNAs) in human cancers. He discovered that one quarter of a typical cancer cell's genome is subjected to whole-arm SCNAs or whole-chromosome SCNAs of aneuploidy (Beroukhim et al 2010). In addition, a strong evidence for preferential gain or loss in whole-chromosome SCNAs across

human cancer lineages was observed in their study, which shows that this is a selective process rather than random alterations. A reinforcement of the results from this study is further supported by the analyses of the Mitelman Database (http://cgap.nci.nih.gov/Chromosomes/Mitelman), which contains the largest repository of cytogenetic information on human cancer and the results of more than 60,000 cases (Ozery-Flato et al 2011). Concurrently, aneuploidy are also observed in several cancer types such as breast cancer (Li and Benezra 1996, Yoon et al 2002), colorectal cancer (Cahill et al 1998, Cardoso et al 2006), Hepatocellular carcinoma (Saeki et al 2002), lung cancer (Weitzel and Vandre 2000), head and neck cancer (Ai et al 2001, Minhas et al 2003), and cervical cancer (Melsheimer et al 2004). In addition, in cases of acute myeloid leukemia (AML), 10-20% gain of chromosome number 8 is identified, as well as in some solid tumors like Ewing's sarcoma and desmoids tumors (Hitzler and Zipursky 2005, Maurici et al 1998, Qi et al 1996). All these data indicate the role as well as occurrences of aneuploidy at an early stage of tumorigenesis, which might support the preceding of cell transformation.

Understanding about how aneuploidy contributes to the phenotypes of human cancer is still the focus in current research. One possibility is the ability of a population of cells reorganizes the whole chromosomes such as that it facilitates the loss of heterozygosity (LOH) of tumor-suppressor gene or gain of an oncogene by duplicating the chromosome that contains the mutated allele. One example that could explain this possibility is the high incidence of loss of chromosome 10 in gliobalstoma, which in turn resulting the inactivation of PTEN tumor-suppressor gene (Wang et al 1997). This study highlights that aneuploidy might contribute to tumor formation without the aid of additional mutations. The second possibility is

the defects or weakening of mitotic spindle checkpoint. In fact, loss in certain key mitotic checkpoint genes leads to aneuploidy and tumorigenesis in mice (Schvartzman et al 2010) as well as in human cancers (Schuyler et al 2012, Weaver and Cleveland 2006). Based on the current studies, it shows that mitotic-spindle-checkpoint genes are often altered at the transcriptional level (Wang et al 2002, Weaver and Cleveland 2006). Unravelling the mechanism behind this mitotic checkpoint and it defects could in the future provide a new prospect of treatment to target cancer.

### 1.2.2 Mad2

Mad2 (mitotic arrest deficient 2) is a 24-kilo Dalton (kDa) small protein without a discerning catalytic domain (Li et al 1997). It is an essential mitotic spindle checkpoint protein. The main role of Mad2 protein is to block the activation of separase and seperation of sister chromatids before the onset of anaphase until the chromosomes are properly aligned and attached at the kinetochores (Sotillo et al 2007). During checkpoint activation, Mad2 is activated with the help of Mad1. Physical interaction between Mad1 and Mad2 will function together in a hetero-tetrameric complex to initiate the “stop anaphase signal” (Chen et al 1999, Yang et al 2008). The Mad1-Mad2 complex will then bind at the unattached kinetochore, where Mad1 becomes hyper-phosphorylated and activated by the kinase monopolar spindle 1 (Mps1) (Hewitt et al 2010) (Figure1.3). Mad1-Mad2 complex at the unattached kinetochore will catalytically form the Mad2-CDC20 complex (Fava et al 2011). After being released from the kinetochore the Mad2-CDC20 heterodimer binds to other checkpoint proteins, which consist of the checkpoint protein Mad3 and Bub3. This Mad2-CDC20-Mad3-Bub3 complex is usually called the mitotic checkpoint complex (MCC). Finally, this MCC

inactivates the APC/C and leads to cell cycle arrest until all the chromosomes align correctly at the kinetochore. This mechanism will prevent the premature anaphase (Chao et al 2012, Musacchio and Salmon 2007). To dissolve MCC from the APC/C, Mad2 is bind to $p31^{comet}$ also known as MAD2L1BP. The binding between Mad2 and p31comet will reactivate APC/C. The reactivation of APC/C will then activate separase and promote entry into anaphase (Varetti et al 2011, Westhorpe et al 2011). With this checkpoint process, MAD2 can help the premature intiation of anaphase until all chromosomes are properly attached and aligned along the kinetochore plate (Murray 2011). Either inactivation or hyperactivation of Mad2 promotes tumorigenesis in mice (Chi et al 2009, Sotillo et al 2007).

Mad2 is an essential gene not only in the tight regulation of cell division but it is also important during embryogenesis, because Mad2 null mice is embryonically lethal (Dobles et al 2000). Thus, complete inactivation of Mad2 has not been identified in human cancers (Michel et al 2004). However, in experimental mouse model, whereby one allele of Mad2 is deleted (Mad2+/-), shows higher cancer rates compared with its wild-type (WT) littermates. Mad2+/- mice developed an enhanced rate of lung adenocarcinoma after a long latency (Michel et al 2001). This suggesting that Mad2 haplo-insufficiency might contribute to aneuploidy and tumorigenesis.

Mad2 dysregulation has long been implicated in various cancers. Attenuation of Mad2 expression associated with loss of mitotic checkpoint control and aneuploidy was observed in adult T-cell leukemia, breast cancer, ovarian cancer, and liver cancer (Weaver and Cleveland 2006). On the other hand, Mad2 overexpression is seen in colorectal cancer (Li et al 2003) and gastric cancer (Wang et al 2009b). In addition, this abberant Mad2 overexpression was

demonstrated to be associated with inactivation of Rb or p53 tumor-suppressor gene, which resulting in mitotic alterations and aneuploidy (Schvartzman et al 2011). Interestingly, only transient Mad2 overexpression can sufficiently promotes tumor formation, and knock down of Mad2 after tumor formation, did not result in shrinkage of existing tumor. This phenomenon shows that Mad2 is not required for tumor maintenance, unlike a classical oncogene. The lack of response of Mad2 withdrawal after tumor formation reflects on the early induction of chromosome instability by Mad2, which would persist after Mad2 expression is normalized (Sotillo et al 2007).

Deregulation of Mad2 function during mitosis might be also cause by the abberant interaction of Mad2 with the other proteins. As an example, overexpression of p31comet, a protein that inhibit mitotic checkpoint by antagonizing Mad2, induces premature degradation of securing and allows exit from mitosis without proper chromosome segregation (Habu et al 2002, Westhorpe et al 2011).

In addition, microinjection of Mad2 antibody to the pro-metaphase of primary human keratinocytes induces premature anaphase, which leads to aneuploidy. However, although it is prematurely proceed to anaphase, the cells show a completed anaphase process including chromatid movement to the spindle pole as well as pole- pole separation post injection with Mad2 antibody. This shows how important Mad2 for the timing of anaphase onset in somatic cells during mitosis (Gorbsky et al 1998). Not only the expression level of Mad2 is important but also the localization of Mad2 in the cells undergoing mitosis is also essential for the exact anaphase entry. Higher eukaryotes change Mad2 localization in a cell cycle-dependent manner (Chen et al 1996). Despite its distribution

throughout the cell, Mad2 is preferentially found on the nuclear periphery (Kallio et al 1998). Fluorescence digital imaging reveals that at or near the onset of mitosis, Mad2 translocates into the nucleus. It localizes at the kinetochore from prophase to anaphase if the spindle attachment is incomplete or the chromosome is not properly aligned. Approximately 10 minutes after cells entered the anaphase, Mad2 fluorescence signal is no longer detectable on the kinetochores. Concomitantly, Mad2 can be found associated with unattached kinetochore after nocodazole treatment, a drug that interfere with microtubule polymerization (Howell et al 2000). Therefore, delocalization of Mad2 from the nucleus during mitosis could also lead to chromosomal instability or aneuploidy.

**1.3 Ubiquitin, ubiquitin-like proteins and cancer**

Since the discovery of ubiquitin pathway and functions in early 1980 (Ciechanover 1994, Hershko and Ciechanover 1998), more and more intense research is focusing to dissect the regulation, mechanism and functions of Ubiquitin and Ubiquitin-like proteins. In fact, accumulation of evidence supports Ubiquitin and UBL to play a major role in wide variety of biological processes, such as DNA replication, DNA damage response, signal transduction, cell cycle control, embryogenesis, cell cycle progression, protein stability, apoptosis, transcriptional regulation, and many other functions (Mukhopadhyay and Riezman 2007, Nakayama and Nakayama 2006, Tu et al 2012). Hence, aberrant or impairment function in the ubiquitin proteasome signaling is implicated in the etiology of many diseases, especially in tumorigenesis (Mani and Gelmann 2005). Moreover, ubiquitin-like proteins such as SUMO (Kim and Baek 2009), ISG15 (Bektas et al 2008), and FAT10 (Lee et al 2003) have also been found to play a role in cancer development

### 1.3.1 Ubiquitin

Ubiquitin is a small protein composed of 76 amino acids that is conserved across evolution from yeast to man and ubiquitously expressed in eukaryotes (Cook et al 1993, Yang et al 2010b). Cells are using ubiquitin as a covalent modifier of other proteins via an isopeptide bond between its C-terminal glycine and the ε-amino group of lysine in the substrate proteins both in order to activate their function as well as to target them for degradation via the 26s proteasome pathway (Hochstrasser 1996a, Hochstrasser 1996b). In a cascade of events that requires participation of three enzymes, ubiquitin is targeting its protein's substrates for degradation. It is namely, the ubiquitin-activating enzyme (E1), the carrier protein (E2), and the ubiquitin ligase (E3) (Glickman and Ciechanover 2002). The ubiquitin-activating enzyme (E1) initiates the ligation of ubiqutin by adenylation in an ATP-dependent manner, and then this ubiquitin molecule is transferred to the active site cysteine of ubiquitin-conjugating enzyme (E2) via trans-thioesterification reaction. In the final step, E2 works together with the ubiquitin ligase (E3) that is responsible for conferring substrate specificity. Ubiquitin is transferred to the internal lysine residue of the target protein and binds to its target via its C-terminal Glycine (Ciechanover and Iwai 2004). Emphasizing on the diversity of ubiquitin's functions as a critical posttranslational modification, there are two different functional consequences to ubiquitin's target proteins: monoubiquitination controls protein functions, ranging from membrane transport to transcriptional regulation(Di Fiore et al 2003), whereas ubiquitin chains that form through their lysine residue at position 48 (Lys48) are known to tag proteins for proteolytic degradation by the 26s proteasome (Hershko and Ciechanover 1998). Conjugation of ubiquitin through other lysine residues (Lys6, Lys11,

Lys27, Lys 33, and Lys63) can form different lengths and shapes of ubiquitin chains. Thus, it shows that different ubiquitin chains' conformation creates a range of molecular signal in the cell (Kim et al 2007).

It is the fact that mutations and alterations in ubiquitination as well as deubiqutination process have been directly implicated in cancers (Ciechanover and Iwai 2004). For instance, the consequences of altered ubiquitination is stabilization of oncogene or destabilization of tumor suppressor gene products, which resulted from improper removal of oncoproteins that sometimes is part of the natural substrates of the ubiqutin system. Indeed, ubiquitin system target proteins that positively regulate cell proliferation, such as N-Myc, c-Myc, c-Fos, c-Jun, and Src-like proteins as well as tumor suppressor proteins such as TP53, and p27 (Confalonieri et al 2009, Sun 2006, Zhao et al 2008). Hence, ubiquitin machinery is recently under intense research in order to find a promising therapeutic target. As an example, a recently approved proteasome drug inhibitor called Velcade (Millenium Pharmaceuticals, Inc., Cambridge, MA, USA) has been used to treat multiple myeloma and mantle cell lymphoma (Orlowski and Kuhn 2008). However, this drug has only a limited function, because it targets only one functions of ubiquitin in protein degradation. Given a wide variety of functions in ubiquitin system, another aspect that needs to be considered are the undesired side effects from the drugs that targeting ubiquitin machinery.

### 1.3.2 Ubiquitin –like modifiers (UBL)

In addition to ubiquitin itself, many ubiquitin-like proteins have been identified. These ubiquitin-like proteins are related with ubiquitin either by its sequence or structure. Like ubiqitin, these proteins are engaged in vast array of vital cellular processes. Ubiquitin-like proteins are divided into 2 subgroups, ubiquitin-like

modifiers and ubiquitin domain proteins (UDP). Ubiquitin like modifiers (UBL) are proteins that contain ubiquitin-like structures (Jentsch and Pyrowolakis 2000). UBL has the same three-dimensional core structure as ubiquitin, where it adopts the conserved β-grasp hold characteristic of ubiquitin (van der Veen and Ploegh 2012). In addition, all UBL proteins comprised of a double glycine residue at its C-terminal. This glycine residue is in charge of the covalent isopeptide binding with the lysine residue in its substrate proteins (Jentsch and Pyrowolakis 2000). First studies about UBL begun in the late 1980 by the discovery of an interferon-stimulated gene product of 15kDA (ISG15). This protein has a sequence similarity with ubiquitin and also covalently modified other proteins (Haas et al 1987). Hitherto, there are 10 UBL proteins that are covalently linked to target proteins; these include NEDD8, FAT10, SUMO, ISG15, UBL5, Ufm1, Urm1, Atg8, Atg12, and FUB1 (Cajee et al 2012, Hochstrasser 2009) (Table1.2). Similar to ubiquitin, UBLs also uses a similar enzymatic cascade to target its substrate proteins (van der Veen and Ploegh 2012), with some exception that some UBL is capable to directly bind to its substrate without E3 (Hochstrasser 2009, Welchman et al 2005). So far, only SUMO2/3 and NEDD8 are known to participate in a chain formation like polyubiquitin chain (Matic et al 2008, Xirodimas et al 2008). UBLs is like ubiquitin, have a wide variety of cellular functions, such as activation of enzymes and transcriptional regulators, routing of proteins to their sub-cellular destination, mediating apoptosis as well as cell proliferation, and ultimately determination of the half-life of the target protein (Cajee et al 2012, Herrmann et al 2007). Apart from FAT10, none of the above-mentioned UBLs have ever been reported to be involved in proteasomal-protein degradation (Kerscher et al 2006, Welchman et al 2005).

From all UBLs, SUMO is the most extensively studied (Herrmann et al 2007). It was first detected in mammals as a protein, which covalently bound to the GTPase activating protein RanGAP1 (Mahajan et al 1997). SUMO regulates various cellular biological processes, which encompass nuclear transport and organization, transcription, chromatin remodeling, DNA repair, cell cycle regulation and ribosomal biogenesis (Gareau and Lima 2010, Wilkinson and Henley 2010). Furthermore, substrate modification by sumoylation can affect protein-protein interactions, change protein intracellular localization, or even directly change the activities of the substrate proteins (Geiss-Friedlander and Melchior 2007). Several receptors and intracellular signaling proteins such as p53 (Gostissa et al 1999), c-Jun (Muller et al 2000), and IκB (Desterro et al 1998) have been demonstrated to be modified by SUMO and therefore contribute to tumorigenesis. Further, SUMO has also associated with several proteins that important in mitosis, these include condesin, Topoisomerase II (Top2), CENP-C/E, and surviving. Dysregulation of these proteins will then cause improper cell cycle process, which leads to aneuploidy and tumorigenesis (Dasso 2008).

## Table 1.2 List of ubiquitin-like modifiers and their function

| Modifier | Functions | Acession | Reference |
|---|---|---|---|
| **ISG15** | Function as an anti viral molecule, Modifying STAT1, SERPINA3G, JAK1, MAPK3/ERK1, PLCG1, EIF2AK2/PKR, MX1/MxA, and RIG-1. Interference with ubiquitin proteasome pathway. | NP_005092 | (van der Veen and Ploegh 2012, Zhao et al 2005) |
| **NEDD8** | Cell Cycle control and embryogenesis, Proteasomal degradation, Possible involvement in aggregosomes formation | NP_006147 | (Odagiri et al 2012, Rabut and Peter 2008) |
| **SUMO-1** | Nuclear transport, DNA replication and repair, mitosis, and signal transduction, cell cycle regulation | NP_001005781 | (Gareau and Lima 2010) |
| **SUMO-2** | Nuclear transport, DNA replication and repair, mitosis, and signal transduction, cell cycle regulation | NP_001005849 | (Gareau and Lima 2010) |
| **SUMO-3** | Nuclear transport, DNA replication and repair, mitosis, and signal transduction, cell cycle regulation | NP_008867 | (Gareau and Lima 2010) |
| **SUMO-4** | Negative regulator of NF-κB dependent transcription, Conjugation of stress defense proteins upon conjugation, modulation of protein subcellular localization | NP_001002255 | (Bohren et al 2004, Wang et al 2009a) |
| **FAT10** | Protein degradation, mitotic non-disjunction and chromosome instability mediator, Regulation of TNF-alpha induced chromosomal instability, Formation of aggresomes when proteasome is saturated or impaired. | NP_006389 | (Kalveram et al 2008, Rani et al 2012, Ren et al 2006, Ren et al 2011b) |
| **UBL5** | p53 negative regulator | NP_001041706 | (Allende-Vega et al 2013) |
| **FUB1** | Regulation of apoptosis in human cells, LPS induced ERK-MAPK cascade | NP_001988 | (Nakamura and Yamaguchi 2006, Pickard et al 2011) |
| **Atg8** | Mediates protein lipidation during autopagy | NP_009475 | (Geng and Klionsky 2008) |
| **Atg12** | Mediator of mitochondrial apoptosis, Negative regulation of type I interferon production | NP_004698 | (Geng and Klionsky 2008, Rubinstein et al 2011) |
| **Ufm1** | Prevention of ER stress induced apoptosis | NP_057701 | (Lemaire et al 2011) |
| **Urm1** | Sulfur donor in biosynthesis pathway | NP_001129419 | (Van der Veen et al 2011) |

Another class of ubiquitin-like molecule is called ubiquitin domain proteins (UDPs). UDPs have a higher primary amino acid sequence similarity compared to UBLs, but they are not conjugated to proteins (Herrmann et al 2007). Their cellular function is as an adaptor protein, whereby it binds non-covalently to ubiquitin or UBLs via its ubiquitin-associated domain (UBA). As an example of UDPs, Rpn10 allows direct recognition of polyubiquitinated proteins by 26s proteasome (Elsasser et al 2002). The dysfunction of UDPs has been implicated to human diseases such as neurodegeneration and neoplasia (Madsen et al 2007).

### 1.3.3 FAT10

FAT10 (human leukocyte antigen **F**-**a**ssociated **t**ranscript **10**) is an 18kDA protein consists of 165 amino acid residues. FAT10 gene was first identified amongst genes in the HLA-F locus of major histocompatability complex (MHC)-class I on chromosome 6, and found to be expressed in lymphoid cell lines. Thus, it was originally speculated to have a function in antigen processing and presentation (Bates et al 1997, Fan et al 1996). It belongs to the ubiquitin-like modifier (UBL) family of proteins and encompasses of two-ubiquitin like domains in tandem array (Jentsch and Pyrowolakis 2000). Thus, it is also known as diubiquitin or ubiqutin D (UBD) (Pelzer and Groettrup 2010). The sequence similarity between FAT10 and ubiquitin at its N- and C-terminal regions are 29% and 36%, respectively. Moreover, FAT10 at the C terminus region conserved the di-glycine residues from ubiquitin that are important for conjugating to its substrate protein. Lysine residue that may be capitalized as a potential site for polyubiquitination is also conserved in N-and C-terminal of FAT10 proteins (Liu et al 1999b). Four Lysine residues that correspond with polyubuquitin-chain formation, like Lys27, Lys33, Lys48, and Lys63, are conserved in both ubiquitin

like domains of FAT10 (Liu et al 1999b) (Figure 1.4). FAT10 is limited only to vertebrates and induced upon specific pro-inflammatory stimuli in specific tissue like spleen and thymus (Fan et al 1996, Gruen et al 1996, Liu et al 1999b). Highest basal expression of FAT10 was found in the cytoplasm of mature dendritic cells and B cells, which might show the involvement of FAT10 in immune response (Canaan et al 2006). The conjugation cascade of FAT10 has involved E1-activating enzyme UBA-6 (UBE1L2, E1-L2, OR MOP-4) (Chiu et al 2007, Pelzer and Groettrup 2010) and UBA-6 specific E2- conjugating enzyme, USE1 (Aichem et al 2010). So far, the specific E3 ligase of FAT10 has not been found. Covalent conjugation of FAT10 substrate proteins (FATylation) via its C-terminal glycine is hypothesized to target these proteins for proteosomal degradation (Hipp et al 2005, Raasi et al 2001). Unlike ubiquitin, FAT10 contains free di-glycine at its C-terminus that does not require prior activation for the binding with its substrate proteins (Hipp et al 2005). Five substrates of FATylation have been found so far. These are its own E1-activating enzyme UBA6 (Chiu et al 2007), E2 conjugating enzyme USE1 (Aichem et al 2010), p53 (Li et al 2011, Zhang et al 2006), huntingtin (Nagashima et al 2011) and autophagic receptor p62 (Aichem et al 2012a). However, FAT10 not only can bind covalently to the other proteins but it can also bind non-covalently with the other proteins. Several studies highlighted non-covalent interaction partners of FAT10 that leads to various cellular functions (Table 1.3). Interestingly, FAT10 can be significantly induced synergistically by pro-inflammatory cytokines such as tumor necrosis factor-α (TNF-α) and interferonγ (IFNγ) of almost all tissue origins (Lukasiak et al 2008b), this has further strengthened the possibility of FAT10's roles in immune response and chronic inflammation. Further, elevated level of TNFα is always detected in the

serum of HCC patients (Ataseven et al 2006) and colorectal cancer (CRC) (Szlosarek et al 2006). Concurrently, FAT10 overexpression was identified to associate with expression of TNFα and IFNγ-dependent proteasome subunit LMP2; supporting that pro-inflammatory cytokines can induce both FAT10 and LMP2 (Lukasiak et al 2008b). Moreover, induction of FAT10 through TNFα activates NF-κB pathway and promotes chromosomal instability in colorectal cancer cells (Ren et al 2011b). Therefore, FAT10 is proposed to be the mediator in the development of chronic inflammation-associated tumorigenesis.

Not only is FAT10 important in immune response, it also plays an important role in tumorigenesis. The important roles of FAT10 in cancer have been highlighted by several observations. Firstly, it is found to be overexpressed in various cancers, such as in 90% of Hepatocellular Carcinoma (HCC), and about 85% of colorectal cancer (CRC) (Lee et al 2003). Secondly, FAT10 knockout mice exhibit spontaneous apoptotic death and are sensitive to endotoxin exposure of lymphocytes (Canaan et al 2006). Thirdly, FAT10 was identified as a potential marker for liver pre-neoplasia (Oliva et al 2008). Furthermore, FAT10 overexpression in colon cancer and gastric cancer patients is reported to be associated with lymph node as well as distant metastasis, tumor staging, and invasiveness of these diseases. In gastric cancer, overexpression of FAT10 is associated with increased mutant p53 expression, which could further induce FAT10 expression and indirectly promote gastric cancer progression (Ji et al 2009, Yan et al 2010). Thus, in these studies, FAT10 protein and mRNA level is recognized as a prognostic marker for these diseases. Finally, FAT10 can also mediate pro-inflammatory cytokines TNF-α in inducing chromosomal instability, which is one of the hallmarks of cancers (Ren et al 2011b). In accordance, FAT10

overexpression has also been reported to induce chromosomal instability (Ren et al 2006). In summary, these observations support the notion that FAT10 plays an important role in tumorigenesis.

Given the fundamental role of FAT10 in tumorigenesis and its pro-survival role, it is important for us to understand how cells can degrade FAT10, when it is no longer needed. Although it is still a debate, whether FAT10's degradation is dependent or independent of ubiquitin, earlier study reported that FAT10-mediated degradation is independent of ubiqutination, as lysine-less FAT10 recedes. However, recent studies by *Buchsbaum and Schimdtke et al*. show that lysine-less FAT10 is degraded by the proteasome but it aggregates in an insoluble protein fraction (Buchsbaum et al 2012, Schmidtke et al 2006). In addition, as an alternative route for FAT10's degradation, upon proteasomal inhibition, FAT10 binds to histone deacetylase 6 (HDAC6) non-covalently and travels to aggresomes (Kalveram et al 2008).

**Table 1.3 Reported FAT10 interaction partners**

| Type of Interaction | Interaction Partner | Interaction Residue | | Function | Reference |
|---|---|---|---|---|---|
| | | Glycine | Lysine | | |
| Covalent | E1-L2 (UBA-6) | ✓ | - | Ubiquitin-activating enzyme (E1) | Mol Cell 2007, 27(6):1014-23 |
| | USE-1 (UBE2Z) | ✓ | - | UBA-6-specific E2 conjugating enzyme | Nature Communication. 2010, 1:13 doi: 10.1038/ncomms1012 |
| | p53 | ✓ | - | Upregulation of p53 transcriptional activity | Arch Biochem Biophys. 2011 doi: 10.1016/j.abb.2011.02.017. |
| | Huntingtin | ✓ | - | Play important role in Huntington disease (HD) development | J Biol Chem. 2011. doi: 10.1074/jbc.M111.261032 |
| | p62 | ✓ | - | proteosomal degradation of p62 | J Cell Sci. 2012 doi: 10.1242/jcs.107789. |
| Non Covalent | Mad2 (mitotic arrest deficient 2) | - | - | Cell cycle checkpoint | Proc Natl Acad Sci U S A. 1999, 96(8):4313-8<br>J Biol Chem. 2006, 281(16):11413-21 |
| | NUB1L | - | - | UBA-6 specific E2 enzyme<br>Auto FAT10lyated in cis | J Biol Chem 2004, 279(16):16503-10 |
| | HDAC6 (Histone deacetylase 6) | - | - | Regulate transcription by modulating chromatin structure<br>has binding domain for UBL-protein | J Cell Sci 2008, 121( 24): 4079-88 |

**A.**

**Ubiquitin 3D structure**

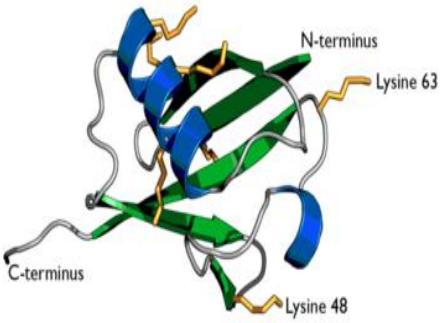


**Predicted FAT10 3D structure**

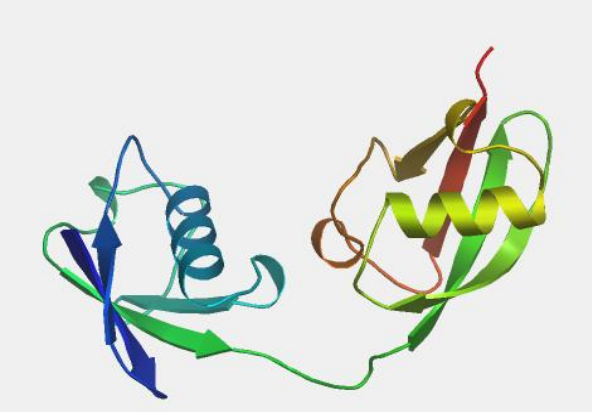

**B.**

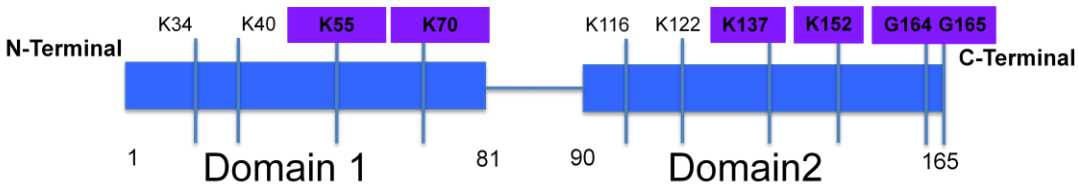


**C.**

```
FAT10 N    MAPNASCLCVHVRSEE-WDLMTFDANPYDSVKKIKEHVRSKT
Ub         MQ-------IFVKTLT-GKTITLDVEPSDSIDNVKQKLQDKE
FAT10 C    PL-------FLVESGDEAKRHLLQVRRSSSVAQVKAMIETKT

FAT10 N    KVPYQDQVLLLGSKILKPRRSLSSYGIDKEKTIHLTLKVVKP
Ub         GIPPDQQRLIFAGKQLEDGRTLSDYNIQKESTLHLVLRLRGG
FAT10 C    GIIPETQIVTCNGKRLEDGKMMADYGIRKGNLLFLASYCIGG
```

**Figure 1.4 Predicted 3D structure of FAT10 in comparison with Ubiquitin as well as its sequence comparison. A.** Ribbon 3D structure of Ubiquitin and predicted 3D structure of FAT10 based on its sequence homology with ISG15 (another di-ubiquitin like protein (http://www.uniprot.org/uniprot/P63072)**. B.** FAT10 consists of two domains, where its sequence is in N-terminal (29%) and C-terminal (36%) identical to ubiqutin. The double glycine motif is conserved in second domain of FAT10. Four Lysine residues (K27, 33, 48. 63), which play role in polyubiquitination chain formation, are also conserved in the two domains of FAT10. **C.** Sequence alignment of FAT10's N- and C-terminal with Ubiquitin. (green: sequence is similar between FAT10's N-terminal and ubiquitin, blue: sequence is similar between FAT10's C-terminal and ubiquitin, red: sequence is similar in FAT10's N-, C-terminal, and ubiquitin.

### 1.4 FAT10 and Mad2

Using yeast-two-hybrid screening of human lymphocyte library, Mad2 is identified as a potential interaction partner of FAT10. Further validation using co-immunoprecipitation reveals that FAT10 interacts with Mad2 non-covalently (Liu et al 1999b). Since Mad2 is a mitotic spindle checkpoint, which plays an important role for spindle assembly during anaphase, disruption of Mad2's function during mitosis can result in chromosome missegregation, which leads to aneuploidy and tumorigenesis (Dobles et al 2000, Sotillo et al 2007). In support to these reports, our previous study demonstrates that FAT10 overexpression reduces Mad2's localization to the kinetochore during pro-metaphase and abbreviates the mitotic duration, which then leads to aneuploidy (Ren et al 2006), one of the hallmarks of cancers (Weaver and Cleveland 2008). Furthermore, upon nocodazole arrest, cells overexpressing FAT10 are observed to escape mitotic arrest and become multinucleated in comparison with its parental cells, suggesting that FAT10 can help the cells escape from mitotic arrest, because its overexpression reduces Mad2 localization at the unattached kinetochore during mitosis, which leads to uncontrolled cell cycle progression and aneuploidy (Ren et al 2006). Further study reveals similar results, when FAT10 is induced with TNF$\alpha$, such as delocalization of Mad2 from kinetochores, acceleration of mitosis duration, and the missegregation of chromosomes. Conversely, upon knockdown of FAT10 using FAT10siRNA, normal phenotype is restored (Ren et al 2011b). These evidences prove that FAT10 could possibly play a major role in driving tumorigenesis through its interaction with mitotic spindle checkpoint Mad2.

## 1.5 Objectives of this thesis

In this thesis, I sought to accomplish three major objectives to elucidate the role of FAT10 in tumorigenesis that are further described below:

1. To validate, whether FAT10 is a potential determinant of malignancy in colorectal cancer (CRC). To answer this question, *in vitro* study using cell proliferation-, apoptosis-, as well as invasion, and cell transformation assay were employed. *In vivo*, subcutaneous injection at the flanking region of nude mice of colorectal cancer cells overexpressing FAT10 is performed and compared with injection of parental cells. Indeed, in vitro and in vivo experiments shows that FAT10 overexpression could increase proliferation, protect these cells from apoptosis, encourage anchorage-independent growth, as well as increase its invasiveness.
2. To find the specific site of FAT10 and Mad2 binding, which potentially could serve as a potential therapeutic target for cancer treatment. In collaboration with A/P Song Jianxing from Department of Biological Science, NUS, Nuclear Magnetic Resonance (NMR) was used to determine the three dimensional structure of FAT10 as crystal structure of FAT10 has yet to be elucidated. Chemical Shift perturbation mapping was used to determine the specific sites where Mad2 binds FAT10. Two-specific regions at domain one of FAT10 were found to be important for FAT10 and Mad2 binding.
3. To validate and characterize, whether the disruption of FAT10 binding to could reverse cell's malignant behaviors, without disrupting FAT10's physiological function. Using mutagenesis study complemented with various cell functional and transformation assays; we demonstrate the

significance of these specific regions of FAT10 and Mad2, which play in tumorigenesis.

**1.6 Significance of this thesis**

In this thesis, we present the first evidence the oncogenic property of FAT10, which could support the malignancy of colorectal cancer cells *in vitro* as well as *in vivo*. Previously, our lab has found that this malignant behavior was linked with FAT10 and Mad2 binding, which resulted in the Mad2 delocalization during metaphase, abbreviation of mitosis and leading to the dysfunction of Mad2 as mitotic spindle checkpoint during mitosis.

I observed that FAT10 overexpression *in vitro* could induce cell proliferation and protect the cells from apoptosis in comparison with cells that did not overexpress FAT10. Additionally, FAT10 overexpression also enhanced the anchorage-independent growth of colorectal cancer cell on soft agar and increased its invasiveness, highlighting the important role of FAT10 as a potential determinant in colorectal cancer malignancy and its pro-survival roles. Finally, *in vivo* study using Xenograft mouse model also revealed that FAT10 could increase the tumor growth of these colorectal cancer cells, which has been injected subcutaneously into the dorsal flanking region of these mice. All these evidences mentioned above, emphasized the potential role of FAT10 as a potential drug target. However, targeting FAT10 as a whole protein could disrupt other important physiological functions of FAT10, since FAT10 is not only important in tumorigenesis, but it is also important in immune response and protein degradation. Therefore, delineating the regions within FAT10 that contributes to tumorigenesis is important.

Significantly, our findings further define the specific mechanism that can be exploited for colorectal cancer treatment. I have demonstrated that it is through targeting Mad2 specific regions within FAT10. Disruption of these specific sites inhibited the cell proliferation and tumor growth, as well decrease anchorage-independent growth and invasiveness of these colorectal cancer cells. Not only could we see the reversed phenotypic effect through this disruption but we can also see that the cells were no longer aneuploid. Notably, I have also shown that disrupting these specific sites will not interrupt FAT10's binding with the other proteins, especially those important proteins that involved for its proteasome degradation function, as FAT10 can still bind to its substrate proteins such as UBA6, and p62 via its C-terminal di-glycine residue, as well as its other non-covalently reported interaction partners such as HDAC6, and NUB1L in these mutants. This work presents a significant improvement in our understanding on FAT10 as potential determinant in colorectal cancer cells malignancy as well as the specific mechanism that could be used as a potential drug target, which previously had been largely unknown.

## Table 1.4 Overview of thesis

| Objective | Findings | Techniques |
|---|---|---|
| To validate FAT10 as a potential determinant of malignancy in colorectal cancer CRC | FAT10 increases cell proliferation | WST-Assay and cell counting |
| | FAT10 protects cells from apoptosis | Flow Cytometry with PE-AnnexinV Staining |
| | FAT10 increases the anchorage-independent growth of CRC cells | Soft agar transformation assay |
| | FAT10 increases cell invasiveness | Transwell-assay, F-Actin/Phalloidin Immunostaining and ELISA of Matrix metallopeptidase9 (MMP9) |
| | FAT10 increases cell adhesion and migration | Adhesion assay with collagen coated plate and Wound healing assay |
| | FAT10 supports tumor growth | Subcutaneous injection of CRC cells on the dorsal area of nude mice |
| To find the specific site of FAT10 and MAD2 binding | Mad2 binds to FAT10 at amino acid sequence number 11,13, 73, 75, and 77 in domain 1. | NMR study followed by chemical perturbation mapping in its HSQC spectrum to predict the specific site of Mad2 binding in FAT10 protein. (This work were performed by our collaborator A/P. Song Jianxing) |
| To characterize and validate the specific site of FAT10 and MAD2 binding, which contributing in tumorigenesis | FAT10 interacts with Mad2 | co-Immunoprecipitation and Proximity Ligation Assay (PLA) |
| | Mutations of FAT10's amino sequence number 11, 13, 73, 75, and 77 abolishes the binding between FAT10 and | co-Immunoprecipitation and Proximity Ligation Assay (PLA) |

| | | |
|---|---|---|
| | Mad2 | |
| | Mutation of FAT10's binding site with Mad2 does not interfere with the other reported protein interaction partners of FAT10 | co-Immunoprecipitation and Proximity Ligation Assay (PLA) |
| | Mutation of FAT10 binding site with Mad2 inhibits cell proliferation | WST-Assay |
| | Mutation of FAT10 and Mad2 binding site prevents the cells from escaping the nocodazole arrest. | Flow cytometry analysis with mitotic protein2 (MPM-2) staining |
| | Mutation of FAT10 and Mad2 prevents the cells from aneuploidy | Karyotyping of the chromosome number |
| | Mutation of FAT10 and Mad2 binding site decreases the CRC cells invasiveness | Transwell-assay, F-Actin/Phalloidin Immunostaining and ELISA of Matrix metallopeptidase9 (MMP9) |
| | Mutation of FAT10 and Mad2 binding site decreases CRC cells adhesion and migration | Adhesion assay with collagen coated plate and Wound healing assay |
| | Mutation of FAT10 and Mad2 binding site inhibits tumor growth | Subcutaneous injection of CRC cells on the dorsal area of nude mice |

# Chapter 2 Material and Methods

## Table 2.1 List of primary antibodies used in thesis

| Primary Antibody | Company | Catalogue Number | Working Dilution | Source |
|---|---|---|---|---|
| FAT10 | In House | | 1:10000 | rabbit polyclonal |
| GAPDH (FL-335) | Santa Cruz | sc-25778 | 1:20000 | rabbit polyclonal |
| HDAC-6 (D-11) | Santa Cruz | sc-28386 | 1:10000 | mouse monoclonal |
| MAD2 | BD Biosciences | 610679 | 1:10000 | mouse monoclonal |
| MTS-1 (X9-7) | Santa Cruz | sc-100784 | 1:5000 | mouse monoclonal |
| NUB1L (C-13) | Santa Cruz | sc-48059 | 1:5000 | goat polyclonal |
| p16 | Santa Cruz | sc-1661 | 1:10000 | mouse monoclonal |
| p62(Nucleoporin) | Santa Cruz | sc-48389 | 1:20000 | mouse monoclonal |
| PCNA (F-2) | Santa Cruz | sc-25280 | 1:20000 | mouse monoclonal |
| UBA6 | Sigma-Aldrich | SAB1400608 | 1:5000 | mouse polyclonal |

**Table 2.2 List of secondary antibodies used in thesis**

| Secondary Antibody | Company | Working Dilution | Source |
|---|---|---|---|
| Goat anti-mouse IgG, HRP conjugated | Pierce | 1:80000 | Goat polyclonal |
| Goat anti-rabbit IgG, HRP conjugated | Pierce | 1:80000 | Goat polyclonal |
| Rabbit anti-goat IgG, HRP conjugated | Pierce | 1:80000 | Rabbit polyclonal |

## 2.1 Mammalian Cell Culture and Assays

### 2.1.1 Mammalian Cell Culture

All cell lines used in this thesis were purchased from American Type Culture Collection (ATCC, Rockville, MD, USA). Human colorectal cancer (CRC) lines HCT116 were cultured in McCoy's 5A medium (Gibco/Invirogen, Carlsbad, CA, USA) supplemented with 10% FBS, while non-transformed immortalized human neonatal hepatocytes NeHepLxHT (ATCC CRL-4020) was cultured in Dulbecco`s Modified Eagle Medium/Nutrient F-12 Ham (Sigma, St Louis, MO, USA) supplemented with 0.2μl/ml of Dexamethasone (Lonza/Clonetics, Allendale, NJ, USA), 0.25μl/ml of Insulin (Lonza/Clonetics, Allendale, NJ, USA), 50μg/ml of G418 (Promega, Madison, WI, USA) and 10% FBS. Flask and culture plates used for culturing of NeHepLxHT cells were coated with 0.03mg/ml rat-tail collagen-type I (BD-Biosciences, Franklin Lakes, NJ, USA). The cell line was incubated at 37°C in a humidified atmosphere containing 5% $CO_2$.

### 2.1.2 Generation of stable HCT116 cell lines stably overexpressing WT-FAT10 or mutant FAT10

To engineer vectors expressing wild type (WT)-FAT10 or its mutants (FAT-mL, FAT-mR, and FAT-mLR), Gateway Cloning Technology (Invitrogen, Carlsbad, CA, USA) was used to clone the FAT10 cDNA or mutant FAT10 cDNA downstream of the N-terminal of the CMV promoter of the destination vectors pcDNA3 (Invitrogen).

To generate stable WT-FAT10 overexpressed cells and its mutants, colorectal cancer cell line (HCT116) was transfected with pcDNA3-FAT10, or pcDNA3-FATmL/mR/mLR using Lipofectamine2000™ (Invitrogen) according to the manufacturer's instruction. Cells were harvested 48 hr post transfection, and

then seeded onto a new 6-well plate with a 1:100 times dilution of cells containing McCoy's5A medium (Sigma Aldrich, St.Louis, MO, USA) supplemented with 10%FBS and 0.8mg/mL G418-sulfate (Promega, Madison, WI, USA). These cells were then incubated for 10 days at 37°C in 5% $CO_2$ humidified incubator. After 10 days several colonies were selected and analyzed for its FAT10 expression by western blot using FAT10 rabbit polyclonal antibody (see Table2.1). Two stably FAT10 overexpressed or FAT10 mutant cells were selected for further functional analyses and studies.

### 2.1.3 Recombinant adenovirus transduction of cells

#### 2.1.3.1 Generation of Recombinant FAT10 Adenoviruses

An invaluable experimental tool used in this thesis is the control (Ad-Ctrl) and FAT10-expressing recombinant adenoviral (AdFAT10) system that facilitated efficient introduction of FAT10 protein into human neonatal hepatocytes NeHepLxHT cells. In this experiment, FAT10cDNA was initially subcloned into the shuttle vector pADTrack-CMV. The FAT10-containing pAdTrack-CMV-FAT10 or control pAdTrack –CMV vectors was linearized using *PmeI* and subsequently co-transformed with enhance green fluorescence protein (EGFP) gene-containing pAdEasy-1 plasmid into BJ5183 *E.Coli* cells. Control and FAT10-expressing recombinant adenoviral vectors were obtained by homologous recombination of the two vectors pAdEasy-1 and pAdTrack-CMV/p-AdTrack-CMV-FAT10 respectively, and successful recombination events were screened using *EcoRV* and *PmeI* restriction endonuclease analyses. Subsequently, pAdControl and pAdFAT10 vectors were digested with *PacI* and transfected using Superfect™ Transfection Reagent (Qiagen, Hilden, Germany) into HEK293 cells

that constitutively express the adenoviral E1 gene product for packaging into control and FAT10-expressing recombinant adenovirus respectively. Finally, the titer of the viruses was determined by monitoring the number of green fluorescence cells after infection with serially diluted viral lysates and expressed as expression-forming units/per ml.

#### 2.1.3.2 Infection of non-transformed immortalized human neonatal hepatocytes NeHepLxHT cells

$6x10^5$ NeHepLxHT cells were seeded at about 60% confluency in each well of 6-well plate and grown for 24 hours. AdControl or AdFAT10 adenoviruses were then introduced to the cells. Cells were transduced with a multiplicity of infection (MOI) of 20 for 24 hours. Fresh media was then added 24 hr post-transduction and cells were incubated for another 24hr before they were used for further analysis. Dark field and phase contrast images were taken 48 hr post transduction (Figure 2.1) to check the transduction`s efficiency rate.

## Figure 2.1

**A.**

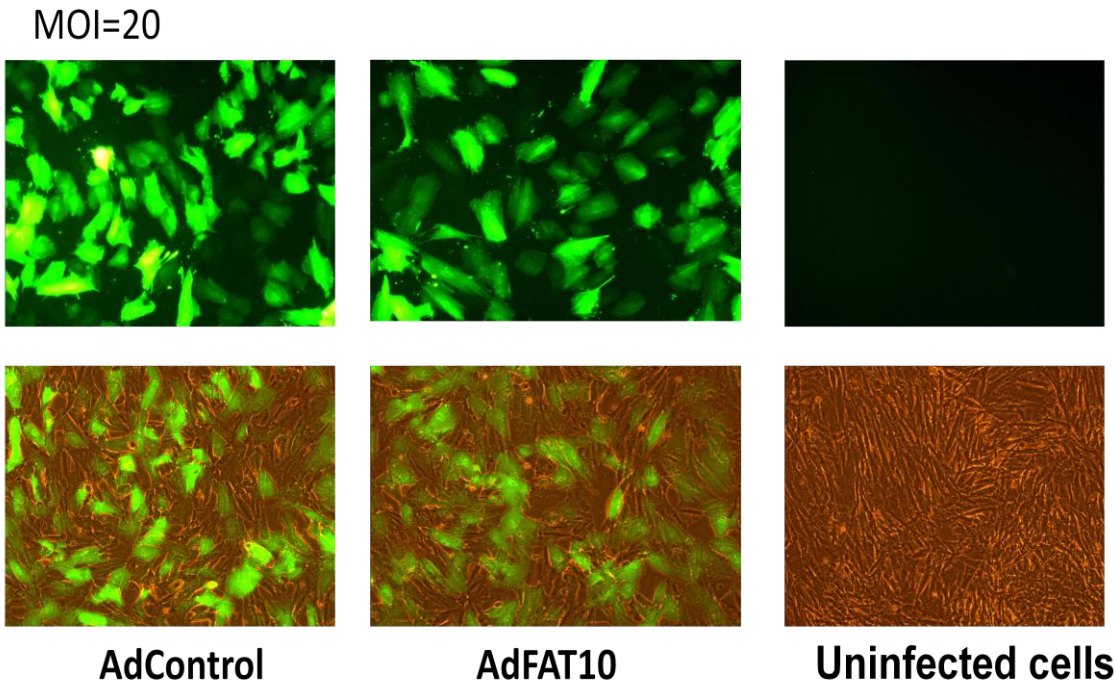


**B.**

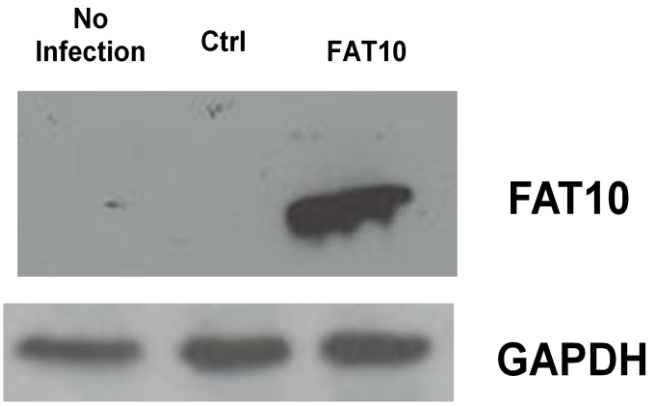


**Figure 2.1 Control and FAT10-overexpressing recombinant adenoviral system. A.** Dark field and dark field overlay with bright field images of the cells infected with the indicated MOI. **B.** Western Blot of FAT10 and GAPDH loading control of the indicated protein lysates to check the infection efficiency.

### 2.1.4 Transient transfection methods of siRNA or plasmid DNA in HCT116 cells

$2x10^6$ HCT116 cells were seeded in each well of 6-well plate. 24 hour post seeding, 100μM of short interfering RNA (siRNAs) or 4μg of plasmid DNA were chemically introduced to the cells using siPORT™ Amine Transfection Reagent (Ambion, Austin, TX, USA) or Lipofectamine2000™ (Invitrogen). These reagents were previously diluted in reduced serum media OPTI-MEM I® (Invitrogen) in a 10μl: 250μl ratio and incubated for 10 min at room temperature. Separately, siRNA or plasmid DNA was also diluted in 250μl OPTI-MEM I®. Subsequently, diluted siPORT™ Amine Transfection Reagent or Lipofectamine2000™ were mixed with the diluted siRNA or plasmid DNA, and incubated for 25 min at room temperature. These transfection complexes were then added onto the adherent cells that were pre-washed with PBS and replaced with fresh culture media. Cells were then harvested 24 hr post-transfection for further analyses. SiRNAs specific for FAT10 (AM16708, Ambion), MAD2 (Hs-42213 and Hs-42214, Sigma) as well as scrambled siRNA (AM4611, Ambion) were used as negative control in this study.

### 2.1.5 Soft agar colony formation assay

Anchorage independent growth using soft agar colony formation assay was performed in six well plates. First, 1.5 ml of 0.8% low-melting agarose solution (Invitrogen, Carlsbad, CA, USA) was added into each well and allowed to solidify. 5000 cells then were mixed with 0.5 % low-melting agarose solution and added on top of the 0.8% solidified agarose gel. After the top layer has been solidified, 3ml of medium supplemented with FBS were given and the cells were cultured for 3 weeks. The medium is continuously changed every 3-4 days during the 3 weeks

incubation. After 3 weeks colonies were stained with 0.01% methylene blue dissolved in 40 % methanol.

### 2.1.6 Cell Growth Assay

#### 2.1.6.1 Cell Counting

The growth profile of HCT116/NeHepLxHT cells was determined by seeding these cells in 6-well culture plate. At various time points (0, 24, 48, 72, 96, 120 hr), cells were harvested, stained with trypan blue, and only viable cells were counted using hemocytometer.

#### 2.1.6.2 Cell proliferation assay

3 x $10^3$ cells were seeded in each well of 96-well culture plate (Corning Inc., New York, NY, USA) in 150 µl of medium. After culturing cells at various time points (24, 48, 72, 96, 120 hr) the supernatant was removed and cell growth was determined using water soluble tetrazolium salt (WST-1) assay (Roche Applied Sciences, Penzberg, Germany) according to instructions given by the manufacturer. Absorbance was measured at 450nm using a microplate reader. All assays were carried out in triplicates.

#### 2.1.6.3 Determination of cell proliferation marker PCNA using FACS

For the analysis of PCNA expression, 1x$10^6$ asynchronous cells were harvested and then fixed in 70% ethanol. Cell pellet was resuspended in Phosphate Buffer Saline (PBS) containing fluorescein isothiocyanate (FITC)-conjugated anti-PCNA or mouse IgG1 (BD Pharmingen) and incubated at room temperature in the dark for 30 min before staining with propidium iodide (PI; Sigma, St Louis, MO, USA). Stained cells were then analyzed using FACS Calibur™ instrument (Becton

Dickinson, San Jose, CA, USA). Dot plots were analyzed using WinMDi 2.9 software.

### 2.1.7 Invasion and cell migration assay

The invasion assays were performed using Matrigel Invasion Chambers (BD Biosciences, CA, USA) and quantitated for the ability of the cells to invade across the coated membranes. Briefly, cells ($5 \times 10^4$/well) were suspended in McCoy's medium supplemented with 0.1% bovine serum albumin and placed in the upper chamber of a 24-well Transwell apparatus containing Matrigel membranes. The lower chambers were filled with 750 µl of McCoy containing 10% FBS as the chemoattractant. After incubation for 36 hours at 37°C, medium was removed; cells were fixed with methanol and stained with Diff Quick (Siemens Healthcare Diagnostics, IL, USA). Cells on the upper surface of each membrane were removed with cotton swabs, whereas cells that had migrated to the bottom surface of the filters were counted using brightfield microscope. Total cell numbers were counted for each well. Each experiment was done with triplicate wells and repeated thrice.

### 2.1.8 Cell adhesion assay

Cell adhesion were performed in 6 well plate coated with collagen. Cells were then added to each well in triplicate and incubated for 30 min at 37°C. Cells were washed 4 times with PBS and the remaining cells attached to the plates were observed under the microscope, harvested, and counted using a Beckman cell coulter counter (Beckman Coulter, IN, USA).

### 2.1.9 Wound healing assay

In brief, cells were plated on culture dishes to create a confluent monolayer. A wound was created by manually scraping the cell monolayer with a yellow tip

and the cells were washed and cultured with medium containing10% FBS. Cell images were then acquired at 0 and 24 hr after wound was created.

### 2.1.10 Actin Cytoskeleton Immunostaining

Cells were seeded on coverslips and incubated for 24 hr at 37°C in a humidified atmosphere of 5% $CO_2$. After 24 hr these coverslips with cells were then fixed with 4% paraformaldehyde in PBS for 15 min, washed with PBS, permeabilized in 1% TritonX-100 in PBS for 10 min, washed, and blocked with PBST with 1%BSA. To visualize the filamentous actin (F-Actin), the cells were stained with rhodamine-phalloidin (Invitrogen) for 30 min at 37°C and washed with PBST. After final wash, coverslips were mounted on the slide glass using mounting medium (Sigma). The cells were then observed under a fluorescence microscope (Zeiss).

### 2.1.11 Apoptosis Assay

$3x10^5$ stable overexpressing FAT10, FAT10 mutants, or wild-type HCT116 cells were seeded in 6-well plate. 24 hr after seeding, cells were subjected to 20μM of Camptothecin (CPT) for 24 hours at 37°C. The apoptosis profiles of the cells were analyzed by PE AnnexinV and 7AAD staining according to the manufacturer's instructions (BD Biosciences Pharmingen™, San Diego, CA, USA), followed by flow cytometry analysis using BD FACSCalibur™ (BD Biosciences). Subsequent analysis of the apoptotic profiles of the cells was analyzed using WinMDI2.9 software (Joe Trotter, USA).

### 2.1.12 Sample preparation for Karyotyping

Cells were first synchronized for 17 hours in media containing 3 mM thymidine (Sigma). After 17 hr cells replace the old medium with a fresh medium without thymidine for 7 hr, then cells were treated with 0.1μg/ml of colcemid

(Invitrogen) for 2 hours. Further, cells were harvested and rinsed with PBS, swelled in 0.06M of KCl solutions and fixed with methanol and glacial acetate acid in a 3 to 1 ratio. Fixed cells were dropped onto microscope slides, partially digested with trypsin, stained with Giemsa (Invitrogen). Chromosome number were counted using BandView software (Applied Spectral Imaging GmbH, Mannheim, Germany) under the phase contrast microscope (Zeiss).

## 2.2 RNA/DNA methodology

### 2.2.1 RNA isolation and reverse transcription polymerase chain reaction

Total RNA was prepared from cells using Rneasy® Mini Kit (Qiagen, Hilden, Germany) according to the manufacturer's instructions. Extracted RNA was then quantified using NanoDrop™ 1000 Spectrophotometer (Thermo Scientific, Waltham, MA, USA). For first strand cDNA synthesis, a 12μl reaction volume consisting of 1μg of RNA, 1 μl of 50 μM oligo dT primers, 1 μl of 10 mM dNTP, RNase/nuclease free water and 1 μl Superscript® II Reverse Transcriptase (Invitrogen). Finally, this mixture was then incubated at 25°C for 15 min followed by 42°C for 1 hr and 70°C for 15 min.

### 2.2.2 Real-time polymerase chain reaction

The abundance of transcription was determined by quantitative real-time PCR (qPCR) using ABI7500 Real Time PCR Detection System (Applied Biosystems™, Life Technologies™, Carlsbad, CA, USA). A 10 μl reaction volume comprising of 5 μl QuantiTect™ SYBR® Green Master PCR mix (Qiagen), 0.25 μl each of forward and reverse primers (Table 2), and Rnase/nuclease free water was prepared. The following qPCR conditions were used: an initial denaturation step at 95°C for 10 min, followed by 40 cycles of 95°C for 30 sec, 58°C for 30 sec

and 72°C for 30 sec. All transcript abundance was normalized against a housekeeping gene β-actin.

### 2.2.3 Mini- and maxi-preparation of plasmid DNA

QIAprep® Miniprep Kit (Qiagen) was used for small scale DNA preparation, whereas NucleoBond® Xtra Maxi EF kit (MACHEREY-NAGEL GmbH&Co., Dueren, Germany) was performed for large scale DNA preparation according to the manufacturer's instructions.

### 2.2.4 Agarose gel electrophoresis

6x DNA loading dye was mixed with DNA and separated on a 1% agarose gel prepared by dissolving agarose in 1x TAE buffer (0.04M Tris-acetate, 0.001M EDTA) with addition of 0.5 μg/ml ethidium bromide. The gel was run using 1 x TAE buffer, at 120 volts. DNA bands were visualized using UV trans-illuminator Gel Doc™ XR (Biorad, Hercules, CA, USA).

### 2.2.5 DNA sequencing

40 ng of plasmid DNA was utilized for ABI BigDye® Terminator Cycle Sequencing (Applied Biosystem), with addition of the following reagents in a 10 μl reaction volume: 2.5 μl BigDye Sequencing buffer, 0.5 μl of 10 μM primer, 0.5 μl BigDye® Terminator v3.1 and deionized water. T3000 Thermocycler (Biometra GmbH, Goettingen, Germany) was used to perform the DNA sequencing with the following conditions: 25 cycles of 96°C for 10 sec, 50°C for 10 sec, 60°C for 4 min, then 4°C on hold. These sequencing extension products were then purified using ethanol precipitation. Concisely to describe this step, 1 μl of 250 mM EDTA, 1 μl 20 mg/ml glycogen and 50 μl 100% ethanol was added into each tube. Tubes were mixed well and centrifuged at 13,300 rpm for 30 min at 4°C. The precipitated

DNA pellets were subsequently washed with 50 μl of 70% ethanol, centrifuged at 13,300 rpm for 15 min at 4°C and air-dried for 15 min at room temperature. Finally, DNA pellets were resuspended in 10 μl highly deionized (Hi-Di) formamide (Applied Biosystem) and sequenced using ABI 3100 Genetic Analyzer (Applied Biosystems).

### 2.2.6 Generation of FAT10 and mutant-FAT10 constructs

To experimentally validate the specific binding sites between FAT10 and MAD2 that has been predicted via nuclear magnetic resonance (NMR) study by our collaborator A/P Song Jianxing, WT-FAT10 and FAT10 mutant constructs (FAT-mL, FATmR, FATmLR) were generated. First, a 1006 bp FAT10 fragment was PCR amplified from genomic DNA of non-tumorous human liver tissue using Expand High Fidelity PCR System (Roche Applied Sciences, Penzberg, Germany) and primers 5`-GAGAGGATCCATGGCTCCAATGCTTCCTG-3`(forward) and 5`-TATAGCGGCCGCCCCTCCAATACAATAAGATGC-3` (reverse) in a total volume of 20μl. The conditions for PCR used are as follows: initial denaturation at 95°C for 2 min, 10 cycles of 95°C for 15 sec, 55°C for 30 sec, and 68°C for 4 min, followed by another 10 cycles of 95°C for 30 sec, 55°C for 30 sec, and 68°C for 4 min with 5 sec cycle elongation of each successive cycle, and a final elongation at 72°C for 7 min. This amplified FAT10 fragment was then gel-purified and cloned behind the CMV promoter into the *BamHI/NotI* in pCDNA3 plasmid (Invitrogen). The plasmid construct also contained ampicillin for plasmid amplification *in E.Coli* as well as Neomycin for stable cells selection. The following mutant FAT10 constructs were generated: a) mutant FAT10 at regions I (FAT-mL), b) mutant FAT10 at regions II (FAT-mR) c) double FAT10 mutant containing mutations at both regions (FAT-mLR) d) mutant FAT10 at its C-terminal double

glycine residue (FAT-Gly) from Glycine to Alanine e) mutant FAT10 at its all lysine residue in both domains (FAT-Lys) from Lysine to Arginine. The mutant FAT10-constructs (FAT-mL, FAT-mR, and FAT-mLR) were generated by fusion PCR using primers consisting the desired mutations (Figure 2.2). We would like to apologize that the exact sequence of the Mad2 interaction regions in FAT10 cannot be revealed in this thesis as we are only in the process of getting it patented.

The fusion PCR conditions are as follows: an initial denaturation at 95°C for 15 min, followed by 20 cycles of 95°C for 30 sec, 50°C for 30 sec, and 72°C for 3 min. The amplified fragments was gel-purified and similarly cloned into the pcDNA3 plasmid downstream of the CMV promoter. Sequencing of all the constructs to verify the DNA sequence's integrity was performed. This will allow us only to choose construct with only the desired mutations.

## Figure 2.2

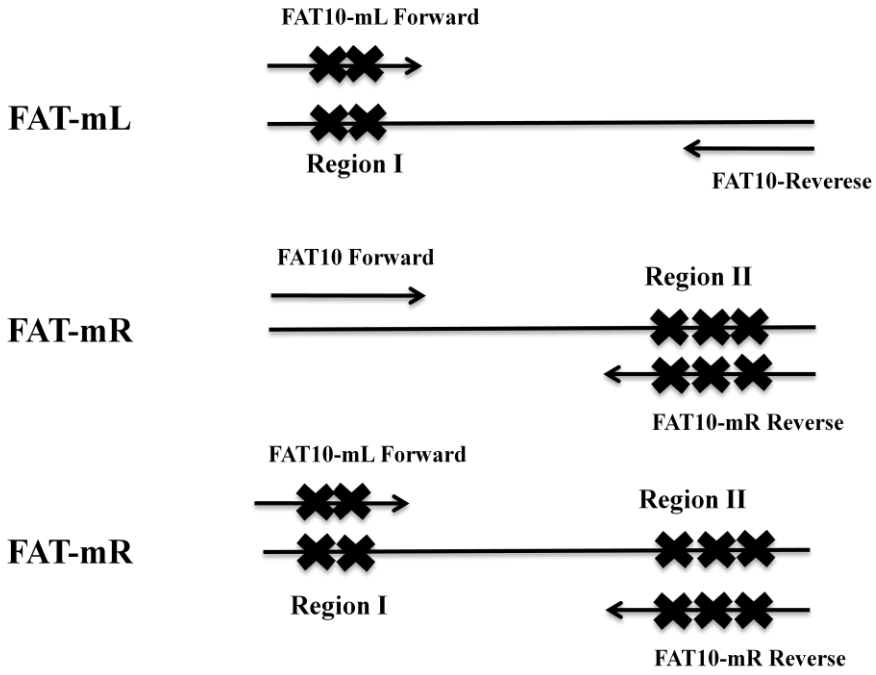


**Figure 2.2 Pictorial diagrams for generation of FAT10 mutant-contructs.** Introduction of mutations in Mad2 interaction regions within FAT10 via fusion-mutagenesis PCR method. The arrows shows the primers used to clone the FAT10 mutant-constructs (FAT-mL, FAT-mR and FAT-mLR).

## 2.3 Protein Methodology

### 2.3.1 Isolation and quantification of proteins from cells

Cells were harvested and pellet down from the cell culture flasks/plates. Cell pellets were then lysed with 100 µl of RIPA buffer (50 mM Tris HCl pH 8, 150 mM NaCl, 1% NP-40, 0.5.5 sodium Deoxycholate, 0.1% SDS) and incubated on ice for 30 min. Cells were sonicated using Bioruptor® (Diagenode Denville, NJ, USA) for 10 min at high setting with 30 sec 'on' followed by 30 sec 'off'. Cell debris was removed by centrifugation at 13,300rpm for 2 min at 4°C and cell lysates were transferred to new tubes. Protein concentrations were determined using Bradford protein assay reagent (Bio-Rad) according to the manufacturer's instructions.

### 2.3.2 Western Blotting

6 x SDS-loading dye was mixed with 60 µg of protein sample. The mixture was boiled for 10 min and subjected to gel electrophoresis on a 13% SDS poly-acrylamide gel. The separated proteins were transferred to a polyvinylidene fluoride membrane (Bio-Rad), blots were blocked for 1 hr using Amersham ECL™ membrane blocking agent (GE Healthcare Biosciences, Uppsala, Sweden). The appropriate primary antibodies (Table 2.1) were then added to the blot and incubated for 1 hr. After primary antibody incubation, blots were washed with PBST (1 x PBS + 1% Tween-20) for 15 min and then incubated for 45 min with the appropriate horseradish peroxidase-conjugated secondary antibodies (Table 2.2). Following the secondary antibodies incubation and washing steps, protein signals were detected using Amersham ECL™ Western Blotting Detection

Reagents (GE Healthcare). Finally, the membrane was exposed on a Koadak® BioMax™ MR film (Kodak Inc., Rochester, NY, USA).

### 2.3.3 Immunoprecipitation

Cells were transfected with Lipofectamine2000™ (Invitrogen) as a control or Lipofectamine2000™ carrying FAT10 gene. After 24 hr, cells were harvested and lysed using RIPA buffer. Cell debris was removed using centrifugation at 13,300rpm and the protein concentration of the protein lysate was measured and adjusted to 3 mg/ml. Immunoprecipitation was performed using the protein G-immunoprecipitation kit (Roche Applied Science, IN, USA) on 600 μg of the protein lysate with 2 μg of either of the following antibodies: p16 antibody (Santa Cruz Biotechnology, Santa Cruz, CA, USA), which served as a nonspecific rabbit IgG control; mouse monoclonal MAD2 antibody (BD Biosciences, Franklin Lakes, NJ, USA); mouse monoclonal UBA6 antibody (Sigma), mouse monoclonal HDAC6 (Santa Cruz); NUB1L goat polyclonal antibody (Santa Cruz) and rabbit FAT10 antibodies generated by our laboratory. The immunoprecipitated proteins were then subjected to gel electrophoresis in 13% SDS poly-acrylamide gel, and western blot analyses was performed as described previously using FAT10, MAD2, UBA6, NUB1L or HDAC6 antibodies.

### 2.3.4 In-situ Proximity Ligation Assay (PLA)

Cells were seeded on an 8-chamber slide (Thermo Scientific, Waltham, MA, USA). PLA (Duolink *in situ* PLA™; Olink Bioscience, Uppsala, Sweden) was carried out to detect the protein-protein interaction between FAT10, MAD2, and the other reported interaction partner of FAT10. Rabbit FAT10 antibody generated by our lab (dilution: 1:300) was incubated together with following antibodies: mouse MAD2 antibody (BD) or mouse UBA6 antibody (Sigma), or mouse

HDAC6 antibody (Santa Cruz), or mouse NUB1 antibody (Santa Cruz), or mouse p16 antibody (negative control) with a dilution of 1:100 was used. The cells were incubated overnight at 4°C with the two antibodies pair mentioned above. To visualize the bound antibody pairs, the Duolink Detection Kit HRP/NovaRED with PLA plus and minus probes for mouse and rabbit (Olink Bioscience) was used, according to the manufacturer's description. After washing, specimens were mounted with the Duolink DAPI Mounting Medium (Olink Bioscience). The PLA signals were then observed under the fluorescence microscope (Zeiss) with 200x magnification. (Figure 2.2)

### 2.4 Statistical analysis of experimental data

Data presented in this study were obtained from at least three independent experiments, unless otherwise stated. Data were presented as mean values of experimental triplicates ± standard error (SE). Data comparing differences between two groups were statistically analyzed using two-sided unpaired Student's t-test. Differences were considered significant when $p\text{-value} < 0.05$.

**Figure 2.3**

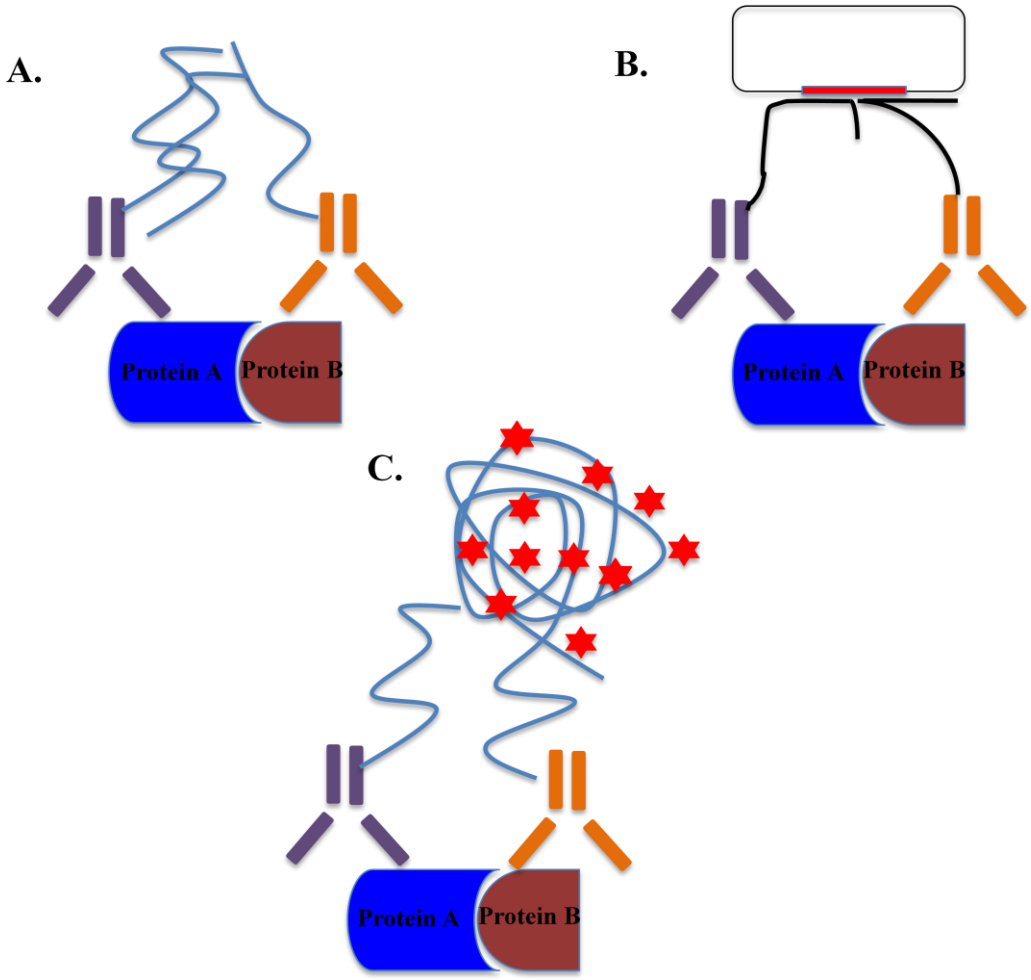


**Figure 2.3 Schematic presentation of *in situ* proximity ligation assay (PLA). A.** Dual binding by a pair of proximity probes that consist of antibodies with attached DNA strands to a target protein complex that interact with each other. **B.** The probes that come in proximity because of the specific protein-protein interaction will serve as the hybridization of circularization of oligonucleotides, which are then joined enzymatically by ligation into a circular DNA molecule. **C.** The circular DNA will then be amplified by rolling circle amplification (RCA) primed by one of the proximity probes. This will create a concatemeric RCA product that remains covalently attached to the proximity probe. Fluorophore-labeled detection primers are then hybridized to the repeated sequence of the rolling circle products, and these will creates a bright signal that could be visualized under the fluorescence microscope.

# Chapter 3 Results

## 3.1 FAT10 enhances cell proliferation of HCT116 colorectal cancer cells

Previous findings in our lab revealed that FAT10 is overexpressed in gastrointestinal cancer and colon cancer and also its ability to induce chromosomal instability (Lee et al 2003, Ren et al 2006). We used wild-type (WT) colorectal cancer HCT116 cell lines, wild type FAT10 stably overexpressing cells (FAT10), and transient knockdown of FAT10 overexpressing stable cells using FAT10siRNA (FATi) to study the malignant transformative potential of FAT10 especially in enhancing cell proliferation, as it is well-known that sustaining cell proliferation is one of the hallmarks of cancers.

In order to answer this question, I generated two stable cell lines, namely two stable cell lines overexpressing wild type FAT10 (FAT-A & FAT-B). As shown in Figure 3.1.A by Western blot as well as real-time PCR, the basal level of FAT10 is undetectable in wild type HCT116 cells and very low in FATi cells, in comparison with FAT10-overexpressing cells, which showed high expression level of FAT10. Cells expressing high levels of FAT10 showed significant enhancement in cell proliferation *in vitro*, as determined by the trypan-blue exclusion cell counting method for a period of 3 days or WST- calorimetric assay over a period of 5 days (Figure 3.1B upper panel). The cell doubling time of FAT10 overexpressing cells were also higher in comparison with the WT cells (Figure 3.1 B bottom panel). Cell proliferation rate of FATi cells was similar to wild-type HCT116 cells (WT) but significantly reduced after FAT10 expression was knocked down in FAT10 overexpressing stable cells (Figure 3.1.B upper panel). These results implicate FAT10's role in modulating cell proliferation.

## Figure 3.1

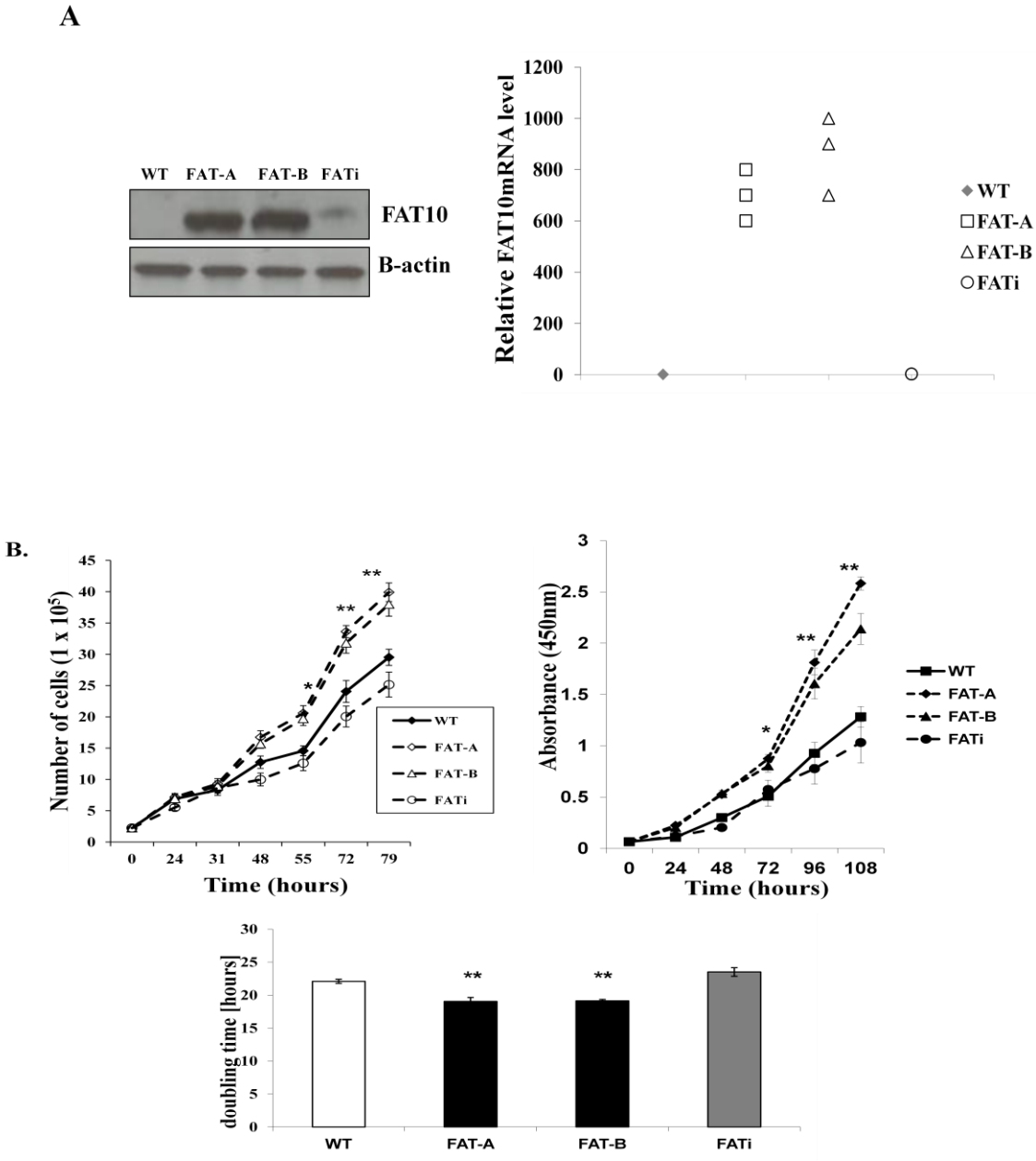


**Figure 3.1 FAT10 enhances cell proliferation. A.** Expression level of FAT10 by Western blot (left panel) and real-time PCR (right panel) in wild type (WT) HCT116, FAT10 stably overexpressing HCT116 (FAT-A, FAT-B) cells, and transient FAT10-knocked-down cells (FATi). **B.** Cell proliferation profile from WT HCT116 and the stably transfected cell lines, determined by trypan blue exclusion cell counting method (top left panel) or by WST-cell proliferation assay (top right panel). Cell doubling time is calculated as $d = \log_2/k$ where $k$ is the growth constant determined by the slope of the linearly regressed line. FAT10-overexpressing cells have significantly shorter cell doubling time compared to WT or FATi (bottom panel). Data is expressed as mean±s.e. of at least three replicates. *denotes statistical significance at *p-value*<0.05 compared with WT, **denotes statistical significance at *p-value*<0.01 compared with WT.

### 3.2 FAT10 upregulates cell proliferation marker Proliferating Cell Nuclear Antigen (PCNA)

Complementary to the proliferation assay described in Figure-3.1, bivariate-flow-cytometric analysis was used, to assess cells expression of proliferation marker, Proliferation Cell Nuclear Antigen (PCNA), which is expressed in the proliferating cells, and propidium iodide (PI) staining for the cell cycle phase. Through flow cytometry analysis using WinMdi2.9 software (Purdue University, USA), we observed that FAT10 overexpressing cells (FAT-A and FAT-B) expressed at least 1.5 times more PCNA positive cells in comparison with WT HCT116 cells (Figure 3.2 A). Western blot analysis to check the protein level of PCNA, as well as real- time PCR to analyze the transcript level of PCNA also showed the upregulation of PCNA expression in FAT10 overexpressing cells. In combination with our data from trypan blue cell counting method and WST-assay, these data together again further strengthened our hypothesis that FAT10 can significantly increase the cell proliferation of HCT116 colorectal cells.

### 3.3 FAT10 encourages anchorage-independent growth of HCT166 cells.

Since FAT10 enhance cell proliferative properties of the cells, I further investigated its impact on supporting anchorage-independent growth. Soft agar transformation assay was used to demonstrate the ability of FAT10 in encouraging the cells to form colonies. The ability of cells to form colonies in anchorage-independent condition is one of the hallmarks of transformed malignant cells. As shown in Figure 3.3, FAT10 significantly increased the colony formation of HCT116. In contrast to WT cells, which in average formed around 52±16.7 colonies of cells in soft agar, FAT10-overexpresing cells have the ability to form a

## Figure3.2

**A.**

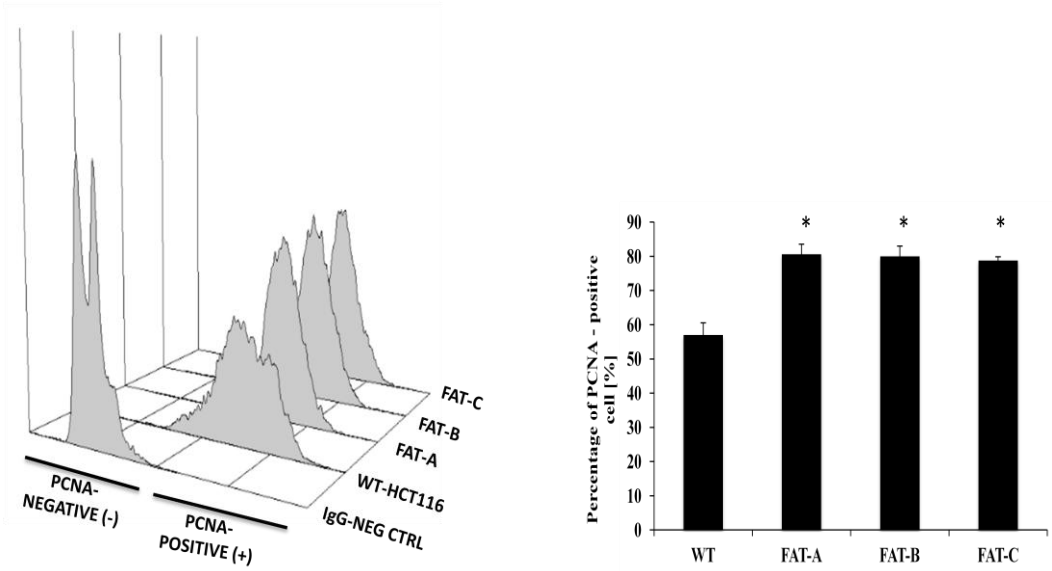


**B.**

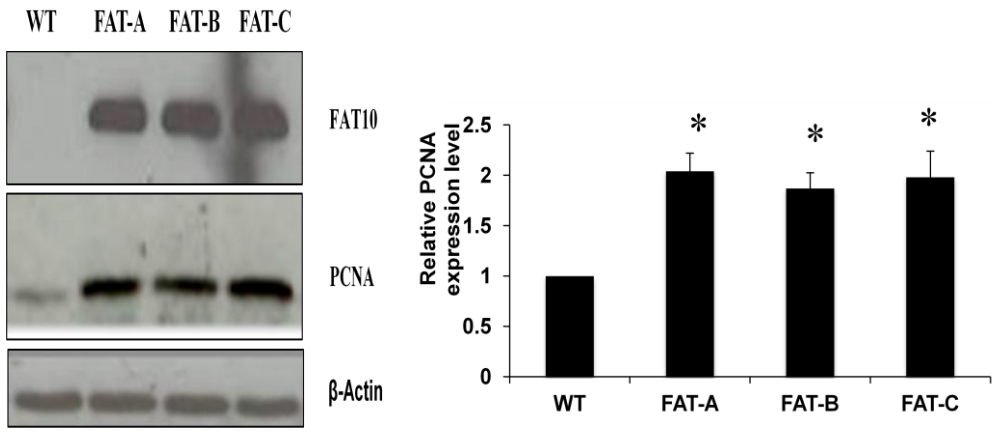


**Figure 3.2 FAT10 increases the level of cell proliferation marker PCNA. A.** Comparison of PCNA positive cells using Flow-Cytometry analysis (FACS) of WT, FAT-A, FAT-B, and FAT-C cells. Prior of the FACS analysis, these cells were stained with PCNA-FITC reagent. The histogram at the upper left represents the comparison of the PCNA-positive cells analyzed using Win.Mdi2.9 software. The graph at the bottom left showed the percentage of PCNA-positive cells based on the FACS analysis. Data is expressed as mean±standard error with at least three replicates (*$p$<0.05). **B.** FAT10 expression level validated by real-time-PCR (upper panel graph) and western blot (lower panel).

higher colonies number (273 ± 63.2 cells in FAT-A, 258 ± 43.5 cells in FAT10-B) (Figure 3.3). However, knockdown of FAT10 using siRNA attenuated the ability of FAT10 stable overexpressing cells to form colonies. An average of 63 ± 8.9 colonies of FATi cells comparable with WT cells were observed in soft agar. FAT10 increased the formation of colonies in soft agar by at least 4 fold compared to WT and FATi cells, which have a low expression of FAT10. This has further strengthened our notion that FAT10 is a potential determinant that can drive the malignant transformation of cancer cells.

### 3.4 FAT10 promotes cellular transformation of non-tumorigenic NeHepLxHT cells

Not only can FAT10 support anchorage-independent growth of HCT116 cells, but it is also able to drive the transformation of non-tumorigenic human neo-natal hepatocytes (NeHepLxHT). Recombinant FAT10 adenovirus were generated and NeHepLxHT cells were infected with the adenovirus-carrying vector control (AdCtrl) or adenovirus overexpressing FAT10 (AdFAT10) under the optimal MOI as shown in Figure 2.1. Only NeHepLxHT cells infected with AdFAT10 were able to form colonies in soft agar (Figure 3.4). An average of ~ 14.5 ±1.66 colonies were observed in NeHepLxHT cells overexpressing FAT10, while no colonies were observed in wild type NeHepLxHT cells and NeHepLxHT cells infected with adenovirus vector control (AdCtrl). The ability of FAT10 infected NeHepLxHT cells to survive under anchorage-independent conditions is one of the evidence that FAT10 can promote the transformation of “normal” cells to become malignant cells.

**Figure 3.3**

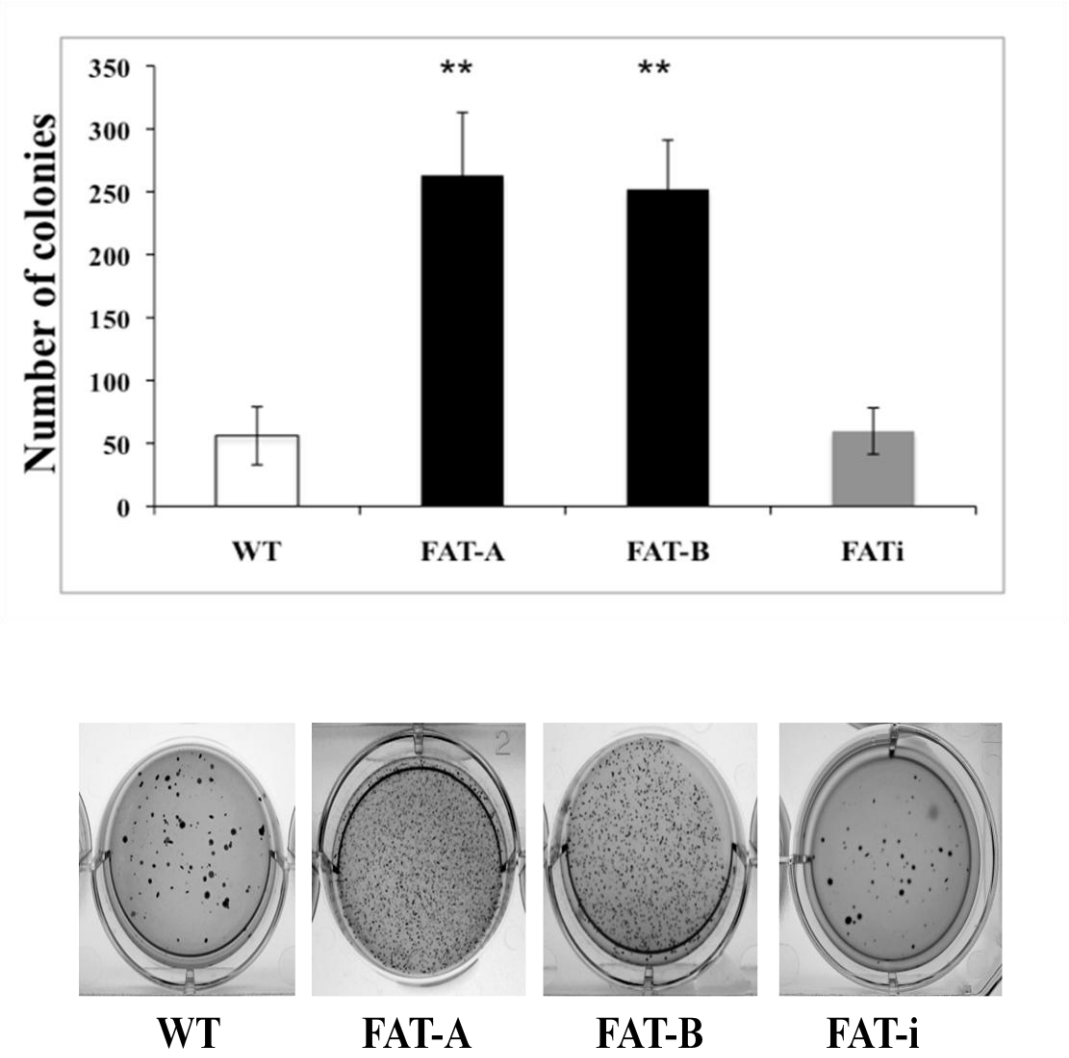


**Figure 3.3 FAT10 supports anchorage-independent growth.** Anchorange-independent growth and colony formation were assessed by growing WT and the stable cell lines in soft agar as described in Material and Methods. 5000 cells were seeded into each well. Cells were grown for 3 weeks at 37°C in 5% humidified $CO_2$ incubator. After 3 weeks soft agar were stained and colony number was quantified. The HCT116 colonies were photographed at 20x magnification (bottom panel). A significant result of FAT10-overexpressing cells exhibit the ability to survive and growth under anchorage-independent condition compared to WT and FATi cells. Data is expressed as mean$\pm$standard error with at least three replicates. ** denotes p-value$< 0.01$.

## Figure 3.4

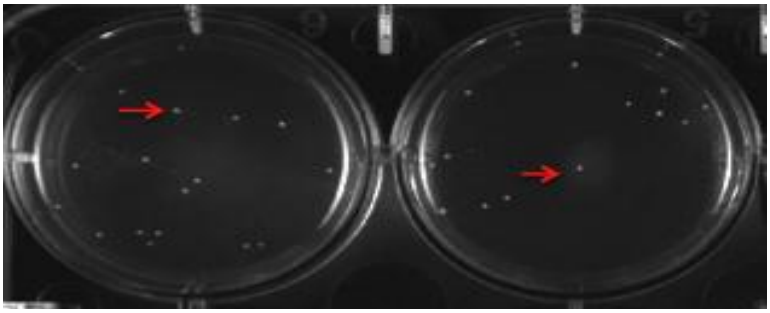

**AdFAT10**

**Ad Ctrl**

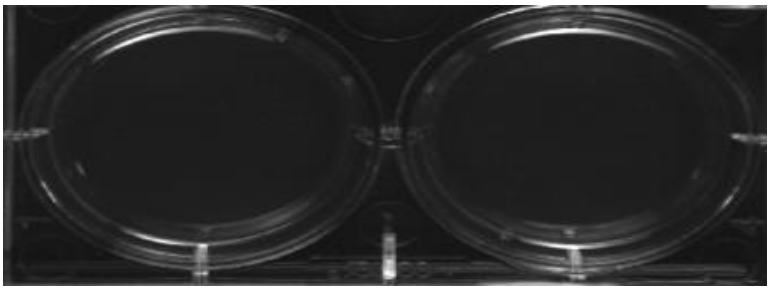

**WT**

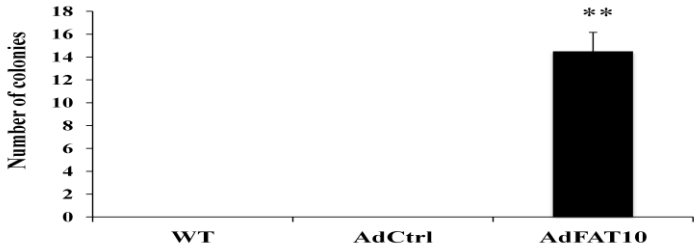


**Figure 3.4 FAT10 promotes cellular transformation of non-tumorigenic hepatocytes (NeHepLxHT)**. As shown in the pictures above only NeHepLxHT cells infected with AdFAT10 are able to form colonies (red arrows indicates the formation of colonies). In average approximately 14.5 ±1.66 colonies were formed (lower panel). Cells were incubated for 4 weeks at 37°C, pictures were taken under microscope with 20x magnification and colonies were then quantified. Results were taken from 3 biological repeats. ** denotes p-value < 0.01. 100.000 cells were plated into each well.

### 3.5 FAT10 protects cells from cytotoxic induced cell death

One of the other hallmarks of cancer is the ability of cells to resist cell death. To demonstrate the ability of FAT10 in protecting the cells from apoptosis, WT HCT116 cells as well as FAT10 and FATi cells were treated with Camptothecin. Camptothecin is a cytotoxic agent that inhibits DNA replication. Cells were treated with 20 μM of Camptothecin for 24 hr. Cells were then harvested and stained with PE-Annexin V followed by flow cytometry analysis. Morphologic features, including the loss of plasma membrane attachment and asymmetry, were used to characterize apoptotic process. In apoptotic cells, the membrane phospholipid phosphatidylserine (PS) is translocated from the inner to the outer site of plasma membrane, therefore exposing its PS to the external cellular environment. Annexin V has a high affinity for PS and binds to cells with exposed PS. Thus, Annexin V-positive cells indicate that the cells are undergoing apoptosis.

PE-Annexin V staining showed that FAT10-overexpression in HCT116 cells conferred protective effect against camptothecin-induced cell death, where the population of apoptotic cells in FAT10 overexpressing cells is approximately around 7.55 $\pm$ 0.6% for FAT-A and 5.59 $\pm$ 0.8% for FAT-B versus 20.46 $\pm$ 1.2% for WT. Similar rate in apoptotic cells population was observed in FATi cells (21.61 $\pm$ 0.4%) compared to WT, when FAT10 expression was inhibited (Figure 3.5A, B). Similarly, using trypan blue cell counting method, where dead cells that were stained with trypan blue dye were counted using haemocytometer (Figure 3.5C). Similar results were observed with PE Annexin V staining, whereby FAT10 protected the cells from cytotoxic induced cell death. These observations indicate that FAT10 overexpression not only enhances cell proliferation but it could also facilitate cells resistance against cell death.

## Figure 3.5

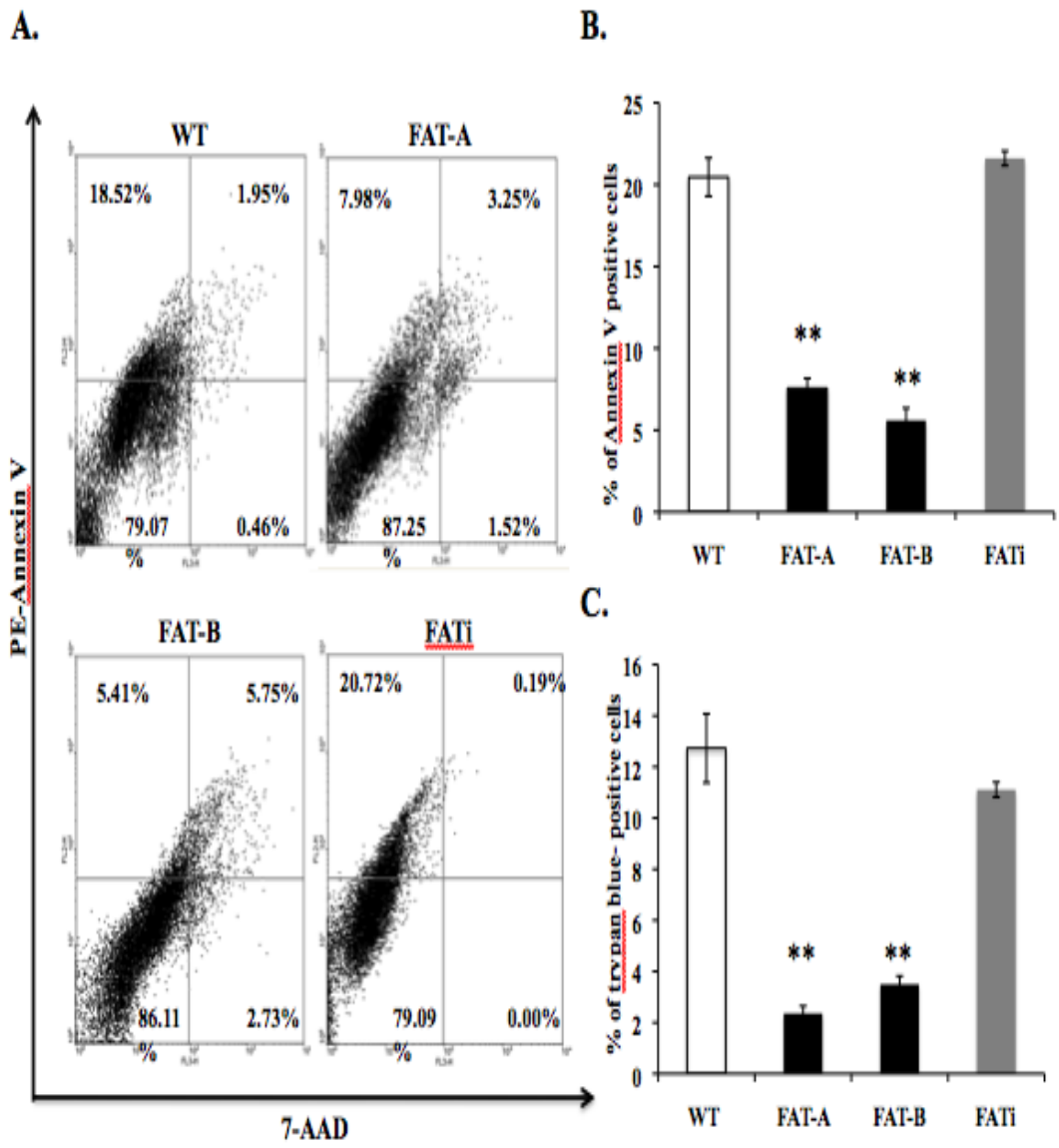


**Figure 3.5 FAT10 protects cells from cytotoxic induced cell death.** Cells were treated with cytotoxic agent 20μM Camptothecin for 24 hr **A.** Shown are staining profiles of a representative set of experiments. The apoptotic cells are depicted in the upper left quadrant (Annexin V positive, 7-AAD negative). **B.** Apoptosis profiles of WT, FAT10 overexpressing, and FATi HCT116 cells determined using PE-Annexin V and 7-AAD staining, followed by flow cytometry detection and analysis. Shown are the percentages of apoptotic cells distribution described in B from 3 independent biological repeats. **C.** Shown are the percentages of dead cells (trypan blue positive cells) from 3 independent experiments in WT, FAT10 overexpressing, and FATi HCT116 cells. Error bars shows SE (Standard error) from 3 different experiments. ** denotes p-value < 0.01.

### 3.6 FAT10 increases HCT116 cells invasiveness

Beside increasing cell proliferation, malignant transformation of cells, and resistance of cell death, the ability of FAT10 to affect cells malignancy, such as the gain of invasive capabilities was also observed. The role of FAT10 in enhancing the invasiveness of HCT116 cells was examined using plates carrying Transwell® inserts, which comprised cell permeable membrane. In order to mimic the presence of tumor cells microenvironment *in vivo*, Transwell® inserts were coated with matrigel. This matrigel will serve as an extracellular matrix, which are normally presents in tumor cells microenvironment and are degraded during invasion process by the tumor cells. By seeding the cells on top of the insert, which has been coated with collagen, plus an additional chemo-attractant (FBS) at the bottom of the inserts, the invasive features of the cells can be determined by staining and counting those cells that have transversed the cell permeable membrane towards the higher concentration of chemo attractant. This assay revealed that FAT10 overexpression significantly augmented the pro-invasive function of FAT10 across the collagen-coated wells by at least 5 fold in comparison with WT HCT116 cells that have a low level of FAT10. (Figure 3.6A).

The dynamic of actin-cytoskeletal remodelling and the formation of protrusive structures in FAT10 overexpressing- and WT HCT116 cells, which are required during the invasion process, were also examined. Rhodamine-phalloidin staining was used to examine the actin cytoskeleton. Phalloidin is one of a group of toxins from death cap (*Amanita phalloides*) and binds specifically to F-actin. As shown in Figure 3.6B, immunofluorescence revealed that FAT10 overexpressing cells displayed more intense F-actin staining than WT cells. Further, FAT10

overexpressing cells also exhibited prominent lamellopodia-migratory structures, which are observed in Figure 3.6B as broad extension from plasma membrane. Taken together, all these data show the role of FAT10 in driving the invasiveness of tumor cells during tumorigenesis.

**3.7 FAT10 promotes cell migration and adhesion**

Other important attributes of malignant cells are its ability to migrate as well as to adhere to extracellular matrix. Therefore, using scratch-wound healing assay, we examined the ability of FAT10 overexpressing cells and WT cells to migrate. This simple and reproducible assay is commonly used to measure the cell migration capability of cells. Cells were grown to confluence and "wound" were introduced by scratching the cells with a pipette tip. Through this assay we could show the directional migratory response of the cells. As shown in Figure 3.7A, 15 hr after the scratching, FAT10 overexpressing cells (FAT-A and FAT-B) can migrate faster in compared to WT cells.

Another central feature of invasion and metastasis is cell adhesion. Figure 3.6B showed that a greater number of adherent cells in FAT10 overexpression cells in comparison with WT cells. This indicated that FAT10 promoted cell adhesion. Moreover, enzyme-linked immunosorbent assay (ELISA) showed an increased in matrix metalloproteinase 9 (MMP-9) concentration by at least 4 fold in FAT10 overexpressing cells. MMP-9 is known for its ability to degrade type IV collagen that is present in the basal membrane. Higher concentration of MMP-9 in FAT10 overexpressing cells facilitated the degradation of the components of the ECM with a higher efficiency, which again showed that FAT10 overexpression could drive these colorectal HCT116 cells to be more invasive (Figure 3.7 C).

## Figure 3.6

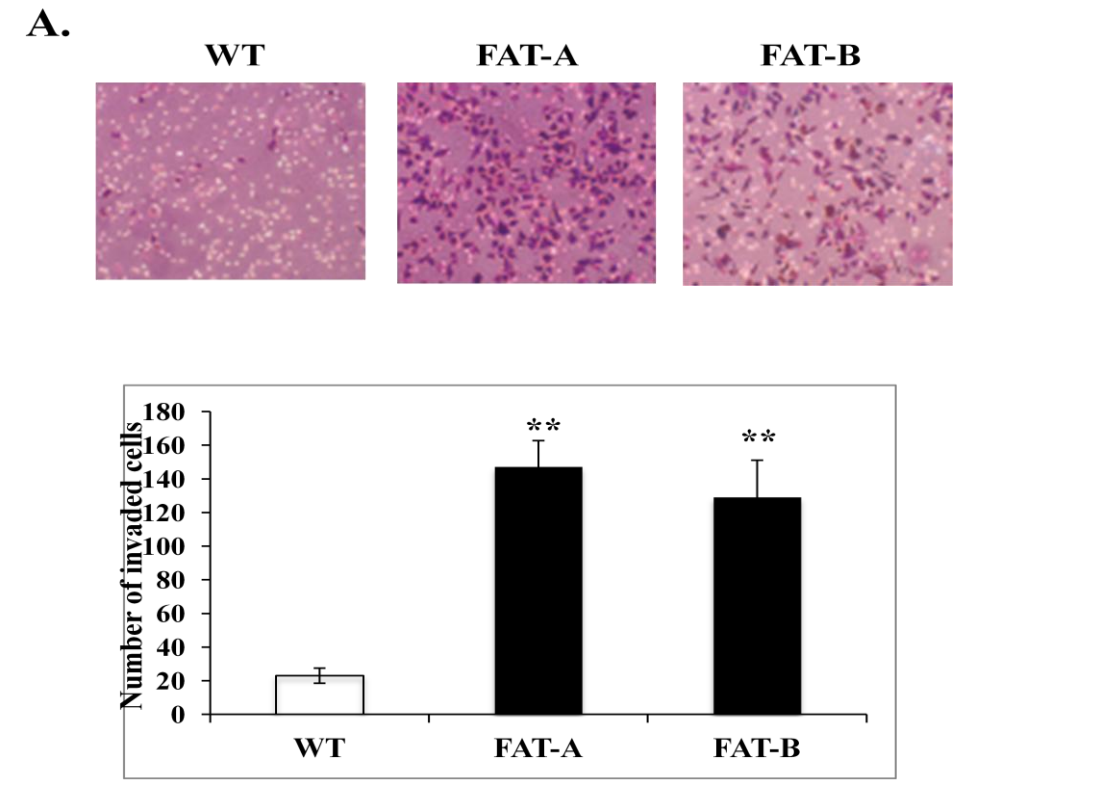


**Figure 3.6 FAT10 promotes cell invasion. A.** Invasion profiles of WT HCT116 and FAT10 stably overexpressing cells. Cells were assayed for invasion using Transwell® inserts coated matrigel for 16 hours, after which the invaded cells were stained and quantified. FAT10 overexpression in HCT116 significantly increased cell invasion compared to WT cells. Representative pictures of the invaded cells are shown below the graphs. The data shown is representative of 3 biological repeats. **B.** Rhodamine-Phalloidin staining to show actin cytoskeleton profiles of cells. The cells were seeded on poly-L-lysine-coated 6-well plate, allowed to adhere for 24 hours and stained with rhodamine-conjugated phalloidin to visualize filamentous actin. Pictures display a representative set of experiments (X 400). Scale bar represents 20µm. * $P < 0.05$, ** $P < 0.01$, *** $P < 0.001$.

**Figure 3.7**

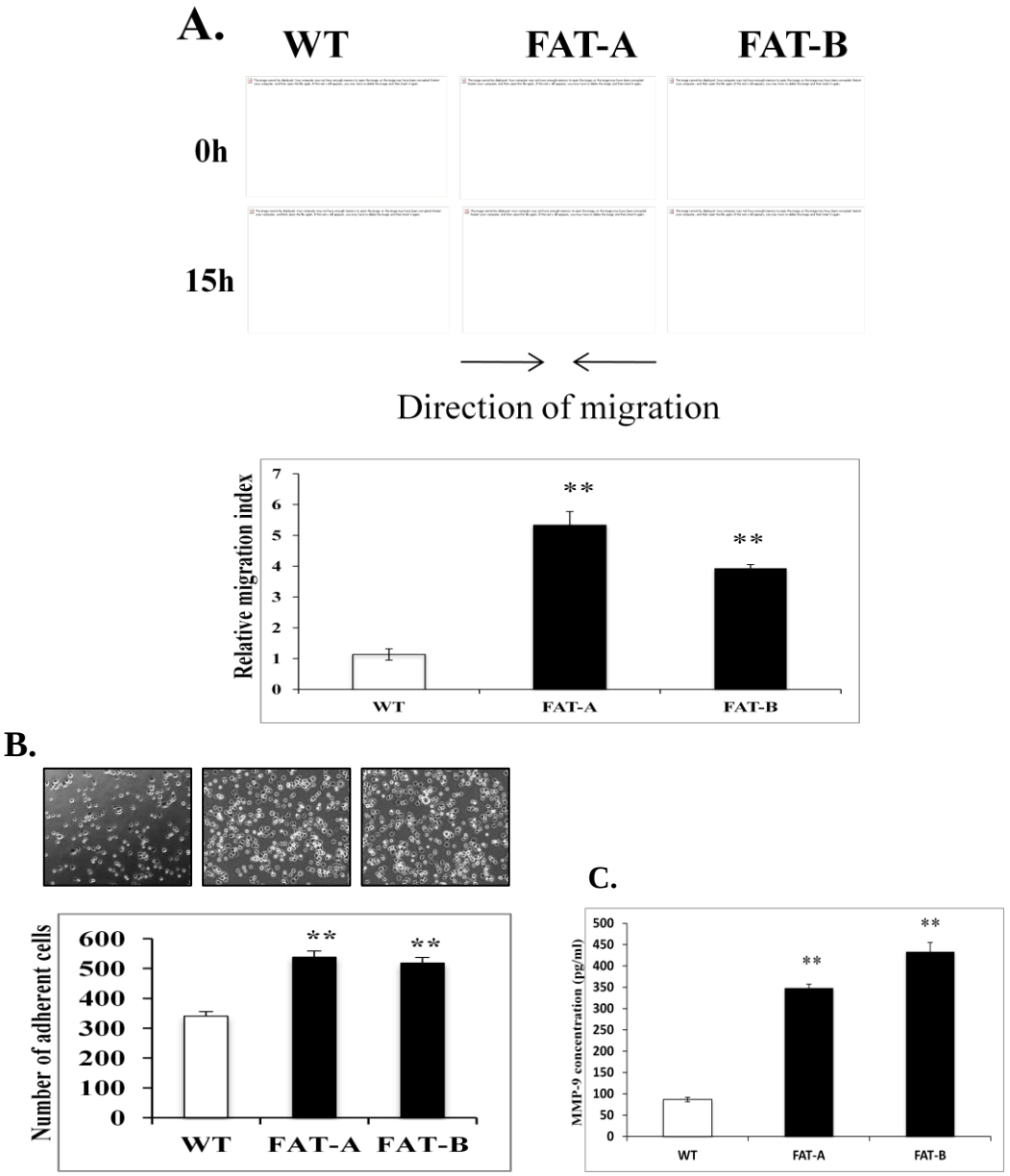


**Figure 3.7 FAT10 supports cell invasion, migration and adhesion. A.** Cell migration of HCT116 assessed by scratch-wound healing assay. Confluent HCT116 cell monolayers were scratched and monitored for 15 hours. The direction of cell migration is showed by the arrows. The furthest distance from HCT116 cells migrated from the edge of scratch was measured in 5 random fields (X200), an inverse correlation of the distance of gap and migration was performed. The graphs show the migration index relative to WT, based on 3 independent experiments. Representative pictures of the invaded cells are shown above the graphs. **B.** Profiles of the adhesive properties of WT HCT116 and FAT10 overexpressing cells (FAT-A and FAT-B). Cells were seeded in collagen IV-coated wells and allowed to adhere for 2 hours, after which adhered cells were quantified in 5 random fields (X200). Graph shows the mean and standard error (SE) of the number of adhered cells. Graph showing a significant higher number of adherent cells in FAT10 stable overexpressing HCT116 cells adhered to collagen. The data shown is representative of 3 experiments. **C.** MMP-9 concentration measured by ELISA from WT and FAT10 overexpressing cells. FAT10 drives a significantly higher concentration of MMP-9.

### 3.8 FAT10 supports tumor growth in nude mice

It is important to address whether the oncogenic properties of FAT10 can also be recapitulated *in vivo*. To address this question, WT and FAT10 overexpressing cells were subcutaneously injected into the left and right flanks of nude mice, respectively. Here, for the first time we were able to show that subcutaneous injection of FAT10 overexpressing HCT116 cells promoted tumor growth as shown by a bigger tumor size in Figure 3.8A. A quantitative measurement of tumor weight after 3 weeks of injection as well as progressive measurement of tumor size was performed using an analytical precision balance and digital caliper, respectively. As shown in the graph in Figure 3.8B, C, mice injected with FAT10 overexpressing cells has a heavier tumor weight as well as a bigger tumor size in comparison with WT HCT116 cells. Collectively, these *in vitro* and *in vivo* results revealed the important role of FAT10 as a determinant of malignancy in colorectal cancer.

## Figure 3.8

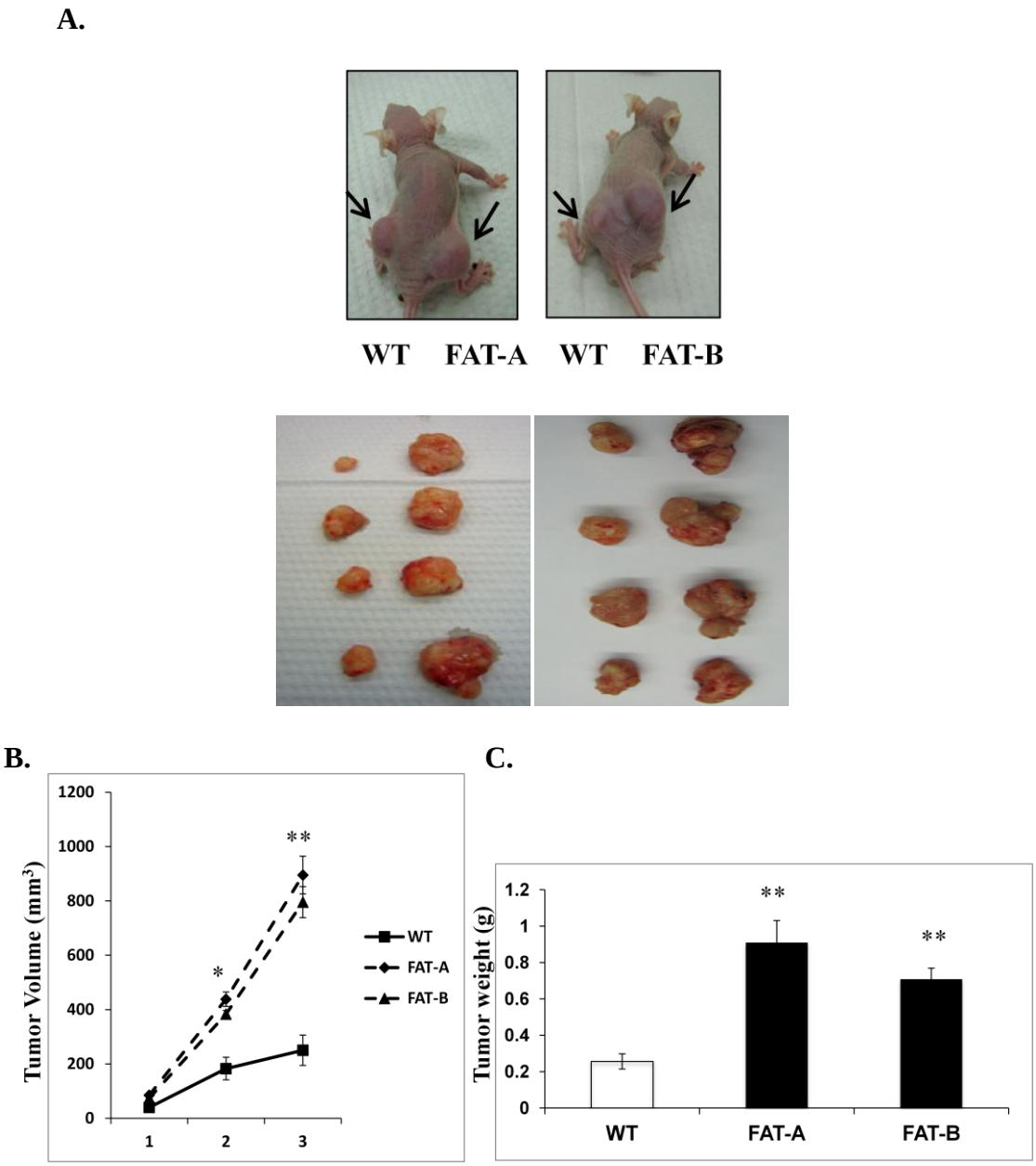


**Figure 3.8 FAT10 supports tumor growth in nude mice. A.** WT and FAT10 stably overexpressing cells were subcutaneously injected into the right and left flank of at least 6 nude mice (n=6), respectively. 3 weeks after the injection, mice were sacrificed and tumors were isolated. FAT10 overexpression in HCT116 significantly increased the tumor growth in compare to WT. **B.** Measurement of tumor weight from each group of injected cells. (n=6 in each group). Data is expressed as mean±s.e. *$p$<0.05; **$p$<0.01. **C.** Tumor size measured every week with digital caliper (n=6 in each group). Tumor volume was calculated using the formula 0.5 x a x $b^2$, where a and b are the largest and smallest diameters, respectively.

## 3.9 Identification of specific binding sites responsible for FAT10 and Mad2 interaction

### 3.9.1 Identification of the specific Mad2 binding sites on FAT10 using Nuclear Magnetic Resonance (NMR)

Our collaborator, A/P Song Jianxing employed a Nuclear Magnetic Resonance (NMR) study to map Mad2 interacting sites on FAT10 upon its binding with Mad2. The specific interaction between FAT10 and Mad2 was identified based on analyzing the $^{1}H$-$^{15}N$-HSQC (Heteronuclear single quantum coherence) spectra. An HSQC spectrum is like a "fingerprint" of the protein because each peak is associated to an NH group of each amino acid residue. The chemical shift in both nitrogen (15N) and proton (1H) is sensitive to the chemical environment of the two nuclei. Examination of the HSQC spectra of $^{15}N$-labelled FAT10 alone, will give a spectra of FAT10 without Mad2. The HSQC spectra were then obtained again but now upon addition of Mad2. Addition of Mad2 into $^{15}N$-labeled FAT10 resulted in a chemical shift in HSQC spectrum, which can be observed by a change in the peaks observed in HSQC spectrum. Since every peak corresponded to an amino acid in FAT10 protein, it is thus possible to specifically map out the specific Mad2 interaction regions within FAT10. Mad2 was found to bind at two specific regions in domain 1 of FAT10 protein. We would like to apologize that the exact sequence of the Mad2 interaction regions in FAT10 cannot be revealed in this thesis as we are only in the process of getting it patented.

Based on the result from this NMR study, we then performed mutagenesis study of the predicted specific regions were mutated using fusion-PCR mutagenesis method. We created five different FAT10 mutants as follows (Figure 2.2): the first mutant (FAT-mutant-Left/FAT-mL) consists mutations at region I of

Mad2 interaction regions within FAT10 The second mutant (FAT-mutant-Right/FAT-mR) consists of mutations at region II of Mad2 interaction regions within FAT10. The third mutant is a combination of mutations from FAT-mL and FAT-mR, whereby we mutated all the NMR-predicted amino residues that are important for Mad2 binding on FAT10. We named this mutant FAT-mutant-Left-Right/FAT-mLR. The fourth mutant is FAT-Lys, where we mutated the entire Lysine residue of FAT10 from Lysine (K) to Arginine (R), which might be important for poly-FATylation. Finally, the fifth mutant is FAT-Gly with mutated double-glycine residue at C-terminal of FAT10 protein that is important for FAT10-covalent conjugation with its substrates.

### 3.9.2 Generation of FAT10 and FAT10 stable mutants

FAT10 and FAT10 stable mutants were generated by transfection of pcDNA3 plasmid carrying wild type FAT10 or FAT10 mutants (FAT-mL, FAT-mR, FAT-mLR, FAT-Lys, and FAT-Gly) and selected with G418 as described in chapter 2.1.2. Here, we show that wild type FAT10 as wells as its mutant derivatives are indeed stably expressed to comparable levels at the protein level (Figure 3.9). Western blot analysis from the whole cell lysate of these stable cell lines were run through SDS-PAGE gels and detected using FAT10 specific antibody. These mutants were generated to validate the FAT10-Mad2 interaction site, identified through NMR as well as to address the functional significance of these sites.

**Figure 3.9**

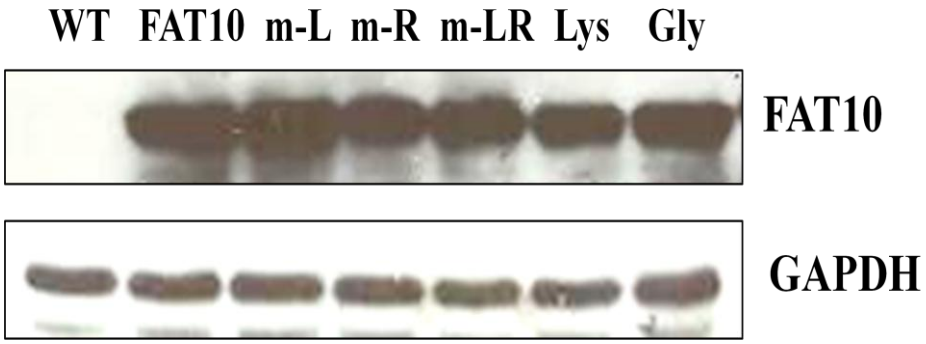


**Figure 3.9 FAT10 protein expressions in FAT10 stable clones and its mutant derivates.** Western blot analysis from the whole cell lysate of the FAT10 stable and FAT10 mutants cells (FAT-mL, FAT-mR, FAT-mLR, FAT-Lys, and FAT-Gly). Western blot shows that we successfully generated a stable cell lines that overexpressed wild type FAT10 or FAT10 mutants.

### 3.9.3 Identification of the specific Mad2 binding sites on FAT10 using co-Immunoprecipitation method

Using all the generated FAT10 mutant stable clones that have been mentioned above, we then performed co-immunoprecipitation experiment to validate, which Mad2 interaction regions within FAT10 is important for FAT10-Mad2 binding. As shown in Figure 3.10, we found that only FAT-m-LR abolished the binding between FAT10 and Mad2, whereas FAT-mL and FAT-mR did not abolish the binding between FAT10 and Mad2. To address whether these sites bind specifically to Mad2 and not other interacting proteins of FAT10, co-Immunoprecipitation was also performed with other reported interaction proteins of FAT10 using WT, FAT10-overexpressing cells and its stable mutants. SDS-PAGE-Western blotting was performed and blots were probed with various antibodies listed in table 2.1 (Mad2, p62, NUB1L, UBA6, and HDAC6).

## Figure 3.10

**A.**

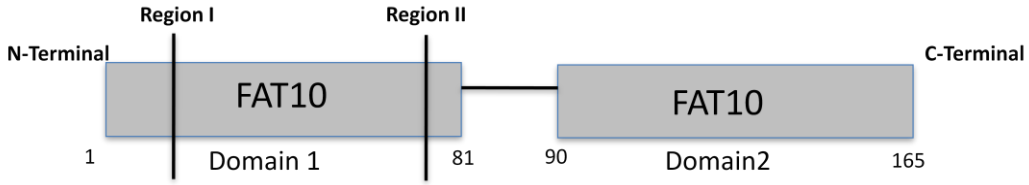


**B.**

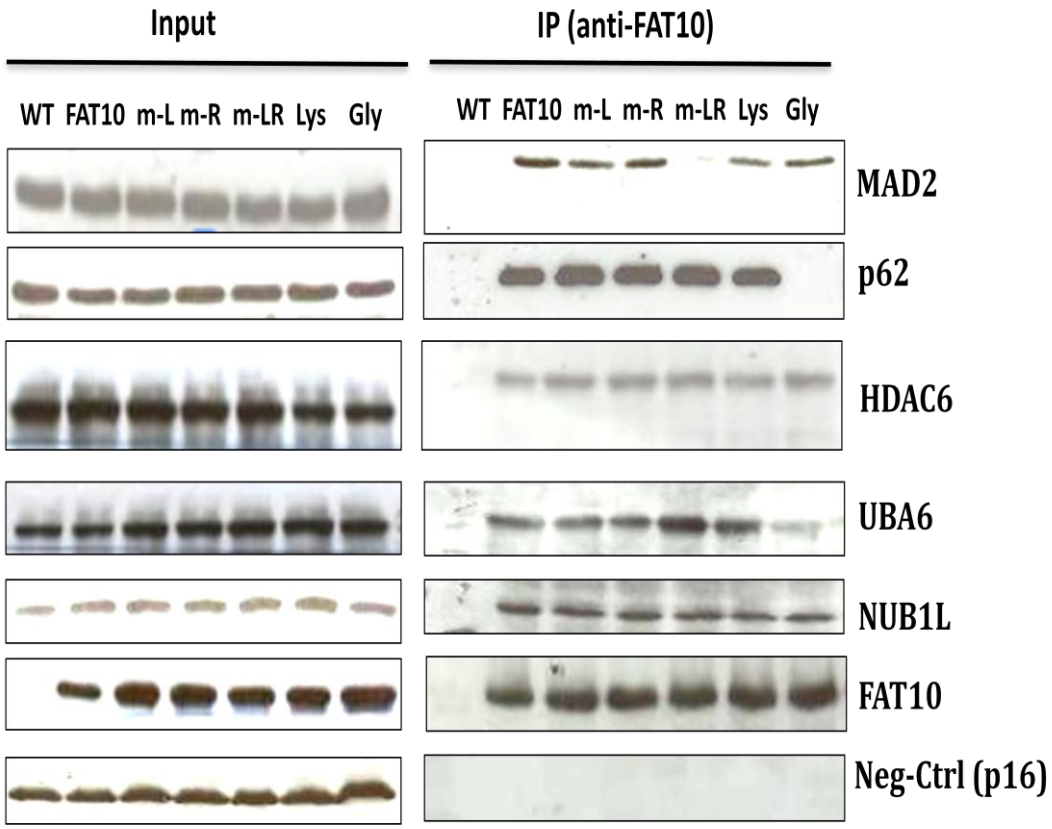


**Figure 3.10 Abolishment of Mad2 binding on FAT10 observed in FAT-mLR**
**A.** Pictorial diagram of mutations generated in FAT10 protein, which are important for the binding with Mad2. **B.** Co-IP-Western blot analysis of interactions between FAT10, Mad2, p62, NUB1L, UBA6, and HDAC6. Mad2, p62, NUB1L, UBA6, and HDAC6 are proteins that have been reported to have an interaction with FAT10. HCT116 cells were transfected with pcDNA3 plasmid carrying FAT10, FAT10 mutants (FAT-mL, FAT-mR, and FAT-mLR), FAT10 Lysine mutant (FAT-Lys), or FAT10 Glysine mutant (FAT-Gly). Total cell lysates of WT, FAT10 overexpressing, and FAT10 mutants (FAT-mL, FAT-mR, FAT-mLR, FAT-Lys, FAT-Gly) were treated with RNase-A and incubated with anti-FAT10 antibody conjugated to agarose beads. The immunoprecipitates were analyzed by SDS-PAGE-Western blotting method and probed with the specific antibodies (MAD2, NUB1L, p62, UBA6, HDAC6). p16 served as loading control and nonspecific control.

We selected to perform the co-IP with these antibodies, because these proteins have been previously reported to interact with FAT10 (Table1.3). Indeed, we found that FAT-mLR was specific only for Mad2 and FAT10 binding as abolishment of these sites did not affect the binding of FAT10 with its other interaction partners like UBA6 (FAT10-E1 activating enzyme), NUB1L, p62, and HDAC6 (Figure 3.10B). On the other hand, FAT-Gly mutant is unable to bind to UBA6 and p62, because these proteins bind covalently to FAT10 through the glycine residue (Aichem et al 2012b, Pelzer and Groettrup 2010). Other non-covalently conjugated interaction partners like HDAC6, and NUB1L were also not affected by the mutation at these FAT10`s residues (Kalveram et al 2008, Schmidtke et al 2006). We used p16 as a loading and random control.

### 3.9.4 Identification of disruption of FAT10 and MAD2 binding using *in situ* Proximity Ligation Assay (PLA) method

To strengthen our previous results from co-IP, we used another method to detect protein-protein interaction between FAT10 and Mad2 as well as other FAT10's interaction partners. This method is called *in situ* proximity ligation assay (PLA). Using *in situ* PLA allowed us to detect protein-protein interaction directly from the cells; therefore it is less tedious than using co-Immunoprecipitation. One can also visualize the interaction at single cell level.

In concordance with co-Immunoprecipitation results mentioned in the previous section, *in situ* PLA also demonstrated that the mutated amino acid residues in FAT-mLR cells was the specific site for FAT10 and Mad2 binding and not for the other reported FAT10 interaction partners (Figure 3.11). Disruption of these binding sites abolished the binding of Mad2 on FAT10 only. As negative control, we used p16 plus FAT10 antibodies to probe the FAT10 overexpressing

HCT116 cells. As mentioned above, to validate the specificity of this PLA assay, we probed the FAT10 overexpressing cells with only one antibody (FAT10 or Mad2 antibody) or no antibody. This validation allowed us to ascertain that PLA's results were reliable, because PLA signal was only observed, when two proteins interacted with each other, otherwise no signal were detected. In this experiment, WT-HCT116 cells, wild type FAT10 overexpressing cells, as well as various FAT10 mutant cells (FAT-mL, FAT-mR, FAT-mLR, FAT-Lys, and FAT-Gly) were used. To test that these amino acid residues were the specific regions that were responsible for FAT10 and Mad2 binding, interaction between FAT10 with its other protein interaction partners such as HDAC6, p62, NUB1L, and UBA6 were also investigated. Collectively, based on two different experiments with two different methods (co-Immunoprecipitation and *in situ* PLA), we demonstrated that only FAT-mLR abolished FAT10 and Mad2 binding. In summary, our results demonstrated the specific binding regions of Mad2 on FAT10. These regions only prevented the binding of FAT10 to Mad2 but not to other proteins reported to interact with FAT10. Hence, altering these amino acid residues of FAT10 is unlikely to alter other cellular functions of FAT10.

## Figure 3.11

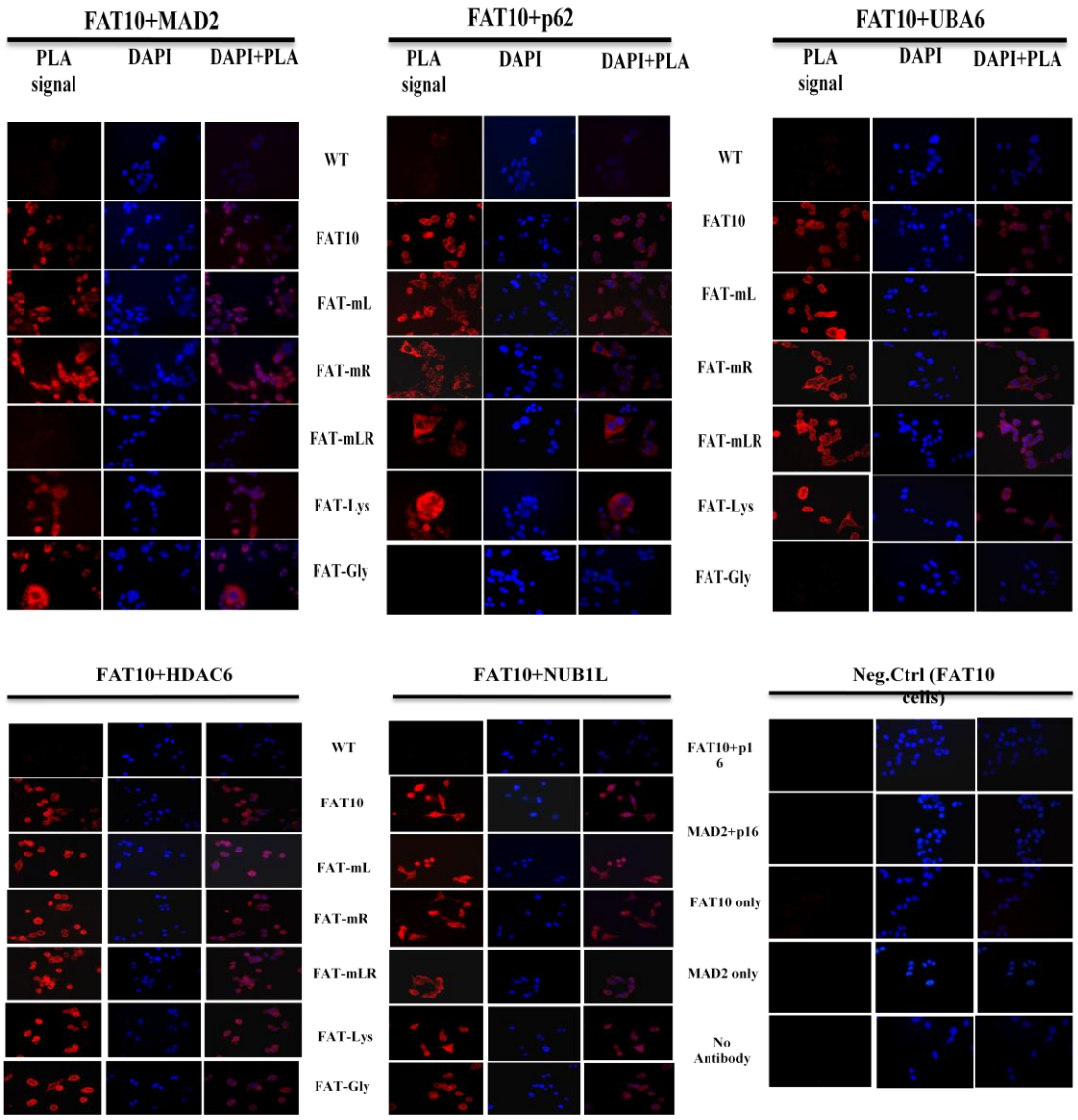


**Figure 3.11 *In situ* PLA results showing Mad2 binding on FAT10 was abolished in FAT-mLR mutants**. *In-situ*-PLA analysis of WT, FAT10 overexpressing, and its derivatives mutants HCT116 cells (FAT-mL, FAT-mR, FAT-mLR, FAT-Lys, and FAT-Gly). Red fluorescence signals represent an interaction detected by the assay (positive PLA signal) targeted by two primary antibodies. In this assay, interaction of FAT10 with 5 different proteins (MAD2, p62, UBA6, HDAC6, and NUB1L) was analyzed. All cells were counterstained with DAPI to visualize nuclei of the cells. As negative control (bottom right panel), FAT10 and p16 antibody were used, because FAT10 did not interact with p16. In addition, a single antibody (FAT10/MAD2 only) was used to check the specificity of PLA. No Antibody refers to control assay, where cells where incubated with only secondary antibodies.

### 3.10 Specific mutations of FAT10 and MAD2 binding sites attenuate cell proliferation of HCT116 cells

Having identified the specific binding regions between FAT10 and Mad2, which plays an important role in aneuploidy and tumorigenesis, we would also like to know whether disruption of these binding regions would affect the cellular function of the cells such as its cell proliferation. Therefore, we measured the cell proliferation rate of WT, two FAT10 overexpressing stable clones, FATi stable clone, FAT-mL, FAT-mR, and two FAT-mLR stable clones using WST-1 cell proliferation assay. Interestingly, we found that FAT-mLR mutants have significantly lower cell proliferation rate by at least 3 fold in comparison with FAT10 overxpressing stable clones and by at least 1.5 fold in compare with WT HCT116 cells (Figure 3.12A). In addition, as shown in Figure 3.12B, FAT-mLR-A (27.05±0.31h) and FAT-mLR-B (26.03±0.40h) have a longer cell doubling time in compare with FAT10 overexpressing cells (FAT-A: 19.83±0.26h, FAT-B: 19.31±0.21h) or WT HCT116 cells (23.42±0.25h). The cell proliferation rate and doubling time of FAT-mLR mutants is almost similar with FAT10 knockdown stable cells (FATi). Therefore, it shows that the disruption of FAT10 and MAD2 binding abated the cell proliferation of colorectal cancer cells HCT116.

### 3.11 Disruption of binding between FAT10 and Mad2 curtailed the anchorage-independent growth of HCT116 cells

Since FAT-mLR mutants could slow down the cell proliferation, we also further investigated the effect of these mutants in supporting anchorage-independent growth in soft agar. Previously, we demonstrated that FAT10 augmented the anchorage-independent growth of colorectal cancer HCT116 cells (Figure 3.3).

## Figure 3.12

**A.**

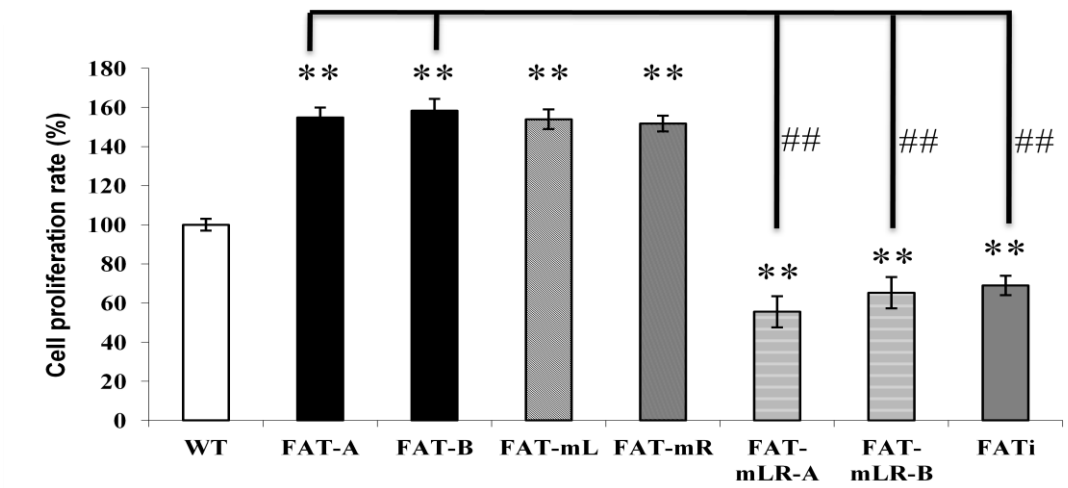


**B.**

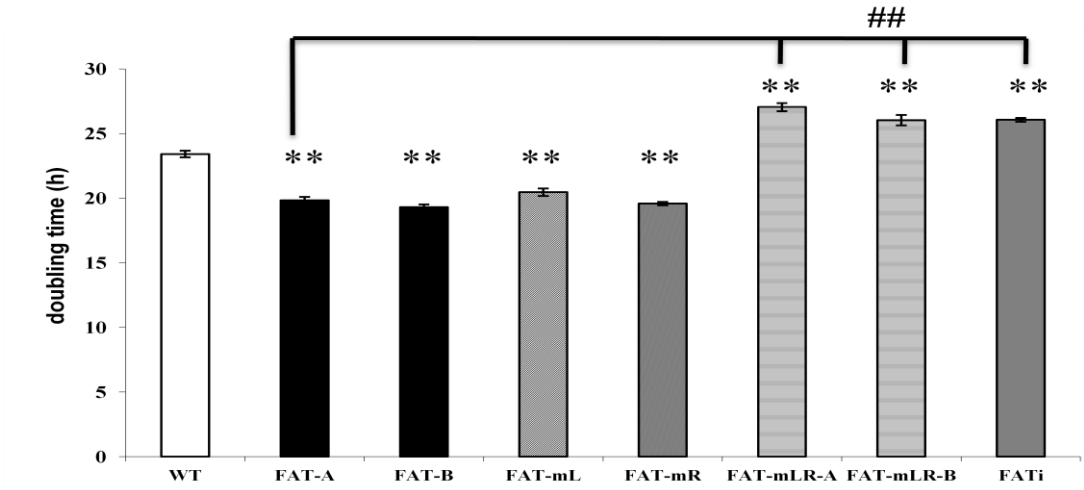


**Figure 3.12 Disruption of FAT10 and MAD2 binding sites via mutations of its binding sites decreased cell proliferation of HCT116 cells**. **A.** Cell proliferation rate of WT, FAT10 overexpressing stable cells (FAT-A, FAT-B), FAT10 mutants (FAT-mL, FAT-mR, and FAT-mLR) and FAT10 stable knockdown cells (FATi). Cells were grown in 96-well plate for 108 hours and cell proliferation was measured using calorimetric WST-1 assay every 24 hours. **B.** Doubling time of WT, FAT10 overexpressing cells, and its mutant derivates. Doubling time is calculated using this following formula (doubling time = $(\ln(2)/ \ln(C_t/C_0))*t$). Data is represented as mean±s.e. from 3 biological repeats. **denotes statistical significance *p-value* <0.01 compared with WT. ## denotes statistical significance at *p-value*<0.01 compared with FAT10 overexpressing cells.

Therefore, we then further investigated, whether the disruption of FAT10 and Mad2 binding regions has an effect on the ability of HCT116 colorectal cancer cells to grow and form colonies in soft agar. The ability of cells to grow in a condition without adherence into a solid substrate shows one of the features of malignant cells. Remarkably, mutation at region I and region II of Mad2 binding regions within FAT10 (FAT-mLR) significantly attenuated the ability of HCT116 cells to form colonies in soft agar ($p<0.001$) compared to FAT10-overexpressing cells. Figure 3.13 shows that FAT-mLR mutants have 8.3±3.5 colony numbers in comparison with FAT10 overexpressing cells that have 471.7±15.5 colony numbers. In addition, mutations at either site of FAT10 and Mad2 binding sites (FAT-mL/FAT-mR) have slightly decreased the formation of colonies in soft agar in compare to FAT10-overexpressing cells (FAT10). However, similar numbers of colonies were observed in FAT-mL (130.3±11.9 colonies) and FAT-mR (74.0±9.5 colonies) as well as WT HCT116 cells (125.7±16.2 colonies). Despite its lower colony numbers, mutations at only one Mad2 regions within FAT10 (FAT-mL and FAT-mR) were still showed a higher colony numbers compared to FAT-mLR cells, where both Mad2 regions within FAT10 have been mutated (FAT-mLR). These results again further strengthened our notion that targeting the specific binding regions between FAT10 and Mad2 reduced the cell malignant transformation.

### 3.12 Interruption of FAT10 and MAD2 binding increases its cytotoxic induced cell death

Having demonstrated the importance of disruption of FAT10 and Mad2 binding in cell proliferation, we next examined the apoptotic profiles of WT,

## Figure 3.13

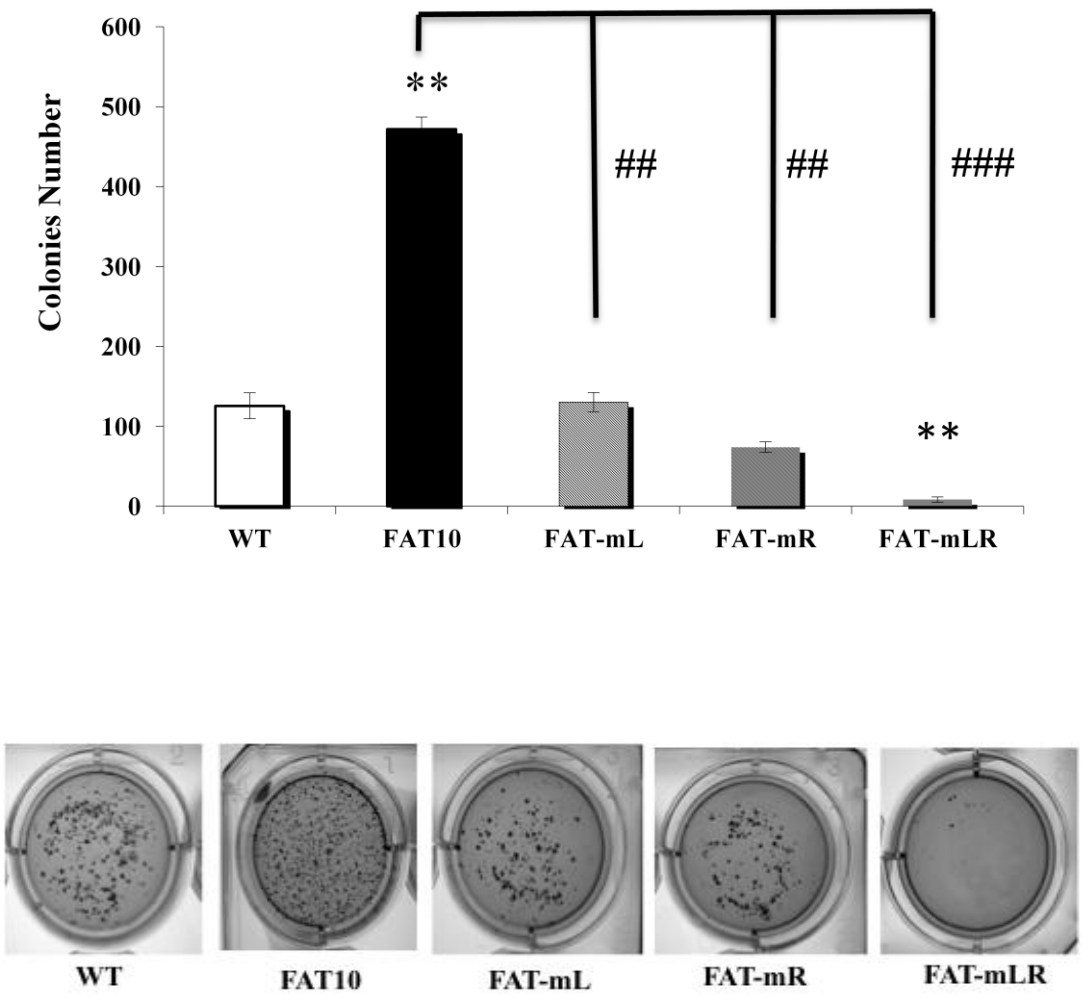


**Figure 3.13 Disruption of FAT10 and MAD2 binding reduces the anchorage-independent growth of HCT116 cells in soft agar.** The graph shows the total number of colonies formed in soft agar. WT, FAT10 overexpressing cells, FAT-mL, FAT-mR, and FAT-mLR stable clones were seeded in 6-well plate. After 3 weeks soft agar were stained and colonies were counted. The pictures is a representative sets from 1 experiment. Data is represented as mean±s.e. from 3 biological repeats. **denotes statistical significance *p-value* <0.01 compared with WT. ## denotes statistical significance at *p-value*<0.01 compared with FAT10 overexpressing cells. ### denotes statistical significance at *p-value*<0.001 compared with FAT10 overexpressing cells.

## Figure 3.14

**A.**

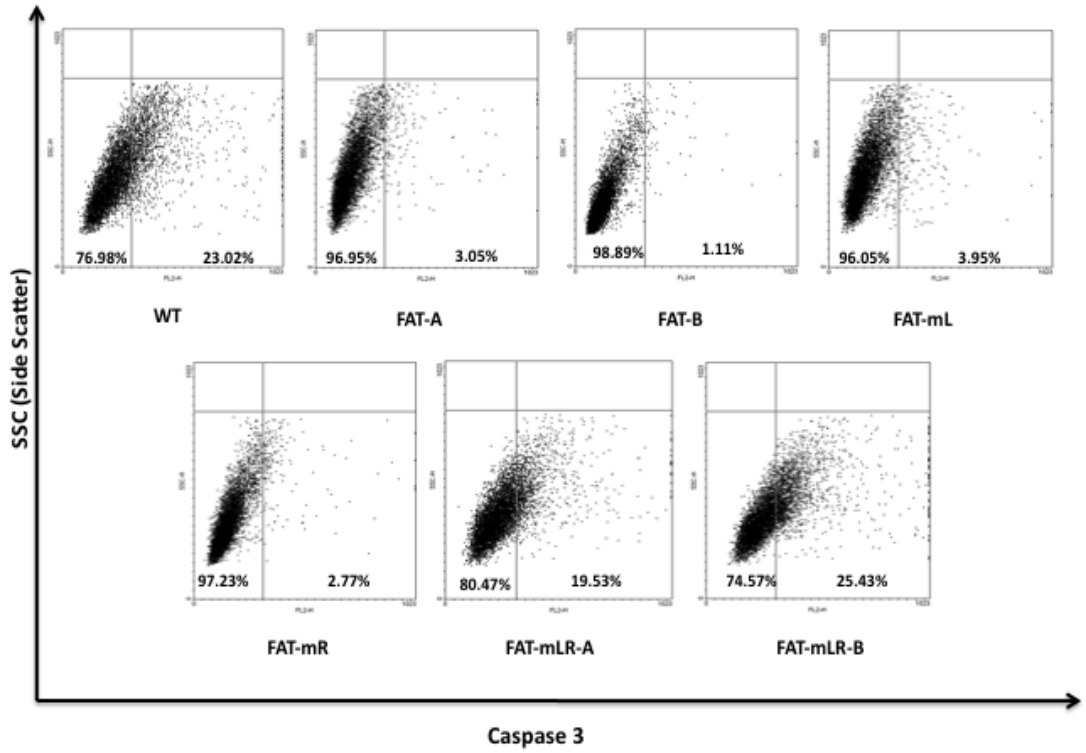


**B.**

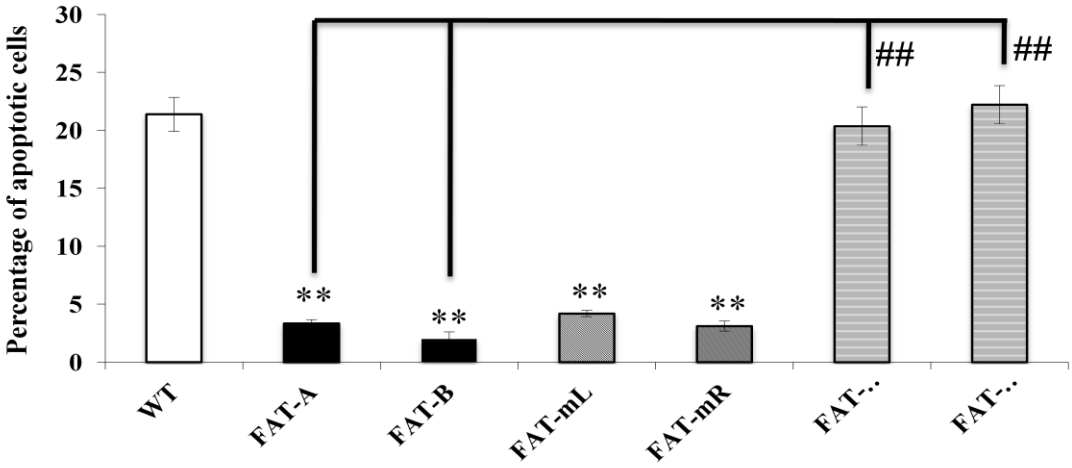


**Figure 3.14 Interference of FAT10 and MAD2 binding increases the percentage of cell death. A.** Representative set of flow cytometry pictures from WT, FAT10 overexpressing stable cells (FAT-A, FAT-B), and FAT10 mutant cells (FAT-mL, FAT-mR, FAT-mLR-A, FAT-mLR-B) stained with FITC-Caspase3. **B.** Percentage of apoptotic cells described in A from 3 independent experiments. The bar chart shown in the graph is mean±s.e. ** denotes p-value<0.01 compared to WT HCT116 cells, ## denotes p-value<0.01 compared to FAT10 overexpressing cells (FAT-A, FAT-B).

wild type FAT10, and its mutants FAT10 stable cells upon Camptothecin-induced cell death. Previously, in Chapter 3.5, we have shown that FAT10 overexpression increased cell survival upon cytotoxic induced cell death. Therefore, we also validated, whether FAT10's pro-survival ability, could be reverted back upon the disruption of MAD2 binding regions within FAT10 protein. Caspase 3 staining followed by flow cytometry analysis was performed to check the effect of the disruption of FAT10 and Mad2 binding sites on cell survival.

Approximately 17% increase in apoptotic cells was observed, when both Mad2 binding sites on FAT10 protein were mutated (Figure3.14 B). As shown, FAT-mLR-A (20.36±1.66%) and FAT-mLR-B (22.22±1.59%) showed a high percentage of apoptotic cells comparable to WT cells (21.38±1.47%) upon cytotoxic treatment. In agreement with our previous finding, we once again demonstrated that FAT10 overexpression (FAT-A: 3.35±0.38%, FAT-B: 1.99±0.69%) promoted cell survival. Interestingly, mutations at one region of Mad2 interaction regions within FAT10 (FAT-mL: 4.19%±0.27%, FAT-mR: 3.11±0.89%) did not significantly increase the rate of apoptosis upon cytotoxic treatment. Hence, FAT-mL and FAT-mR cells were able to evade apoptosis.

**3.13 Disruption of FAT10 and Mad2 binding abrogates cell invasiveness of HCT116 cells**

The gain of invasive and migratory capabilities of FAT10 overexpressing cells, which has been showed previously in Chapter 3.6, were reduced by the disruption of FAT10 and Mad2 binding. Through fusion-PCR-mutagenesis experiments, we mutated Mad2 interaction regions within FAT10 protein. As shown in Figure 3.15A, only FAT-mLR mutants reduced the ability of HCT116 cells to migrate and invade the matrigel-coated transwell® membrane by at least

## Figure 3.15

**A.**

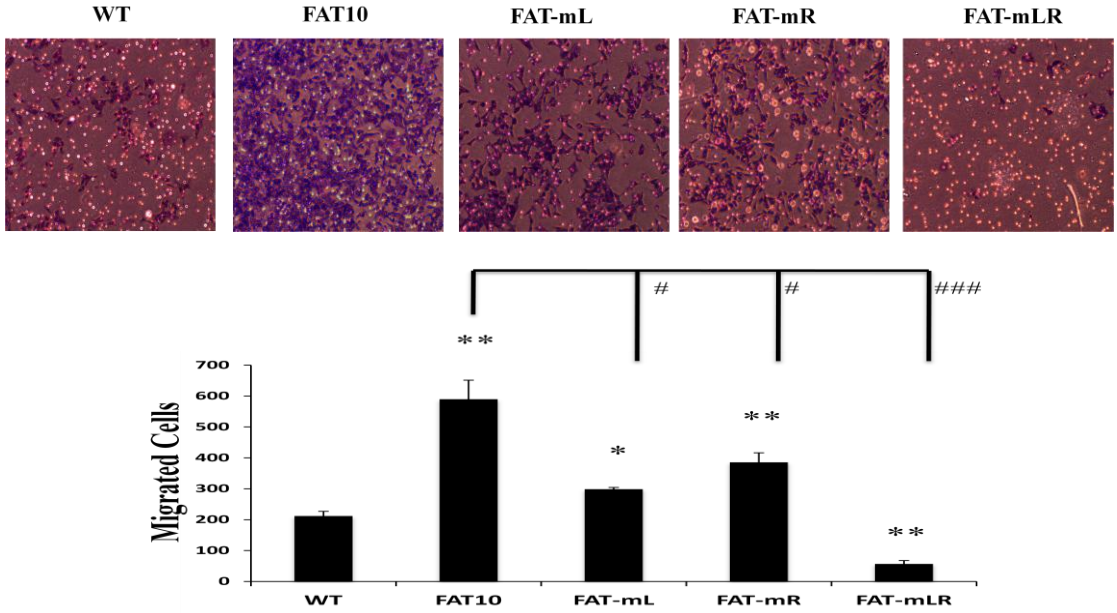


**B.**

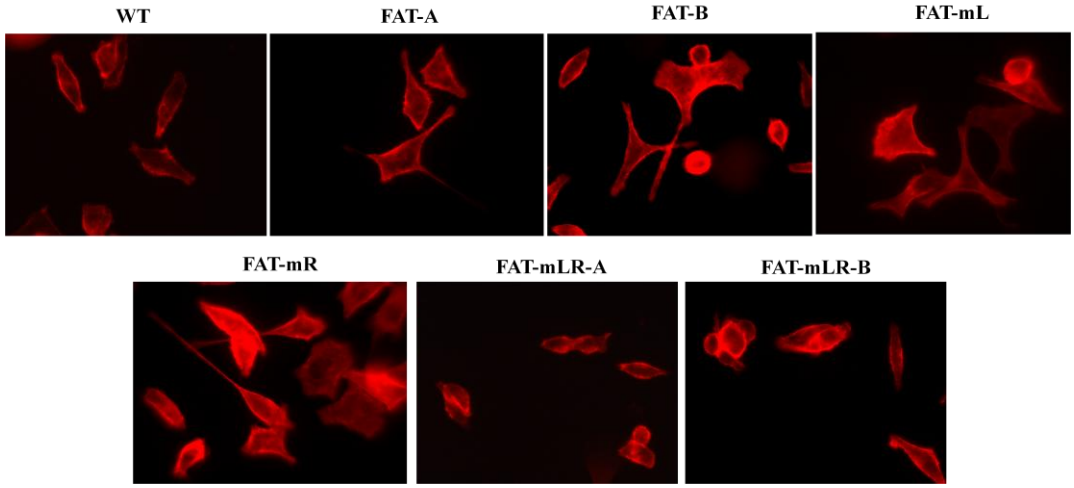


**Figure 3.15 The importance of FAT10 and MAD2 binding in cell invasion. A.** Migration and invasion profile of WT, FAT10 overexpressing cells and its mutant derivates (FAT-mL. FAT-mR, FAT-mLR). The pictures show the migrated cells after 24 hours taken under the microscope with 40x magnification after staining with Diff Quick. The graph shows the number of migrated cells, which represents the degree of invasiveness of these cells *in vitro*. Data is represented as mean±s.e. (*p<0.05, **p<0.01 compared to WT, #p<0.05, ###p<0.001 compared to FAT10 overexpressing cells) **B.** Actin cytoskeleton profiles in HCT116 cells. The cells were seeded on poly-L-lysine-coated 6-well plate, incubated for 24 hours for the cells to adhere and stained with rhodamine-conjugated phalloidin to visualize filamentous actin. Pictures are shown as representative sets from at least 3 independent experiments.

compared to FAT10-overexpressing cells. However, mutations of amino acid residues only at region I (FAT-mL) or region II (FAT-mR) of Mad2 interaction regions within FAT10 protein attenuated the invasiveness of HCT116 cells by 2 fold and 1.5 fold, respectively in comparison with FAT10 overexpressing cells. Nevertheless, only the invasiveness of FAT-mLR was significantly decreased compared to wild type HCT116 cells.

The ability of cells to invade and migrate requires dynamic actin cytoskeletal remodelling and the formation of protrusive structures. Hence, we investigated the actin cytoskeleton features of the cells using rhodamine-phalloidin staining. In general, immunofluorescence indicated that only FAT-mLR and WT HCT116 cells did not show enriched lamellipodia structures unlike the FAT10-overpressing, FAT-mL, and FAT-mR stable cells. The disappearance of lamellopodia structures, which were required for active cytoskeletal turnover at the edge of migrating cells, indicated that FAT-mLR mutant was less invasive. Consistently, with our previous findings disruption of FAT10 and Mad2 binding were not only diminished the cell proliferation and cell survival of rate, but it also reduced the cell invasion.

### 3.14 Cell adhesion and migration is decelerated by the disruption of FAT10 and Mad2 binding

Having shown that FAT-mLR reduced cell proliferation, cell survival, and cell invasion rate of HCT116 cells. Further, effect of these FAT10 stable mutants (FAT-mL, FAT-mR, and FAT-mLR) on cell adhesion to an extracellular matrix were investigated, since cancer metastasis tumors that spread through the circulatory system capitalize mechanisms of cell adhesion to establish new tumors.

## Figure 3.16

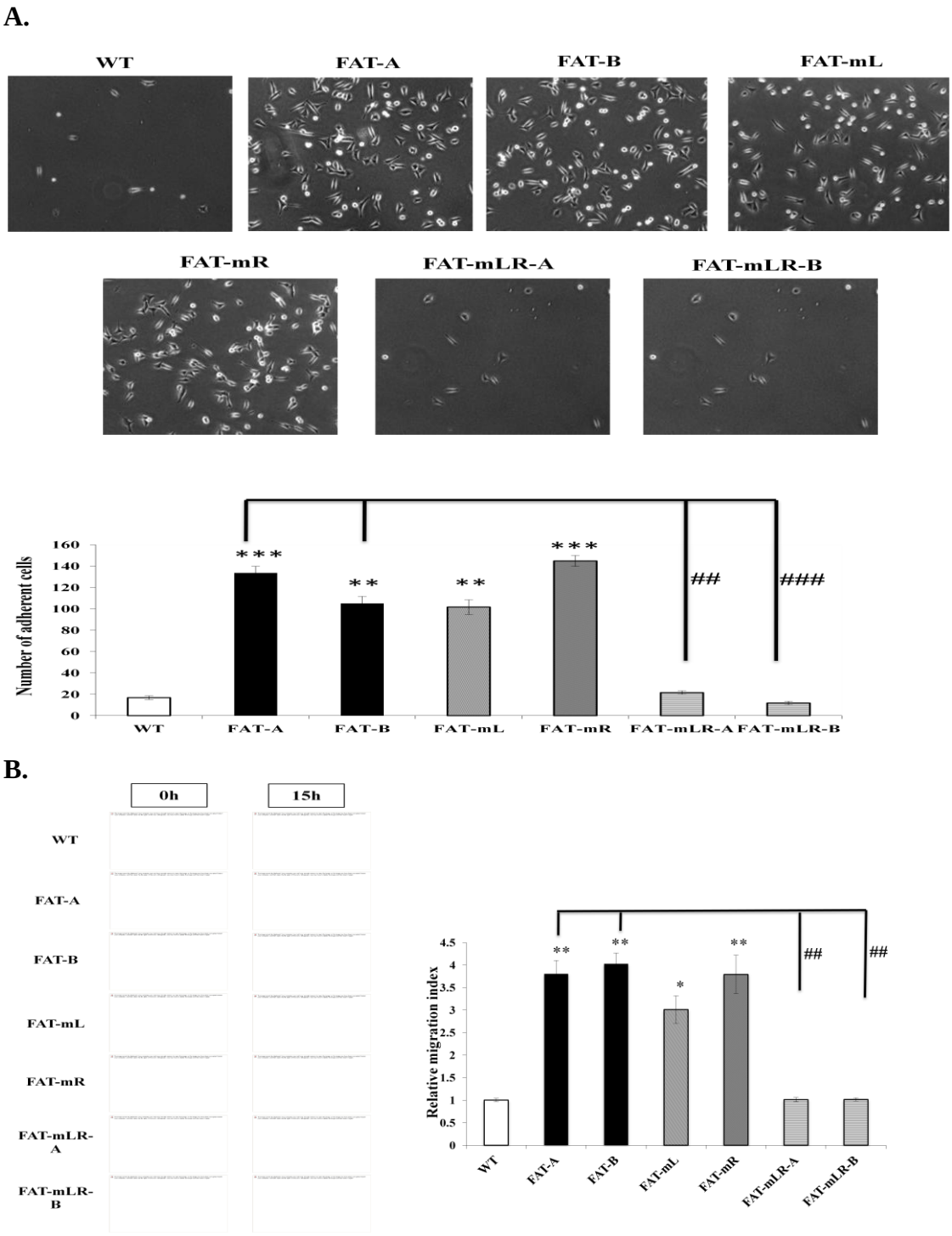


**Figure 3.16 Deceleration of cell adhesion and migration caused by disruption of FAT10 and MAD2 binding.** A. Cell adhesion profile of WT, FAT10 overexpressing cells (FAT-A, FAT-B), and FAT10 mutants (FAT-mL, FAT-mR, FAT-mLR-A, FAT-mLR-B). B. The migration ability of WT, FAT10 overexpressing cells, and its mutant derivates after introduction of "wound". Data is expressed in mean±s.e from three independent experiments. (*p<0.05,**p<0.01,***p<0.001 compared to WT; ##p<0.01, ###p<0.001 compared to FAT10 overexpressing cells).

As shown, Figure 3.16A shows less adherent cells in FAT-mLR mutants compared to FAT10-overexpressing, FAT-mL, and FAT-mR stable cells. Scratch-wound-healing assay to check the migration ability of these FAT10 mutant cells were also performed. The closure of the "wound" measured the migration ability of these cells. As shown in Figure 3.16B, 15 hours post "wound" introduction, FAT-mLR has a slower migration ability to close the "wound-gap" compared to FAT10-overexpressing cells, since the "wound" in FAT10-overexpressing cells was almost closed. Consistent with the results from transwell invasion assay and F-actin staining, FAT-mL and FAT-mR mutants showed a similar distance of "wound-gap closure" as FAT10 overexpressing cells. Taken together, these results conferred the importance of FAT10 and Mad2 binding in cell invasion, adhesion as well as migration. Thus, targeting this specific interaction between FAT10 and Mad2 abrogated the invasion and migration of colorectal cancer HCT116 cells.

**3.15 Disruption of FAT10 and Mad2 binding prevents cells from escaping the mitotic cell arrest.**

In our previous finding, we found that overexpression of FAT10 led the cells to escape from mitotic cells arrest and became multinucleated upon prolong mitotic arrest. Therefore, to address the question, whether disruption of FAT10 and Mad2 binding help the cells to escape mitotic cell arrest, we treated WT, wild type FAT10-overexpressing cells and mutants FAT10 stable cells (FAT-mL, FAT-mR, FAT-mLR, FAT-Lys, and FAT-Gly) with 200ng/ml nocodazole for 8h, prior the nocodazole treatment we synchronized the cells at G1/S phase using 3mM thymidine for 17h. Post 8h of nocodazole treatment, mitotic-specific antibody (MPM2) was used to stain specifically mitotic cells,

**Figure 3.17**

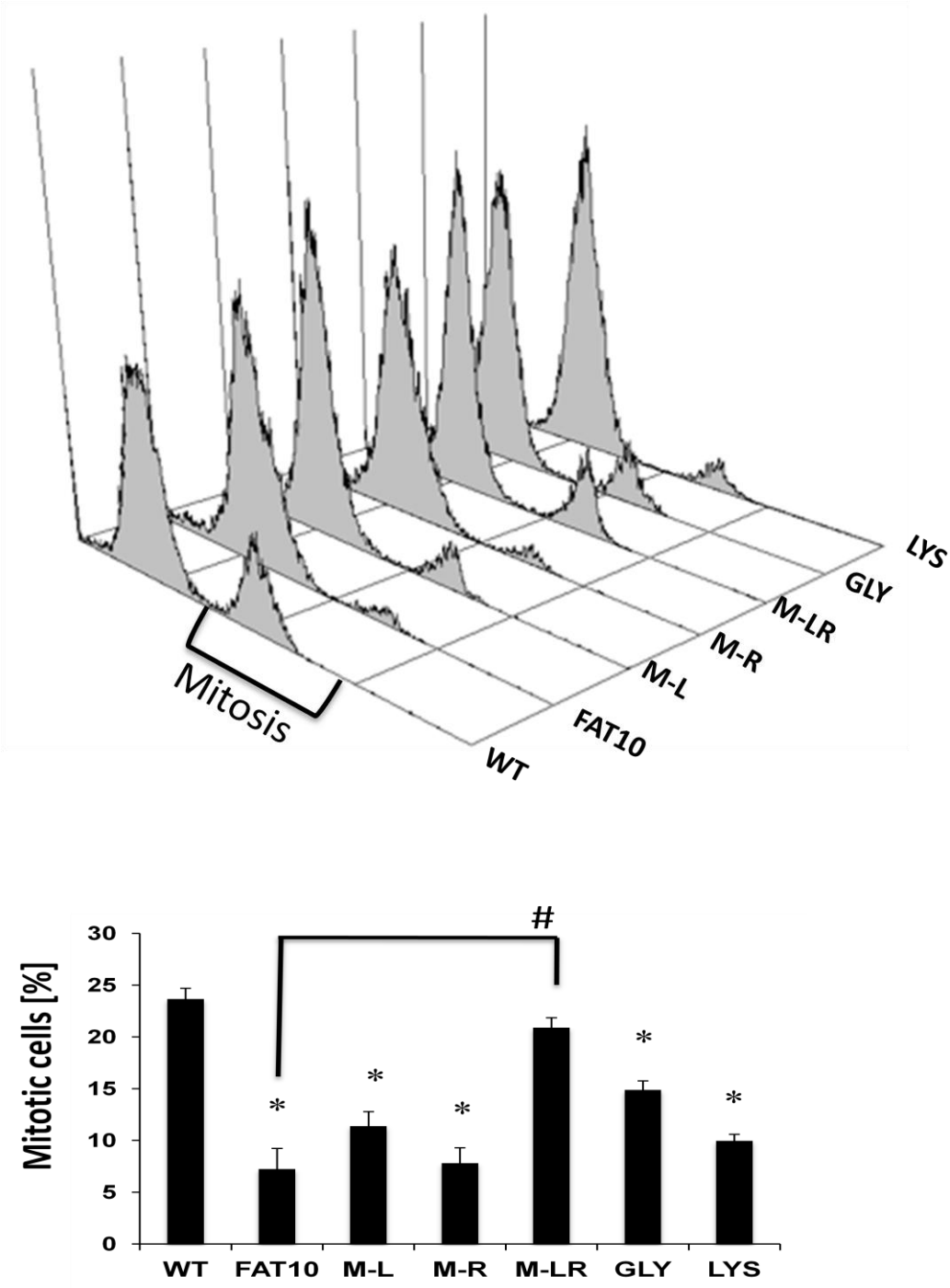


**Figure 3.17. A reduce level of cells escaping from mitotic arrest observed in FAT-mLR mutants.** Representative histograms showing the fluorescence-activated cell sorting profile of cells probed with MPM-2 antibody. The graph shows the average percentage of mitotic cells with MPM-2 positive staining from 3 independent experiments. All error bars show standard error (s.e.) of the mean. (**$p$-value<0.01 compared to WT, and #$p$-value<0.05 compared to FAT10 overexpressing cells).

followed by Alexafluor488 staining as dye that can be detected by FACS and at the last step these cells were analyzed using FACS Calibur® flow cytometer.

As shown in Figure 3.17 approx. around 10% more WT and FAT-mLR cells were arrested at mitosis compared to FAT10-overexpressing, FAT-mL, and FAT-mR cells. These results suggest that disruption of FAT10 and Mad2 binding reverted back the ability of these cells to escape the mitotic arrest. However, mutations only at one region of Mad2 interaction regions within FAT10 (FAT-mL and FAT-mR) helped the cells to escape from the mitotic arrest compared to WT and FAT-mLR cells. Interestingly, mutation of all the lysine residues (FAT-Lys) or double-glycine residues (FAT-Gly) did not enhance the ability of these cells to escape from mitotic cell arrest.

**3.16 Disruption of FAT10 and Mad2 binding prevents aneuploidy**

Based on our previous study, we found that FAT10 overexpression induced numerical chromosomal instability (CIN). Therefore, we further examined, if disruption of FAT10 and Mad2 binding can prevent CIN. WT, wild type FAT10 and mutants FAT10 that were stably expressed in HCT116 cells (FAT-mL, FAT-mR and FAT-mLR) were cultured for approx. 50 passages (~150 doubling time), before karyotyping analysis were performed. A relatively stable karyotype was observed from WT HCT116 cells. As shown in Figure 3.18B, majority of WT HCT116 cells (84%) have 40-49 chromosomes/cell. Only a smaller percentage of cells were observed to have more than 80-90 chromosomes/cell and none of the WT cells contained more than 100 chromosomes/cell. Similar karyotype trends as WT cells were observed in FAT-mLR mutant cells, whereas FAT10 overexpressing cells, FAT-mL and FAT-mR mutants (71%, 68% and 65%, respectively) were in majority observed to

## Figure 3.18

**A.**

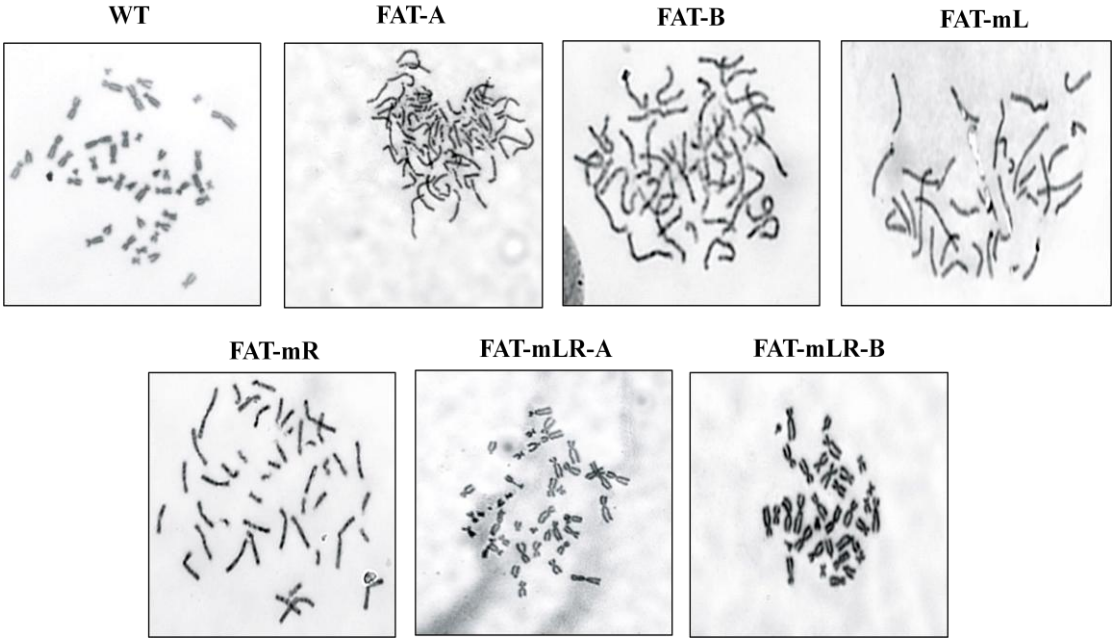


**B.**

| Chromosome number per cell | Percentage of cells(%) | | | | | | |
|---|---|---|---|---|---|---|---|
| | WT | FAT-A | FAT-B | FAT-mL | FAT-mR | FAT-mLR-A | FAT-mLR-B |
| 30-39 | 4.9 | 3.7 | 2.8 | 3.1 | 4.2 | 2.2 | 3.8 |
| 40-49 | 84.1 | 6.5 | 8.5 | 11.2 | 13.8 | 83.6 | 79.8 |
| 50-59 | 2.1 | 0.7 | 0.4 | 4.8 | 3.6 | 4.8 | 5.7 |
| 60-69 | 1.4 | 3.1 | 1.3 | 1.1 | 1.3 | 1.6 | 1.2 |
| 70-79 | 3.3 | 10.5 | 11.5 | 10.7 | 10.9 | 3.1 | 2.9 |
| 80-89 | 2.7 | 71.2 | 73.1 | 68 | 65 | 3.3 | 5.8 |
| 90-99 | 1.5 | 1.2 | 0 | 0 | 0.5 | 1.4 | 0.8 |
| ≥100 | 0.0 | 3.1 | 2.4 | 1.1 | 0.7 | 0 | 0 |
| Total number of cells examined | 100 | 95 | 93 | 90 | 92 | 95 | 96 |

**Figure 3.18 Complete disruption of FAT10 and MAD2 binding prevents aneuploidy. A.** Representative pictures of chromosome morphology from WT, 2 stable clones of FAT10 overexpressing cells (FAT-A, FAT-B), and its mutant derivatives stable cells (FAT-mL, FAT-mR, FAT-mLR-A, Fat-mLR-B). Metaphase spread from FAT-mLRA and FAT-mLRB displaying a normal sister chromatid separation with completely condensed chromosome unlike FAT-A, FAT-B, FAT-mL, and FAT-mR. **B.** Table showing the karyotyping profile of cells based on its chromosome numbers.

carry 80-90 chromosomes per cell. Thus, it suggests that disruption of FAT10 and Mad2 binding prevented the cells to become aneuploid.

Through karyotyping experiment, not only numerical chromosomal instability were observed, but interestingly, altered chromosome morphology were also observed in FAT10-overexpressing, FAT-mL and FAT-mR mutants stable cells. As evidence, Figure 3.18A shows the abnormal chromosome morphology, where the sister chromatid separation to have incomplete condensed chromosome in FAT10 overexpressing, FAT-mL and FAT-mR cells. Incomplete condensed chromosome morphology was not observed in FAT-mLR mutants and WT HCT116 cells. As shown in Figure 3.18A, normal condensed chromosome morphology during metaphase looked like a ribbon, whereas altered chromosome morphology looked like a strand without a proper separation of chromosome arms. Taken together, these data revealed that FAT10-overexpressing, FAT-mL and FAT-mR exhibited premature sister chromatid separation with incomplete condensed chromosome and more aneuploid cells. This phenomenon can be reverted by the disruption of FAT10 and MAD2 binding as shown by the normal karyotype profile of FAT-mLR mutant cells.

**3.17 Disruption of FAT10 and Mad2 binding diminishes tumor growth in xenograft nude mice model**

In order to reaffirm the importance of the disruption of FAT10 and Mad2 binding in affecting the cellular phenotypes such as cell proliferation obtained from the *in vitro* study. Next, we performed an *in vivo* study, where we injected WT, FAT10-overexpressing cells, and FAT10 mutants cells (FAT-mL, FAT-mR and FAT-mLR) subcutaneously into the left and right flank of nude mice. In this experiment, four different groups of mice were used as follows: WT vs. FAT10

## Figure 3.19

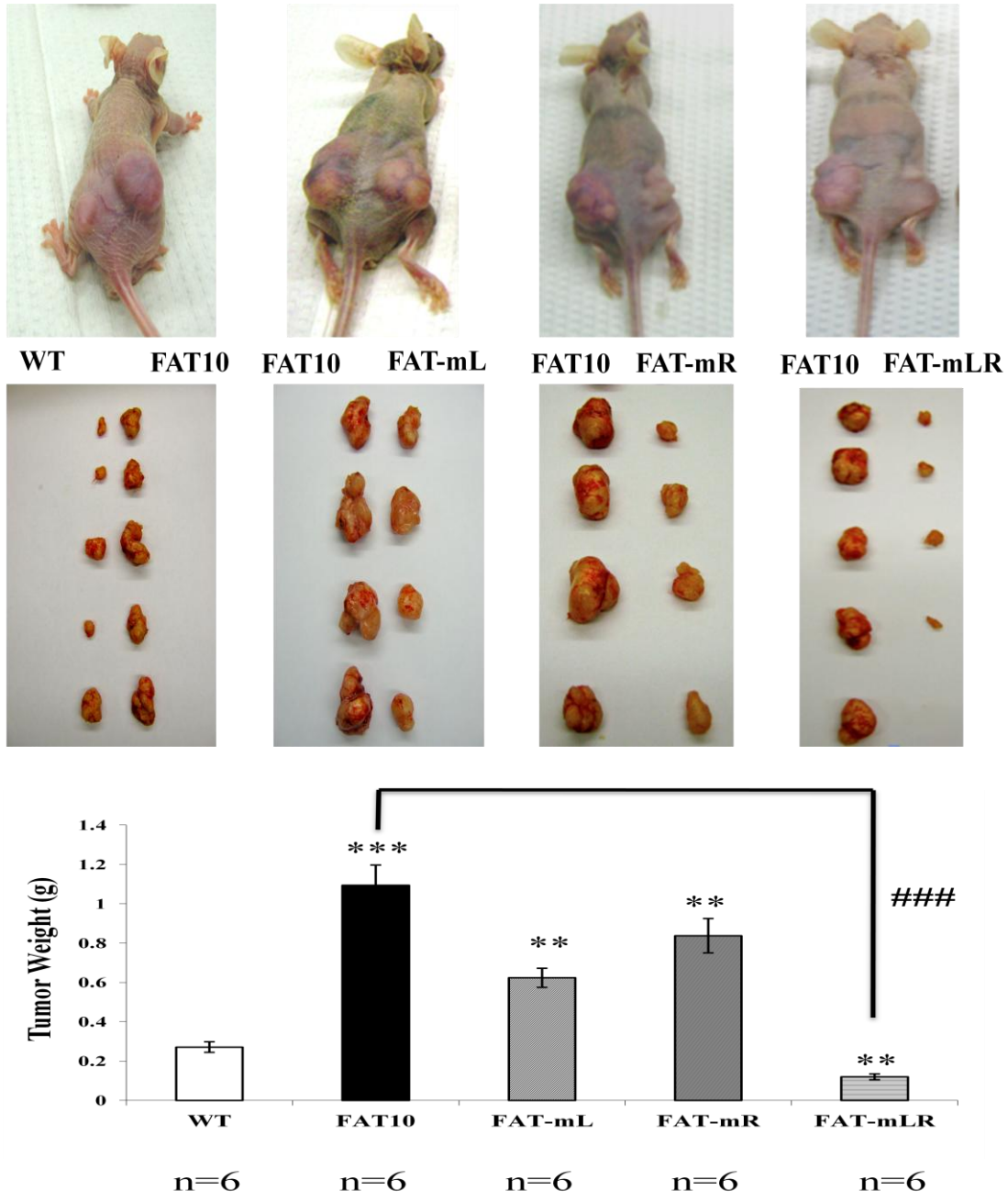


**Figure 3.19 Abolishing FAT10 and MAD2 binding abates tumor growth in nude mice model.** The representative set of pictures above shows the tumor growth of WT, FAT10 overexpressing (FAT10), FAT-mL, FAT-mR, and FAT-mLR stable cells injected subcutaneously. The graph shows the tumor weight of 6 nude mice measured with precision balance, 3 weeks after the subcutaneous injection into the nude mice. The middle picture shows the tumors isolated from the nude mice. Data is expressed mean±s.e. (***p-value*<0.01,****p-value*<0.001 compared to WT, and ###*p-value*<0.001 compared to FAT10 overexpressing cells).

overexpressing cells, FAT10 overexpressing cells vs. FAT-mL mutants, FAT10 overexpressing cells vs. FAT-mR mutants, and FAT10 overexpressing cells vs. FAT-mLR mutants. In each group six mice were used.

In accordance with our previous finding, where we overexpressed FAT10, we once again observed a greater promotion of tumor growth of FAT10-overexpressing stable cells in comparison with WT HCT116 cells in nude mice model. Notably, as shown in Figure 3.19, we also found that FAT-mLR stable mutant cells have an impaired tumor growth compared to FAT10-overexpressing cells. Remarkably, these FAT-mLR mutant cells have significantly smaller tumors than WT HCT116 cells. However, FAT10 mutants harboring only one mutated Mad2 binding regions within FAT10 (FAT-mL and FAT-mR) only showed a marginal decrement of tumor growth in comparison to FAT10-overexpressing cells. An augmented tumor growth in these mutant cells (FAT-mL and FAT-mR) was still observed compared to WT, although one Mad2 binding regions within FAT10 were mutated. These results clearly suggest that we need to abolish both binding regions of Mad2 interaction regions within FAT10 in order to abate the tumor growth. Therefore, based on our *in vivo* study, FAT10 and Mad2 binding played an important role in tumorigenesis, and the interference of these binding negated the pro-survival role of FAT10.

**3.18 FAT10 overexpression phenocopies Mad2 knockdown effects to escape from mitotic cell arrest.**

Previously, our laboratory has reported that FAT10 overexpression reduced the localization of Mad2 at the kinetochores during mitosis, which led to abbreviation of mitotic duration and aneuploidy. Therefore, in order to validate

## Figure3.20

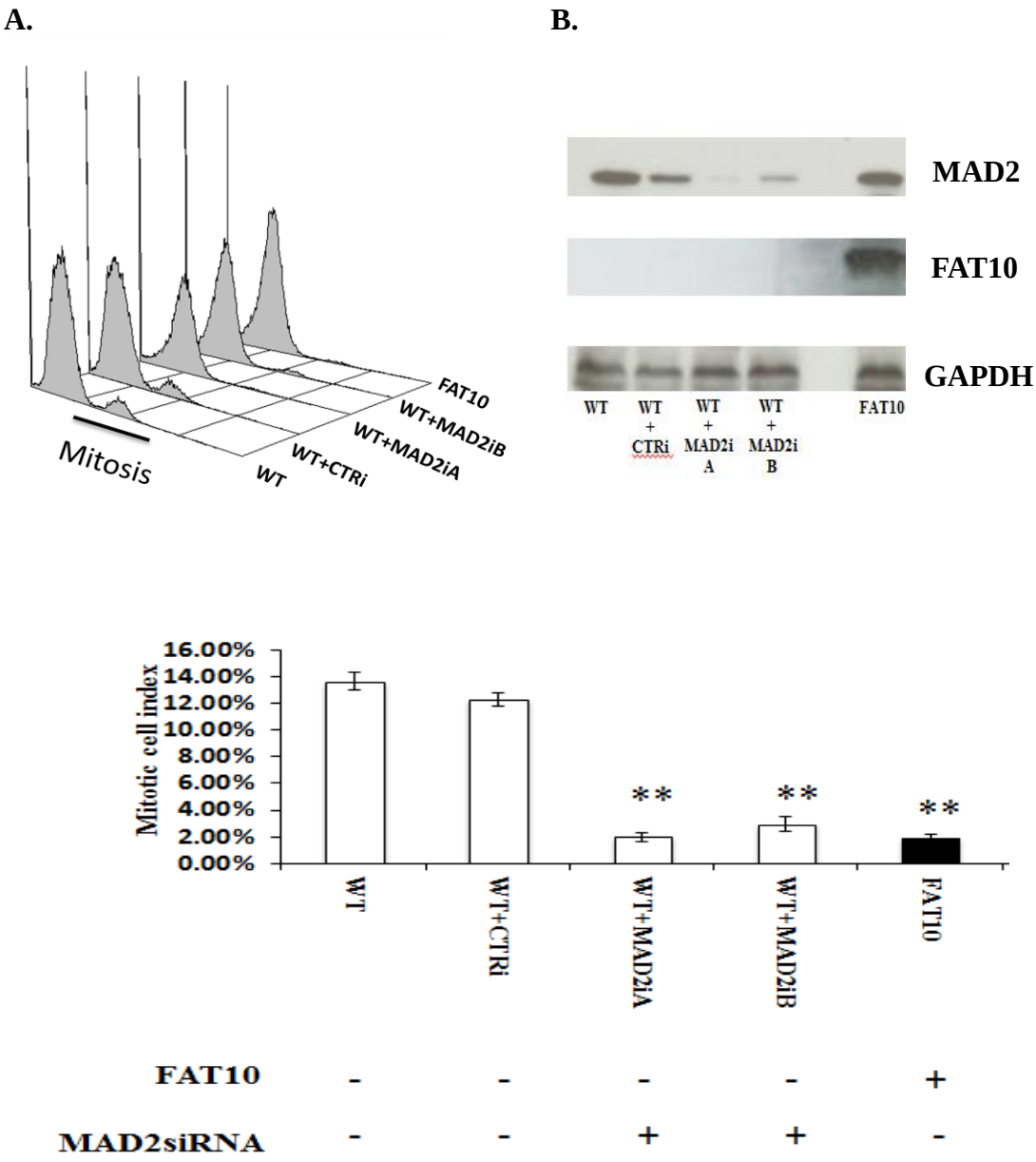


**Figure 3.20 FAT10 overexpression or MAD2 knockdown can help the cells to escape from mitotic arrest** A. The Histogram (Upper left panel) shows the representative of FACS data analyzed with WinMDi2.9 software. WT, and FAT10 overexpressing cells were used in this experiment and two different MAD2siRNA (MAD2iA, and MAD2iB) as well as scramble siRNA (CTRi). The graph (bottom panel) shows the percentage of mitotic cells that positively stained with mitotic specific antibody (MPM-2). Data is represented as mean±s.e. from 3 independent experiments. ** denotes p-value <0.01, *** denotes p-value <0.001 compared to WT cells. **B.**Western blot analysis of MAD2 and FAT10 protein expression in WT and with a long term treatment of MAD2siRNA or scramble siRNA (CTRi) and FAT10-overexpressing cells to check the efficiency of MAD2 knockdown and FAT10 overexpression. GAPDH was used as loading control.

whether Mad2 knockdown or FAT10 overexpression exerts a similar effect on mitotic escape and aneuploidy, we employed siRNA knockdown against Mad2. WT and FAT10- overexpressing stable HCT116 cells were repeatedly transfected with two different MAD2 siRNA (MAD2iA, MAD2iB) or scrambled siRNA (CTRi) within a period of at least 20 passages (~100 doubling times). The introduction of these siRNAs over a prolonged period will allow us to examine the effect of Mad2 knockdown on these colorectal cancer HCT116 cells. After 20 passages, these cells were then synchronized with 3mM of thymidine, followed by nocodazole treatment to arrest the cells at mitotic phase. These cells were then stained with mitotic specific antibody (MPM-2), which is a marker of mitosis, and analyzed using fluorescence cell sorting (FACS).

As shown in Figure 3.20A, either FAT10 overexpression or Mad2 knockdown were found to help the cells to escape from mitotic arrest. This result is in agreement with our previous findings, which showed that FAT10 interacted with Mad2, and induced Mad2 delocalization from the kinetochores during pro-metaphase.

Validation of Mad2 and FAT10 protein expression level on cells used for this experiment and subsequent experiments is showed in Figure 3.20B by performing Western blot using the cell lysates. Western blot analysis showed an efficient knockdown of Mad2 over a long-term treatment of cells with MAD2siRNA treatment. WT and FAT10-overexpressing cells treated with scramble siRNA (CTRi) in parallel were also used as control.

### 3.19 Reduced Mad2 expression or FAT10 overexpression promotes aneuploidy in HCT116 cells

Having demonstrated similar phenotypes between FAT10 overexpression and Mad2 knockdown in escape of mitotic cell arrest, we further investigated, whether the proportion of aneuploid cell population in FAT10-overexpressing cells is similar to that of Mad2-knockdown cells. Therefore, we utilized the WT and FAT10- overexpressing cells that has been treated with MAD2 siRNA over a long-term period (20 passages) for analysis of the number of chromosomes in cells.

Consistent with our previous findings in Chapter 3.18, we also found that FAT10 overexpression or reduction of Mad2 level resulted in increased proportion of aneuploidy cells (Figure 3.21A, B). In addition, around 72% of FAT10-overexpressing cells or 70% of Mad2-knockdown cells alone are having 80-89 chromosomes per cell. In contrast, 81% of WT cells have 40-49 chromosomes per cell. Thus, this further strengthens our previous data, which showed that FAT10 overexpression led to a reduction of Mad2 localization at the kinethochore during mitosis. There is no statistical difference between the number of chromosomes in FAT10-overexpressing cells and Mad2-knockdown cells.

## Figure 3.21

**A.**

| Chromosome number per cell | Percentage of cells(%) | | | | |
|---|---|---|---|---|---|
| | WT | WT+CTRi | WT+MAD2iA | WT+MAD2iB | FAT10 |
| 30-39 | 3.8 | 5.2 | 2.4 | 3.5 | 2.5 |
| 40-49 | 81.6 | 80.4 | 15.7 | 17.2 | 11.1 |
| 50-59 | 3.7 | 4.6 | 2.3 | 1.5 | 1.7 |
| 60-69 | 2.4 | 1.2 | 1.8 | 1.8 | 1.2 |
| 70-79 | 3.8 | 2.6 | 3.9 | 5.3 | 9.6 |
| 80-89 | 3.3 | 4.8 | 69.8 | 68.0 | 72.6 |
| 90-99 | 1.4 | 1.2 | 0.2 | 1.1 | 0 |
| ≥100 | 0 | 0 | 2.0 | 1.6 | 1.3 |
| Total number of cells examined | 50 | 50 | 53 | 53 | 50 |

**B.**

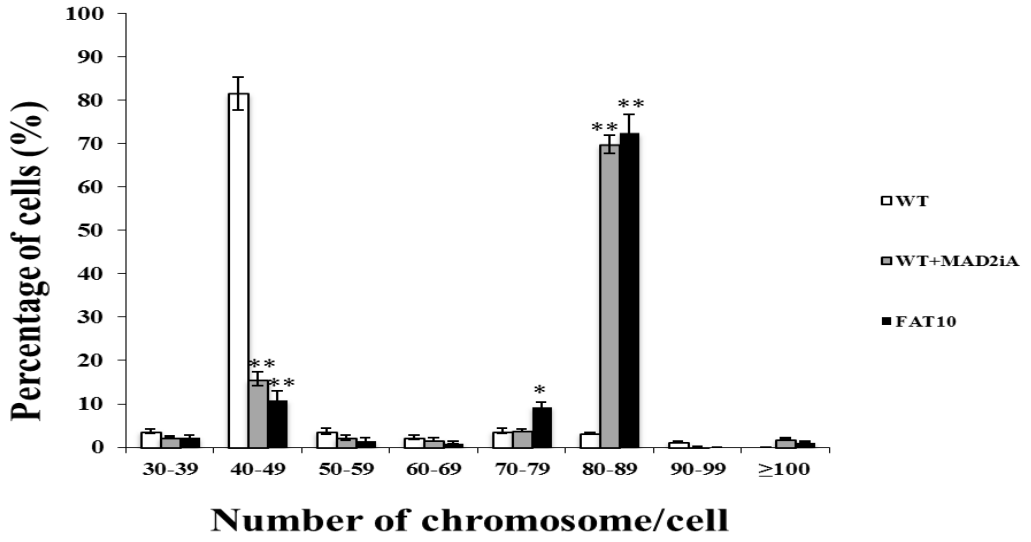


**Figure 3.21 FAT10 overexpression or reduction of Mad2 level resulted in increased proportion of aneuploid cells. A.** Table showing the profile of chromosome number in WT, WT+CTRi, WT+MAD2iA, WT+MAD2iB, and FAT10-overexpressing cells. Two different MAD2siRNAs were utilized in this experiment. **B.** Representative graph showing the chromosome number per cell of WT, WT+MAD2iA, and FAT10-overexpressing stable cells (FAT10) obtained from karyotyping experiments. Data is expressed in mean±s.e. * denotes p-value<0.05, ** denotes p-value <0.01.

# Chapter 4 Discussion

## 4.1 Fundamental background of this thesis

FAT10 overexpression was found in several different types of cancers, such as colorectal cancer, hepatocellular carcinoma, stomach cancer, and gynecological cancer (Lee et al 2003, Lim et al 2006). Additionally, pro-inflammatory cytokines TNFα and IFNγ synergistically induced FAT10 overexpression in colon and liver cancer cell line (Lukasiak et al 2008b). Taken together, these studies suggested that FAT10 might play a role in tumorigenesis. A study by *Liu et al* reported non-covalent interaction between FAT10 and a mitosis spindle checkpoint Mad2 (Liu et al 1999b). Based on this report, we then examined the role of FAT10 and Mad2 interaction in tumorigenesis. Mad2 is an important mitotic spindle checkpoint and its deregulation is widely known to cause improper chromosome segregation leads to aneuploidy, one of the hallmarks of cancers (Hanahan and Weinberg 2011). Therefore, this interaction suggests a role of FAT10 in the regulation of cell division. Indeed, our previous finding highlighted the role of FAT10 overexpression in causing chromosomal instability (CIN) through reduced localization of Mad2 at the kinetochore during mitosis, which then caused the abbreviation of mitosis duration, chromosome missseggregation and aneuploidy (Ren et al 2006). Further, inhibition of FAT10 expression caused normal Mad2 localization at the kinetochore during pro-metaphase with significantly reduced aneuploid cells (Ren et al 2011b). Hence, based on these findings found so far, a more comprehensive understanding about the role of FAT10 in tumorigenesis as well as targeting its specific cellular function that contributes to tumorigenesis was necessary to be further investigated.

To study the role of FAT10 in tumorigenesis as well as finding the underlying mechanism, which contributes to tumorigensis, we chose to investigate the oncogenic properties of FAT10 in driving tumorigenesis through its effects in the important cellular functions such as in cell proliferation, migration, adhesion and invasion. Additionally, we also further examined, whether disruption of FAT10 and Mad2 interaction alleviated the tumorigenic role of FAT10. So far, FAT10 has only been reported to cause aneuploidy and upregulated in tumors from cancer patients, however solid evidence about FAT10's pro-malignancy properties in driving tumor growth and progression has never been elucidated. In order to give a comprehensive and direct evidence about the pro-malignancy role of FAT10 in tumorigenesis, *in vitro* assays such as wound healing assay, cell transformation assay, apoptosis assay, cell proliferation assay, invasion assay and adhesion assay were employed. *In vivo* approach using xenograft mice model was also used to further strengthen the *in vitro* assays.

Since FAT10 crystal structure yet to be elucidated and FAT10 is a small protein molecule, in collaboration with A/P Song Jianxing, NMR study, which can be utilized to unveil the specific binding sites between FAT10 and Mad2 were employed in this thesis. Disruption of these binding sites by fusion-PCR-mutagenesis study helped us to dissect the specific role of FAT10 in tumorigensis and specifically target the tumorigenic role of FAT10 without disrupting its physiological function. Furthermore, reduced Mad2 protein expression level or FAT10 protein overexpression allowed us to unravel, whether FAT10 exerted its oncogenic role through aberrant regulation and function of mitotic spindle checkpoint Mad2.

## 4.2 The significance of FAT10 overexpression in supporting cell proliferation, transformation and survival

Current literature provides contradictory results on the role of FAT10 in cell survival role. FAT10's pro-survival role has been supported by the following observations from various studies. Firstly, FAT10 was overexpressed in several types of cancers (Lee et al 2003, Lim et al 2006), Secondly, absence of FAT10 in knockout mice led to spontaneous apoptosis of lymphocytes (Canaan et al 2006), Thirdly, its high level of expression was correlated with colon cancer progression and recurrence (Yan et al 2010), and finally, FAT10 has also been proposed as an epigenetic marker for liver neoplasia (Oliva et al 2008). All these studies only infer the pro-survival role of FAT10. However, concrete evidence on the role of FAT10 in driving tumorigenesis has not yet been fully elucidated and shown. In contrast, a study from *Raasi et al.* reported a role for FAT10 in inducing apoptosis (Raasi et al 2001). A possible reason for this contradictory observationis that *Raasi et al*. used HeLa cells (cervical cancer cell line) and murine fibroblast cells in their studies, and there are no reports of FAT10 upregulation in these cells. In contrast, FAT10 overexpression was reported in colon and liver cancer cells (Lee et al 2003, Lukasiak et al 2008a). Therefore, it is possible that the pro-survival role of FAT10 maybe cell- or tissue-specific. Another possibility is that electroporation was used to introduce the ectopic expression of FAT10 in this study may have also contributed to the observed cell death. In our hands, the introduction of FAT10-overexpressing plasmid by Lipofectamine in colorectal cancer cell lines (HCT116, SW620), liver cancer cell lines (HepG2, Hep3B), as well as infection of "immortalized" normal hepatocytes (NeHepLxHT, THLE) with adenovirus vector carrying FAT10 did not increase cell death or apoptosis.

Consistent with the possible pro-survival role of FAT10 reported by several studies mentioned earlier, we also found that FAT10 overexpression increased the proliferation of HCT116 cells and supported its malignant cell transformation in soft agar, where we observed more colonies in FAT10 overexpressing cells than in WT HCT116 cells. In contrast, reduction of FAT10 expression in FATi stable cells abated cell proliferation and also greatly impaired the malignant transformation of these cells, as evidenced by its ability to form colonies in soft agar. Two different methods (trypan blue exclusion cell counting and WST-1 assay) to measure the cell proliferation rate of FAT10 stable overexpressing cells, WT, and FAT10 knockdown cells (FATi) were used in order to draw more conclusive results. The increase in cell proliferation rate as well as augmented self-anchorage independent growth were observed, when FAT10 was overexpressed, strongly supporting the role of FAT10 in driving cell malignancy.

The characteristics of malignant cells are not only based on the ability of the cells to proliferate faster with enhanced malignant transformation ability alone, but it also depends on its ability to evade apoptosis. Thus, investigating the ability of FAT10 overexpressing cells to evade apoptosis is also as important as its proliferation and transformation ability. Importantly, we found that upon cytotoxic challenge, cells that overexpressed FAT10 were more resistant towards this cytotoxic induced cell death compared to its parental cells (WT HCT116). Taken together, these results have demonstrated that FAT10 upregulation increases cell proliferation, cell malignant transformation as well as cell survival.

## 4.3 Importance of FAT10 as a determinant in enhancing cell migration, adhesion and invasion of cells

Other than cell proliferation, cell survival and malignant transformation of cells, other important cellular features such as acquisition of adhesive, invasive and migratory capabilities are also important in tumor development and progression. Therefore we investigated, whether FAT10 also contributes to cell migration, adhesion and invasion? The first clues came from earlier studies, where high level of FAT10 expression was observed in stage II-III of colon cancer (Yan et al 2010) and a strong correlation was found between high FAT10 expression and cancer invasion, lymph node metastasis, distant metastasis, as well as the overall survival rate of colon and gastric cancer patients (Ji et al 2009, Qing et al 2011, Yan et al 2010). Although, these correlative studies demonstrated a link between FAT10 overexpression and the above-mentioned malignant features in tumors, a definitive study that demonstrate the role of FAT10 in increasing the cell invasion, adhesion, and migration remains to be investigated.

To address this question, we performed cell invasion assay using transwell® cell culture plate coated with matrigel to assess the capability of FAT10 cells to invade the matrigel and to migrate to the other side of the well. Remarkably, our data showed that FAT10 enhanced the cell invasiveness of HCT116 cells. Further, we also demonstrated that FAT10 supported the adhesion of cells to the extracellular matrix as well as significantly increased the cells migratory capabilities. Additionally, we found that stable cells overexpressing FAT10 secreted a higher level of matrix metalloproteinase 9 (MMP-9) compared to WT and FAT10 knockdown cells using an ELISA assay. MMP-9 is widely known for its contribution in invasion and metastasis of tumor cells by degrading the

surrounding basement membrane and extracellular matrix barriers, which enables cells to migrate and spread to a distant site (Choi et al 2011, Egeblad and Werb 2002, Wagenaar-Miller et al 2004). Taken together, these characteristics of malignant cells observed in FAT10 overexpressing cells supports the notion that FAT10 is an important determinant in malignancy rather than just a ”bystander”. As a whole, based on our *in vitro* observations, FAT10 protein likely plays an important role as a pro-malignant and pro-survival factor in tumorigenesis.

### 4.4 Significance of FAT10 overexpression *in vivo*

To reaffirm the oncogenic role of FAT10 observed in our *in vitro* study, we utilized a xenograft mouse model to evaluate the effect of FAT10 *in vivo*. In agreement with previous findings from FAT10 knockout mice that the lymphocytes of these knockout mice were more susceptible to spontaneous apoptosis (Canaan et al 2006), we also found that FAT10 overexpression greatly enhanced tumor growth. Bigger and heavier tumors were observed in mice injected with FAT10-overexpressing cells. In summary, based on our *in vitro* and *in vivo* findings, this thesis provides strong evidence that FAT10 functions as a novel pro-survival and pro-malignant factor in tumorigenesis. Further in depth research on the mechanism of FAT10 that contributes to cell malignancy will provide new insights in cancer progression as well as present opportunities to target FAT10 in cancer. Therefore, based on our previous findings where FAT10 interaction with Mad2 as spindle mitotic checkpoint caused reduced localization of Mad2 at the kinetochore and subsequent aneuploidy, suggested FAT10 contribution in tumorigenesis was potentially through its interaction with Mad2, which then caused its aberrant function. To gain a better understanding whether this

mechanism was truly the fundamental mechanism that contributed to tumorigenesis, we further analyzed the potential role of FAT10 and Mad2 interaction.

### 4.5 Identification of specific Mad2 binding sites on FAT10

As mentioned earlier that FAT10 and Mad2 interaction played an important role in FAT10's pro-malignancy role and aneuploidy, we further extensively examined the importance of this protein-protein interaction. In order to find the specific site where MAD2 protein binds to FAT10 protein, we need to elucidate the FAT10 protein structure. Since the FAT10 crystal structure has not been resolved to date. Hence, in collaboration with A/P Song Jianxing from National University of Singapore (NUS), nuclear magnetic resonance (NMR) was employed to identify the specific amino acid residues that may be important for its interaction with Mad2. Since FAT10 and Mad2 are small protein molecules, which consist of 17-kilo Dalton (kDa) and 24-kilo Dalton (kDa) respectively, they will form a complex that is less than 100 kDa, which is amenable to NMR elucidation of its protein-protein interaction. This is because small proteins allows detection of a distinct chemical shift or perturbation upon building of complexes in $^{1}H$-$^{15}N$-HSQC spectrums, unlike large proteins, which has thousands of one dimensional spectrums and has a higher possibility of signal overlaps (Marintchev et al 2007, Nishida and Shimada 2012). Typically, $^{1}H$-$^{15}N$ HSQC spectrums were used to analyze the protein structure of an isotope-labeled protein (Liu et al 2005, Wuthrich 1990). Analysis of HSQC spectrum of $^{15}N$-labeled-FAT10 proteins obtained from the NMR study facilitated the "fingerprint" of each FAT10 amino acid residues. A subsequent addition of unlabelled-Mad2 protein into FAT10

protein solution allowed Mad2 to interact with FAT10 and caused the changes in FAT10's amino acid equilibrium, which resulted in "shifting" in $^{1}H$-$^{15}N$-HSQC spectrums. Finally, by mapping the $^{1}H$-$^{15}N$-HSQC spectrums from FAT10 protein alone across the $^{1}H$-$^{15}N$-HSQC spectrums from FAT10 and Mad2 complex, one can identify the specific amino acid residues in FAT10 that were responsible for its binding with Mad2 protein, since the signals will shift in $^{1}H$-$^{15}N$-HSQC spectrums upon the addition of Mad2 protein. The NMR study unraveled two interaction regions within FAT10 that are important for binding with Mad2.

To validate the results obtained from NMR study, fusion-PCR mutagenesis approach was employed to generate the mutant constructs and subsequently obtaining the various FAT10 stable mutants. After the successful generation of FAT10 overexpressing stable cells and its various mutant FAT10 stable cells, we used two different methods to examine, whether the NMR-predicted regions were specific for FAT10 and Mad2 binding and did not interfere with other FAT10's interaction partners. We used co-Immunoprecipitation and in-situ proximity ligation assay (PLA) (Clausson et al 2011, Leuchowius et al 2011) to ascertain the protein-protein interaction between FAT10 and Mad2. As shown, in Figure 3.10 and 3.11, only mutations at both predicted Mad2 interaction regions in FAT10 protein abolished its interaction with Mad2. Notably, mutation at these regions did not affect the interaction of FAT10 with the other proteins, which has been previously reported to interact with FAT10 either covalently such as with p62 and UBA6 proteins or non-covalently with HDAC6, and NUB1L proteins (Table1.3). In conclusion, the specific interaction sites between FAT10 and Mad2 protein that were important for their binding to each other was identified. The identification of specific regions in FAT10 that affect its binding with Mad2 but not other proteins

suggest that its other functions of FAT10 such as its function in immune response (Canaan et al 2006, Liu et al 1999b) (Ren et al 2011b) and protein degradation (Schmidtke et al 2006) may not be affected. Further investigation to reveal the effect of disruption of FAT10 and Mad2binding in tumorigenesis was also performed in this thesis and will be described in the next section.

## 4.6 The implications of the abolishment of FAT10 and Mad2 binding in tumorigenesis

Having identified the specific FAT10 amino acid residues that are important for its binding to Mad2 protein, we then further investigated the effect of disruption from FAT10 and Mad2 binding in influencing cellular functions and tumorigenesis (transformation, invasion, and migration abilities). *In vitro* assays such as cell proliferation assay, apoptosis assay, soft agar cell transformation assay, adhesion assay, wound-healing assay, F-actin staining and invasion assay were employed to check the importance of FAT10 and Mad2 binding in FAT10's oncogenic role using the wild type FAT10 and mutant FAT10 that we generated.

Several key observations were made: firstly, disruption of FAT10 and Mad2 binding at both sites decreased the cell proliferation rate and cell malignant transformation ability. Secondly, this disruption also enabled the cells to be more prone to cytotoxic-induced cell death. Thirdly, adhesive properties of FAT10 mutant stable cells were also significantly reduced compared to wild type FAT10 stable overexpressing cells. Finally, the migratory and invasive capabilities of these mutant cells where FAT10 interaction with Mad2, is disrupted were also greatly abated. Taken together, all these *in vitro* experiments show that the abolishment of FAT10 and Mad2 binding can reverse the cell malignant features

of cancer cells. Hence, suggesting a novel mechanism of FAT10 that important in tumorigenesis. Our findings strongly suggest that its interaction with Mad2 mediates FAT10 role in tumorigenesis. Targeting this mechanism through the disruption of FAT10 interaction with Mad2 reduced the pro-survival and pro-malignant roles of FAT10 significantly.

In corroboration with our *in vitro* findings mentioned earlier, we also observed a negative effect of the disruption FAT10 and Mad2 binding on tumor growth in xenograft mice model. Significantly, smaller tumors were observed in mice injected with FAT10 stable mutants, where its interaction with Mad2 is disrupted. However, mutations at only a single region of Mad2 interaction regions within FAT10 did not significantly reduce the size of tumors isolated from the nude mice 3 weeks after subcutaneous injection of these FAT10 stable mutants into the flanking region of these nude mice. Thus, these *in vivo* observations have further strengthened our observation that the oncogenic role of FAT10 is largely attributable to its interaction with Mad2, and disruption of this interaction significantly reduced the malignancy of cancer cells. Having confirmed the significance of FAT10 and Mad2 interaction, we then asked, if the disruption of FAT10 and Mad2 binding site will also affects the rate of aneuploidy of the cells, since FAT10 overexpression has been previously reported to cause reduced localization of Mad2 at kinetochore during mitosis, which then led to aneuploidy. Interestingly, we discovered that the abolishment of FAT10 and Mad2 binding reduced cell aneuploidy based on our karyotyping profile of FAT10 mutant cells carrying mutations at both interaction sites. Moreover, we also demonstrated that these FAT10 mutants were unable to escape the mitotic arrest unlike their wild type FAT10 stable cells counterparts, which were able to induce a greater escape

from mitotic arrest. In concordance with our previous findings, we also found that mutations only at one region of FAT10 and Mad2 interaction regions did not increase the level of aneuploidy nor did it help the cells to escape from mitotic arrest. Hence, not only have we shown that complete disruption of FAT10 and Mad2 binding at both sites reduced the malignant attributes of the cells but we have also successfully demontrated its role in the reduction of aneuploidy, which is widely recognized to play a major role in oncogenesis (Hede 2005). In summary, through *in vitro* as well as *in vivo* studies we have clearly revealed the important mechanism of FAT10 that contributes to tumorigenesis.

### 4.7 Aberrant Mad2 function is the mechanism for FAT10 to cause aneuploidy

Having shown that FAT10 overexpression induces aneuploidy in cells and disruption of FAT10 and Mad2 interaction reduces aneuploidy. Going forward, we examined whether FAT10 promoted aneuploidy through Mad2 or if there were any other mechanisms involved in this process? Through this investigation we then were able to dissect the specific mechanism of FAT10 that contributed in tumorigenesis.

A reduction of Mad2 levels by siRNA or FAT10 overexpression was used to examine if FAT10-overexpressing cells phenocopied the effect of Mad2 knock down on aneuploidy. Remarkably, we found that FAT10 overexpression phenocopies Mad2 knockdown. Therefore, the results strongly suggest that FAT10's role in aneuploidy is linked with aberrant Mad2 function. On the other hand, if aneuploidy observed in FAT10 overexpressing cells were not linked with dysregulation of Mad2 function than similar phenotypes from FAT10-overexpressing cells and Mad2 knock down cells would not have been observed.

However, since FAT10 overexpression or Mad2 knockdown were able to reduce Mad2 level or caused an aberrant Mad2 function, a similar proportion of chromosome number were observed either when FAT10 was overexpressed, or when Mad2 was knocked down.

Next, we further investigated, whether FAT10 overexpression or Mad2 knockdown had also a similar effect on its ability to help cells escape mitotic arrest. Similar to our previous findings, we found that either FAT10 overexpression or Mad2 knockdown were also equally efficient in enhancing the ability of the cells to escape from mitotic arrest. In summary, all the data presented in this thesis have highlighted the importance of FAT10 overexpression in driving tumorigenesis, as well as the fundamental mechanism in which FAT10 contributed to tumorigenesis, through its interaction with Mad2, which then aberrantly altered Mad2 function during cell cycle progression.

### 4.8 The impact of our work on the field of cancer research

Elucidating the role of FAT10 in tumorigenesis not only provided new insights on the ability of FAT10 to drive tumorigenesis and the role of FAT10 in promoting cell malignancy, but it also highlighted the important mechanism by which FAT10 initiates tumorigenesis, which is via Mad2-binding. We have shown that abrogation of the Mad2-binding function in FAT10 did not affect FAT10 binding to its other interaction partners, therefore making the targeting residues within FAT10 that binds to Mad2 an attractive therapeutic option.

FAT10 has been previously reported to be associated with inflammation as its expression was inducible by pro-inflammatory cytokines such as TNF-α and IFN-γ in immune cells and cancer cells (Liu et al 1999a, Lukasiak et al 2008b, Ren et al

2011a). Likewise, FAT10 was also highly expressed in organs of the immune system and inflammation-associated cancers (Bates et al 1997, Lee et al 2003). Interestingly, in the colorectal cancer cell line HCT116 induction of FAT10 through TNF-α required NF-κB activation (Ren et al 2011b). Anti-TNF-α drugs such as adalimumab (humira), infliximab (remicade), and etanercept (enbrel) have been marketed and used to treat cancers. However, since TNF-α is part of immune system and it protects the body from infection, long-term treatment of TNF-α-antagonist has been reported to increase a patient's susceptibility to fatal infections (Frank et al 2009). Moreover, TNF-α inhibitors have been reported to have great adverse drug reactions (Fiorino et al 2011, Wolfe and Michaud 2004). Likewise, for NFkB inhibitors many other important cellular functions will be affected, since NFkB is a major transcription factor of many important genes. Therefore, targeting FAT10 directly may be a more favorable approach.

Thus far the associations of FAT10 in tumorigenesis have been mostly inferential, based on correlative expression study of FAT10 in tumor samples. The direct evidence of FAT10's ability as a driving force to initiate or drive the tumor growth and cell malignancy has not been examined. Although FAT10 has been previously reported to induce aneuploidy by binding to mitotic spindle checkpoint Mad2 and causing the reduction of its localization at the kinetochores during pro-metaphase, it remains unclear whether FAT10 and Mad2 interaction is the key mechanism that can potentially drive cells from aneuploidy state to become cancerous. Our study has paved the way for the use of FAT10 as a potential therapeutic target in cancer.

For the first time, the work in this thesis provided strong evidence to show that indeed FAT10 enhanced cancer cells malignancy by inducing cell growth, cell

survival, cell invasion, cell migration and cell aneuploidy. Additionally, FAT10 overexpression initiated cell malignant transformation in non-tumorigenic cells. Abolishment of FAT10 and Mad2 interaction led to tumor regression and weakened cell malignancy. Thus our data gave us a more comprehensive understanding on FAT10's mechanism in driving tumorigenesis. Characterization of FAT10 overexpression in the *in vivo* environment was also for the first time demonstrated in this thesis. Our findings on FAT10's pro-malignancy role and its mechanism provided us with a new potential cancer therapeutic target.

### 4.9 Conclusion and future perspectives

Taken together, we have characterized the pro-malignancy function of FAT10. We have demonstrated that FAT10 hijacks the spindle checkpoint role of Mad2 during mitosis through its interaction with Mad2, resulting in the delocalization of Mad2 from the kinetochores and leading to abnormal chromosomes segregation, aneuploidy, and finally cancer development.

Importantly, we have successfully identified the specific Mad2 interaction sites on FAT10. This is a significant step in enabling the mechanisms by which FAT10 exerts its pro-malignancy effects. The use of FAT10 mutants with abrogated Mad2 binding in various cellular functional assays and xenograft mice model provided strong evidence that FAT10 induces tumorigenesis by binding to Mad2.

We have found that mutating the Mad2-binding sites on FAT10 does not affect the interaction of FAT10 with its other interaction partners. This marks FAT10 as a potential therapeutic target for cancer. For future work, we propose the synthesis of a small-molecule FAT10 inhibitor which binds to the Mad2-binding

sites on FAT10 to create a steric hindrance effect, and thus, preventing Mad2 from binding to these sites.

This would be useful in our effort to translate our findings from bench to bedside. Given that FAT10 is an ubiquitin-like protein which has been activated through a cascade of enzymes through its double glycine residues, a more in depth study about the role of these glysine residues in FAT10 pro-malignancy will also be important and interesting for future explorations. In addition, we propose that these studies on the pro-malignancy role of FAT10 be extended to non-tumorigenic cells in addition to using cancer cells. This will give us an insight on the role of FAT10 on cancer initiation.

In summary, in this thesis we have demonstrated FAT10's ability in increasing the malignancy including tumor growth of colorectal cancer HCT116 cells. In addition, using non-tumorigenic immortalized human neo-natal hepatocytes cells (NeHepLxHT), we were able to initiate the malignant cell transformation of these normal hepatocytes in soft agar, showing the capability of FAT10 in driving and initiating tumorigenesis. Based on our findings on the significance of disruption of Mad2 binding site on FAT10 in reducing tumor growth *in vivo*, our results have paved the way for the development of a potential drug that can specifically bind to these sites and prevent Mad2 binding to these sites without affecting FAT10's interaction with its other interaction partners. Thus, our results demonstrated the translational potential of our study.

Ai H, Barrera JE, Meyers AD, Shroyer KR, Varella-Garcia M (2001). Chromosomal aneuploidy precedes morphological changes and supports multifocality in head and neck lesions. *Laryngoscope* **111:** 1853-1858.

Aichem A, Pelzer C, Lukasiak S, Kalveram B, Sheppard PW, Rani N *et al* (2010). USE1 is a bispecific conjugating enzyme for ubiquitin and FAT10, which FAT10ylates itself in cis. *Nat Commun* **1:** 13.

Aichem A, Kalveram B, Spinnenhirn V, Kluge K, Catone N, Johansen T *et al* (2012a). The proteomic analysis of endogenous FAT10 substrates identifies p62/SQSTM1 as a substrate of FAT10ylation. *J Cell Sci* **125:** 4576-4585.

Aichem A, Kalveram B, Spinnenhirn V, Kluge K, Catone N, Johansen T *et al* (2012b). The proteomic analysis of endogenous FAT10 substrates identifies p62/SQSTM1 as a substrate of FAT10ylation. *J Cell Sci*.

Allende-Vega N, Dayal S, Agarwala U, Sparks A, Bourdon JC, Saville MK (2013). p53 is activated in response to disruption of the pre-mRNA splicing machinery. *Oncogene* **32:** 1-14.

Amersi F, Agustin M, Ko CY (2005). Colorectal cancer: epidemiology, risk factors, and health services. *Clin Colon Rectal Surg* **18:** 133-140.

Ataseven H, Bahcecioglu IH, Kuzu N, Yalniz M, Celebi S, Erensoy A *et al* (2006). The levels of ghrelin, leptin, TNF-alpha, and IL-6 in liver cirrhosis and hepatocellular carcinoma due to HBV and HDV infection. *Mediators Inflamm* **2006:** 78380.

Baker DJ, Jeganathan KB, Malureanu L, Perez-Terzic C, Terzic A, van Deursen JM (2006). Early aging-associated phenotypes in Bub3/Rae1 haploinsufficient mice. *J Cell Biol* **172:** 529-540.

Baker DJ, Dawlaty MM, Wijshake T, Jeganathan KB, Malureanu L, van Ree JH *et al* (2012). Increased expression of BubR1 protects against aneuploidy and cancer and extends healthy lifespan. *Nat Cell Biol* **15:** 96-102.

Bates EE, Ravel O, Dieu MC, Ho S, Guret C, Bridon JM *et al* (1997). Identification and analysis of a novel member of the ubiquitin family expressed in dendritic cells and mature B cells. *Eur J Immunol* **27:** 2471-2477.

Bektas N, Noetzel E, Veeck J, Press MF, Kristiansen G, Naami A *et al* (2008). The ubiquitin-like molecule interferon-stimulated gene 15 (ISG15) is a potential prognostic marker in human breast cancer. *Breast Cancer Res* **10:** R58.

Beroukhim R, Mermel CH, Porter D, Wei G, Raychaudhuri S, Donovan J *et al* (2010). The landscape of somatic copy-number alteration across human cancers. *Nature* **463:** 899-905.

Birchler JA, Veitia RA (2007). The gene balance hypothesis: from classical genetics to modern genomics. *Plant Cell* **19:** 395-402.

Bohren KM, Nadkarni V, Song JH, Gabbay KH, Owerbach D (2004). A M55V polymorphism in a novel SUMO gene (SUMO-4) differentially activates heat shock transcription factors and is associated with susceptibility to type I diabetes mellitus. *J Biol Chem* **279:** 27233-27238.

Buchsbaum S, Bercovich B, Ciechanover A (2012). FAT10 is a proteasomal degradation signal that is itself regulated by ubiquitination. *Mol Biol Cell* **23:** 225-232.

Buffin E, Lefebvre C, Huang J, Gagou ME, Karess RE (2005). Recruitment of Mad2 to the kinetochore requires the Rod/Zw10 complex. *Curr Biol* **15:** 856-861.

Cahill DP, Lengauer C, Yu J, Riggins GJ, Willson JK, Markowitz SD *et al* (1998). Mutations of mitotic checkpoint genes in human cancers. *Nature* **392:** 300-303.

Cajee UF, Hull R, Ntwasa M (2012). Modification by ubiquitin-like proteins: significance in apoptosis and autophagy pathways. *Int J Mol Sci* **13:** 11804-11831.

Canaan A, Yu X, Booth CJ, Lian J, Lazar I, Gamfi SL *et al* (2006). FAT10/diubiquitin-like protein-deficient mice exhibit minimal phenotypic differences. *Mol Cell Biol* **26:** 5180-5189.

Cannon-Albright LA, Skolnick MH, Bishop DT, Lee RG, Burt RW (1988). Common inheritance of susceptibility to colonic adenomatous polyps and associated colorectal cancers. *N Engl J Med* **319:** 533-537.

Cardoso J, Molenaar L, de Menezes RX, van Leerdam M, Rosenberg C, Moslein G *et al* (2006). Chromosomal instability in MYH- and APC-mutant adenomatous polyps. *Cancer Res* **66:** 2514-2519.

Chao WC, Kulkarni K, Zhang Z, Kong EH, Barford D (2012). Structure of the mitotic checkpoint complex. *Nature* **484:** 208-213.

Chen RH, Waters JC, Salmon ED, Murray AW (1996). Association of spindle assembly checkpoint component XMAD2 with unattached kinetochores. *Science* **274:** 242-246.

Chen RH, Brady DM, Smith D, Murray AW, Hardwick KG (1999). The spindle checkpoint of budding yeast depends on a tight complex between the Mad1 and Mad2 proteins. *Mol Biol Cell* **10:** 2607-2618.

Chi YH, Ward JM, Cheng LI, Yasunaga J, Jeang KT (2009). Spindle assembly checkpoint and p53 deficiencies cooperate for tumorigenesis in mice. *Int J Cancer* **124:** 1483-1489.

Chiu YH, Sun Q, Chen ZJ (2007). E1-L2 activates both ubiquitin and FAT10. *Mol Cell* **27:** 1014-1023.

Choi BD, Jeong SJ, Wang G, Park JJ, Lim DS, Kim BH *et al* (2011). Secretory leukocyte protease inhibitor is associated with MMP-2 and MMP-9 to promote migration and invasion in SNU638 gastric cancer cells. *Int J Mol Med* **28:** 527-534.

Ciechanover A (1994). The ubiquitin-proteasome proteolytic pathway. *Cell* **79:** 13-21.

Ciechanover A, Iwai K (2004). The ubiquitin system: from basic mechanisms to the patient bed. *IUBMB Life* **56:** 193-201.

Clausson CM, Allalou A, Weibrecht I, Mahmoudi S, Farnebo M, Landegren U *et al* (2011). Increasing the dynamic range of in situ PLA. *Nat Methods* **8:** 892-893.

Cleveland DW, Mao Y, Sullivan KF (2003). Centromeres and kinetochores: from epigenetics to mitotic checkpoint signaling. *Cell* **112:** 407-421.

Confalonieri S, Quarto M, Goisis G, Nuciforo P, Donzelli M, Jodice G *et al* (2009). Alterations of ubiquitin ligases in human cancer and their association with the natural history of the tumor. *Oncogene* **28:** 2959-2968.

Cook WJ, Jeffrey LC, Xu Y, Chau V (1993). Tertiary structures of class I ubiquitin-conjugating enzymes are highly conserved: crystal structure of yeast Ubc4. *Biochemistry* **32:** 13809-13817.

Dasso M (2008). Emerging roles of the SUMO pathway in mitosis. *Cell Div* **3:** 5.

De Antoni A, Pearson CG, Cimini D, Canman JC, Sala V, Nezi L *et al* (2005). The Mad1/Mad2 complex as a template for Mad2 activation in the spindle assembly checkpoint. *Curr Biol* **15:** 214-225.

Desterro JM, Rodriguez MS, Hay RT (1998). SUMO-1 modification of IkappaBalpha inhibits NF-kappaB activation. *Mol Cell* **2:** 233-239.

DeVita VT, Jr., Rosenberg SA (2012). Two hundred years of cancer research. *N Engl J Med* **366:** 2207-2214.

Di Fiore PP, Polo S, Hofmann K (2003). When ubiquitin meets ubiquitin receptors: a signalling connection. *Nat Rev Mol Cell Biol* **4:** 491-497.

Dobles M, Liberal V, Scott ML, Benezra R, Sorger PK (2000). Chromosome missegregation and apoptosis in mice lacking the mitotic checkpoint protein Mad2. *Cell* **101:** 635-645.

Duesberg P, Rasnick D (2000). Aneuploidy, the somatic mutation that makes cancer a species of its own. *Cell Motil Cytoskeleton* **47:** 81-107.

Egeblad M, Werb Z (2002). New functions for the matrix metalloproteinases in cancer progression. *Nat Rev Cancer* **2:** 161-174.

Elsasser S, Gali RR, Schwickart M, Larsen CN, Leggett DS, Muller B *et al* (2002). Proteasome subunit Rpn1 binds ubiquitin-like protein domains. *Nat Cell Biol* **4:** 725-730.

Fan W, Cai W, Parimoo S, Schwarz DC, Lennon GG, Weissman SM (1996). Identification of seven new human MHC class I region genes around the HLA-F locus. *Immunogenetics* **44:** 97-103.

Fang G, Yu H, Kirschner MW (1998). The checkpoint protein MAD2 and the mitotic regulator CDC20 form a ternary complex with the anaphase-promoting complex to control anaphase initiation. *Genes Dev* **12:** 1871-1883.

Fang G (2002). Checkpoint protein BubR1 acts synergistically with Mad2 to inhibit anaphase-promoting complex. *Mol Biol Cell* **13:** 755-766.

Fava LL, Kaulich M, Nigg EA, Santamaria A (2011). Probing the in vivo function of Mad1:C-Mad2 in the spindle assembly checkpoint. *Embo J* **30:** 3322-3336.

Fiorino G, Peyrin-Biroulet L, Repici A, Malesci A, Danese S (2011). Adalimumab in ulcerative colitis: hypes and hopes. *Expert Opin Biol Ther* **11:** 109-116.

Frank KM, Hogarth DK, Miller JL, Mandal S, Mease PJ, Samulski RJ *et al* (2009). Investigation of the cause of death in a gene-therapy trial. *N Engl J Med* **361:** 161-169.

Galandiuk S, Wieand HS, Moertel CG, Cha SS, Fitzgibbons RJ, Jr., Pemberton JH *et al* (1992). Patterns of recurrence after curative resection of carcinoma of the colon and rectum. *Surg Gynecol Obstet* **174:** 27-32.

Gareau JR, Lima CD (2010). The SUMO pathway: emerging mechanisms that shape specificity, conjugation and recognition. *Nat Rev Mol Cell Biol* **11:** 861-871.

Geiss-Friedlander R, Melchior F (2007). Concepts in sumoylation: a decade on. *Nat Rev Mol Cell Biol* **8:** 947-956.

Geng J, Klionsky DJ (2008). The Atg8 and Atg12 ubiquitin-like conjugation systems in macroautophagy. 'Protein modifications: beyond the usual suspects' review series. *EMBO Rep* **9:** 859-864.

Glickman MH, Ciechanover A (2002). The ubiquitin-proteasome proteolytic pathway: destruction for the sake of construction. *Physiol Rev* **82:** 373-428.

Gorbsky GJ, Chen RH, Murray AW (1998). Microinjection of antibody to Mad2 protein into mammalian cells in mitosis induces premature anaphase. *J Cell Biol* **141:** 1193-1205.

Gordon DJ, Resio B, Pellman D (2012). Causes and consequences of aneuploidy in cancer. *Nat Rev Genet* **13:** 189-203.

Gostissa M, Hengstermann A, Fogal V, Sandy P, Schwarz SE, Scheffner M *et al* (1999). Activation of p53 by conjugation to the ubiquitin-like protein SUMO-1. *Embo J* **18:** 6462-6471.

Gruen JR, Nalabolu SR, Chu TW, Bowlus C, Fan WF, Goei VL *et al* (1996). A transcription map of the major histocompatibility complex (MHC) class I region. *Genomics* **36:** 70-85.

Haas AL, Ahrens P, Bright PM, Ankel H (1987). Interferon induces a 15-kilodalton protein exhibiting marked homology to ubiquitin. *J Biol Chem* **262:** 11315-11323.

Habu T, Kim SH, Weinstein J, Matsumoto T (2002). Identification of a MAD2-binding protein, CMT2, and its role in mitosis. *Embo J* **21:** 6419-6428.

Hanahan D, Weinberg RA (2000). The hallmarks of cancer. *Cell* **100:** 57-70.

Hanahan D, Weinberg RA (2011). Hallmarks of cancer: the next generation. *Cell* **144:** 646-674.

Hanks S, Coleman K, Reid S, Plaja A, Firth H, Fitzpatrick D *et al* (2004). Constitutional aneuploidy and cancer predisposition caused by biallelic mutations in BUB1B. *Nat Genet* **36:** 1159-1161.

Hede K (2005). Which came first? Studies clarify role of aneuploidy in cancer. *J Natl Cancer Inst* **97:** 87-89.

Herrmann J, Lerman LO, Lerman A (2007). Ubiquitin and ubiquitin-like proteins in protein regulation. *Circ Res* **100:** 1276-1291.

Hershko A, Ciechanover A (1998). The ubiquitin system. *Annu Rev Biochem* **67:** 425-479.

Herszenyi L, Tulassay Z (2010). Epidemiology of gastrointestinal and liver tumors. *Eur Rev Med Pharmacol Sci* **14:** 249-258.

Hewitt L, Tighe A, Santaguida S, White AM, Jones CD, Musacchio A *et al* (2010). Sustained Mps1 activity is required in mitosis to recruit O-Mad2 to the Mad1-C-Mad2 core complex. *J Cell Biol* **190:** 25-34.

Hipp MS, Kalveram B, Raasi S, Groettrup M, Schmidtke G (2005). FAT10, a ubiquitin-independent signal for proteasomal degradation. *Mol Cell Biol* **25:** 3483-3491.

Hitzler JK, Zipursky A (2005). Origins of leukaemia in children with Down syndrome. *Nat Rev Cancer* **5:** 11-20.

Hochstrasser M (1996a). Protein degradation or regulation: Ub the judge. *Cell* **84:** 813-815.

Hochstrasser M (1996b). Ubiquitin-dependent protein degradation. *Annu Rev Genet* **30:** 405-439.

Hochstrasser M (2009). Origin and function of ubiquitin-like proteins. *Nature* **458:** 422-429.

Howell BJ, Hoffman DB, Fang G, Murray AW, Salmon ED (2000). Visualization of Mad2 dynamics at kinetochores, along spindle fibers, and at spindle poles in living cells. *J Cell Biol* **150:** 1233-1250.

Howell BJ, Moree B, Farrar EM, Stewart S, Fang G, Salmon ED (2004). Spindle checkpoint protein dynamics at kinetochores in living cells. *Curr Biol* **14:** 953-964.

Jemal A, Center MM, DeSantis C, Ward EM (2010a). Global patterns of cancer incidence and mortality rates and trends. *Cancer Epidemiol Biomarkers Prev* **19:** 1893-1907.

Jemal A, Siegel R, Xu J, Ward E (2010b). Cancer statistics, 2010. *CA Cancer J Clin* **60:** 277-300.

Jentsch S, Pyrowolakis G (2000). Ubiquitin and its kin: how close are the family ties? *Trends Cell Biol* **10:** 335-342.

Ji F, Jin X, Jiao CH, Xu QW, Wang ZW, Chen YL (2009). FAT10 level in human gastric cancer and its relation with mutant p53 level, lymph node metastasis and TNM staging. *World J Gastroenterol* **15:** 2228-2233.

Kallio M, Weinstein J, Daum JR, Burke DJ, Gorbsky GJ (1998). Mammalian p55CDC mediates association of the spindle checkpoint protein Mad2 with the cyclosome/anaphase-promoting complex, and is involved in regulating anaphase onset and late mitotic events. *J Cell Biol* **141:** 1393-1406.

Kalveram B, Schmidtke G, Groettrup M (2008). The ubiquitin-like modifier FAT10 interacts with HDAC6 and localizes to aggresomes under proteasome inhibition. *J Cell Sci* **121:** 4079-4088.

Karess R (2005). Rod-Zw10-Zwilch: a key player in the spindle checkpoint. *Trends Cell Biol* **15:** 386-392.

Kerscher O, Felberbaum R, Hochstrasser M (2006). Modification of proteins by ubiquitin and ubiquitin-like proteins. *Annu Rev Cell Dev Biol* **22:** 159-180.

Khodjakov A, Rieder CL (2009). The nature of cell-cycle checkpoints: facts and fallacies. *J Biol* **8:** 88.

Kim HT, Kim KP, Lledias F, Kisselev AF, Scaglione KM, Skowyra D *et al* (2007). Certain pairs of ubiquitin-conjugating enzymes (E2s) and ubiquitin-protein ligases (E3s) synthesize nondegradable forked ubiquitin chains containing all possible isopeptide linkages. *J Biol Chem* **282:** 17375-17386.

Kim KI, Baek SH (2009). Small ubiquitin-like modifiers in cellular malignancy and metastasis. *Int Rev Cell Mol Biol* **273:** 265-311.

Kinzler KW, Vogelstein B (1996). Lessons from hereditary colorectal cancer. *Cell* **87:** 159-170.

Knekt P, Hakama M, Jarvinen R, Pukkala E, Heliovaara M (1998). Smoking and risk of colorectal cancer. *Br J Cancer* **78:** 136-139.

Kops GJ, Kim Y, Weaver BA, Mao Y, McLeod I, Yates JR, 3rd *et al* (2005a). ZW10 links mitotic checkpoint signaling to the structural kinetochore. *J Cell Biol* **169:** 49-60.

Kops GJ, Weaver BA, Cleveland DW (2005b). On the road to cancer: aneuploidy and the mitotic checkpoint. *Nat Rev Cancer* **5:** 773-785.

Kucej M, Zou H (2010). DNA-dependent cohesin cleavage by separase. *Nucleus* **1:** 4-7.

Lampson MA, Kapoor TM (2005). The human mitotic checkpoint protein BubR1 regulates chromosome-spindle attachments. *Nat Cell Biol* **7:** 93-98.

Lee CG, Ren J, Cheong IS, Ban KH, Ooi LL, Yong Tan S *et al* (2003). Expression of the FAT10 gene is highly upregulated in hepatocellular carcinoma and other gastrointestinal and gynecological cancers. *Oncogene* **22:** 2592-2603.

Lemaire K, Moura RF, Granvik M, Igoillo-Esteve M, Hohmeier HE, Hendrickx N *et al* (2011). Ubiquitin fold modifier 1 (UFM1) and its target UFBP1 protect pancreatic beta cells from ER stress-induced apoptosis. *PLoS One* **6:** e18517.

Leuchowius KJ, Weibrecht I, Soderberg O (2011). In situ proximity ligation assay for microscopy and flow cytometry. *Curr Protoc Cytom* **Chapter 9:** Unit 9 36.

Li GQ, Li H, Zhang HF (2003). Mad2 and p53 expression profiles in colorectal cancer and its clinical significance. *World J Gastroenterol* **9:** 1972-1975.

Li R, Sonik A, Stindl R, Rasnick D, Duesberg P (2000). Aneuploidy vs. gene mutation hypothesis of cancer: recent study claims mutation but is found to support aneuploidy. *Proc Natl Acad Sci U S A* **97:** 3236-3241.

Li T, Santockyte R, Yu S, Shen RF, Tekle E, Lee CG *et al* (2011). FAT10 modifies p53 and upregulates its transcriptional activity. *Arch Biochem Biophys* **509:** 164-169.

Li Y, Benezra R (1996). Identification of a human mitotic checkpoint gene: hsMAD2. *Science* **274:** 246-248.

Li Y, Gorbea C, Mahaffey D, Rechsteiner M, Benezra R (1997). MAD2 associates with the cyclosome/anaphase-promoting complex and inhibits its activity. *Proc Natl Acad Sci U S A* **94:** 12431-12436.

Lim CB, Zhang D, Lee CG (2006). FAT10, a gene up-regulated in various cancers, is cell-cycle regulated. *Cell Div* **1:** 20.

Liu G, Shen Y, Atreya HS, Parish D, Shao Y, Sukumaran DK *et al* (2005). NMR data collection and analysis protocol for high-throughput protein structure determination. *Proc Natl Acad Sci U S A* **102:** 10487-10492.

Liu YC, Pan J, Zhang C, Fan W, Collinge M, Bender JR *et al* (1999a). A MHC-encoded ubiquitin-like protein (FAT10) binds noncovalently to the spindle assembly checkpoint protein MAD2. *Proc Natl Acad Sci U S A* **96:** 4313-4318.

Liu YC, Pan J, Zhang C, Fan W, Collinge M, Bender JR *et al* (1999b). A MHC-encoded ubiquitin-like protein (FAT10) binds noncovalently to the spindle assembly checkpoint protein MAD2. *Proc Natl Acad Sci U S A* **96:** 4313-4318.

Logarinho E, Resende T, Torres C, Bousbaa H (2008). The human spindle assembly checkpoint protein Bub3 is required for the establishment of efficient kinetochore-microtubule attachments. *Mol Biol Cell* **19:** 1798-1813.

Lukasiak S, Breuhahn K, Schiller C, Schmidtke G, Groettrup M (2008a). Quantitative analysis of gene expression relative to 18S rRNA in carcinoma samples using the LightCycler instrument and a SYBR GreenI-based assay: determining FAT10 mRNA levels in hepatocellular carcinoma. *Methods Mol Biol* **429:** 59-72.

Lukasiak S, Schiller C, Oehlschlaeger P, Schmidtke G, Krause P, Legler DF *et al* (2008b). Proinflammatory cytokines cause FAT10 upregulation in cancers of liver and colon. *Oncogene* **27:** 6068-6074.

Madsen L, Schulze A, Seeger M, Hartmann-Petersen R (2007). Ubiquitin domain proteins in disease. *BMC Biochem* **8 Suppl 1:** S1.

Mahajan R, Delphin C, Guan T, Gerace L, Melchior F (1997). A small ubiquitin-related polypeptide involved in targeting RanGAP1 to nuclear pore complex protein RanBP2. *Cell* **88:** 97-107.

Mani A, Gelmann EP (2005). The ubiquitin-proteasome pathway and its role in cancer. *J Clin Oncol* **23:** 4776-4789.

Marin JJ, Sanchez de Medina F, Castano B, Bujanda L, Romero MR, Martinez-Augustin O *et al* (2012). Chemoprevention, chemotherapy, and chemoresistance in colorectal cancer. *Drug Metab Rev* **44:** 148-172.

Marintchev A, Frueh D, Wagner G (2007). NMR methods for studying protein-protein interactions involved in translation initiation. *Methods Enzymol* **430:** 283-331.

Markowitz SD, Dawson DM, Willis J, Willson JK (2002). Focus on colon cancer. *Cancer Cell* **1:** 233-236.

Markowitz SD, Bertagnolli MM (2009). Molecular origins of cancer: Molecular basis of colorectal cancer. *N Engl J Med* **361:** 2449-2460.

Matic I, van Hagen M, Schimmel J, Macek B, Ogg SC, Tatham MH *et al* (2008). In vivo identification of human small ubiquitin-like modifier polymerization sites by high accuracy mass spectrometry and an in vitro to in vivo strategy. *Mol Cell Proteomics* **7:** 132-144.

Maurici D, Perez-Atayde A, Grier HE, Baldini N, Serra M, Fletcher JA (1998). Frequency and implications of chromosome 8 and 12 gains in Ewing sarcoma. *Cancer Genet Cytogenet* **100:** 106-110.

Melsheimer P, Vinokurova S, Wentzensen N, Bastert G, von Knebel Doeberitz M (2004). DNA aneuploidy and integration of human papillomavirus type 16 e6/e7 oncogenes in intraepithelial neoplasia and invasive squamous cell carcinoma of the cervix uteri. *Clin Cancer Res* **10:** 3059-3063.

Michel L, Diaz-Rodriguez E, Narayan G, Hernando E, Murty VV, Benezra R (2004). Complete loss of the tumor suppressor MAD2 causes premature cyclin B degradation and mitotic failure in human somatic cells. *Proc Natl Acad Sci U S A* **101:** 4459-4464.

Michel LS, Liberal V, Chatterjee A, Kirchwegger R, Pasche B, Gerald W *et al* (2001). MAD2 haplo-insufficiency causes premature anaphase and chromosome instability in mammalian cells. *Nature* **409:** 355-359.

Minhas KM, Singh B, Jiang WW, Sidransky D, Califano JA (2003). Spindle assembly checkpoint defects and chromosomal instability in head and neck squamous cell carcinoma. *Int J Cancer* **107:** 46-52.

Morin V, Prieto S, Melines S, Hem S, Rossignol M, Lorca T *et al* (2012). CDK-dependent potentiation of MPS1 kinase activity is essential to the mitotic checkpoint. *Curr Biol* **22:** 289-295.

Mukhopadhyay D, Riezman H (2007). Proteasome-independent functions of ubiquitin in endocytosis and signaling. *Science* **315:** 201-205.

Muller S, Berger M, Lehembre F, Seeler JS, Haupt Y, Dejean A (2000). c-Jun and p53 activity is modulated by SUMO-1 modification. *J Biol Chem* **275:** 13321-13329.

Murray AW (2011). A brief history of error. *Nat Cell Biol* **13:** 1178-1182.

Musacchio A, Salmon ED (2007). The spindle-assembly checkpoint in space and time. *Nat Rev Mol Cell Biol* **8:** 379-393.

Nagashima Y, Kowa H, Tsuji S, Iwata A (2011). FAT10 protein binds to polyglutamine proteins and modulates their solubility. *J Biol Chem* **286:** 29594-29600.

Nakamura M, Yamaguchi S (2006). The ubiquitin-like protein MNSFbeta regulates ERK-MAPK cascade. *J Biol Chem* **281:** 16861-16869.

Nakayama KI, Nakayama K (2006). Ubiquitin ligases: cell-cycle control and cancer. *Nat Rev Cancer* **6:** 369-381.

Nishida N, Shimada I (2012). An NMR method to study protein-protein interactions. *Methods Mol Biol* **757:** 129-137.

Odagiri S, Tanji K, Mori F, Kakita A, Takahashi H, Kamitani T *et al* (2012). Immunohistochemical analysis of Marinesco bodies, using antibodies against proteins implicated in the ubiquitin-proteasome system, autophagy and aggresome formation. *Neuropathology* **32:** 261-266.

Oliva J, Bardag-Gorce F, French BA, Li J, McPhaul L, Amidi F *et al* (2008). Fat10 is an epigenetic marker for liver preneoplasia in a drug-primed mouse model of tumorigenesis. *Exp Mol Pathol* **84:** 102-112.

Orlowski RZ, Kuhn DJ (2008). Proteasome inhibitors in cancer therapy: lessons from the first decade. *Clin Cancer Res* **14:** 1649-1657.

Ozery-Flato M, Linhart C, Trakhtenbrot L, Izraeli S, Shamir R (2011). Large-scale analysis of chromosomal aberrations in cancer karyotypes reveals two distinct paths to aneuploidy. *Genome Biol* **12:** R61.

Pelzer C, Groettrup M (2010). FAT10 : Activated by UBA6 and Functioning in Protein Degradation. *Subcell Biochem* **54:** 238-246.

Peters JM (2002). The anaphase-promoting complex: proteolysis in mitosis and beyond. *Mol Cell* **9:** 931-943.

Pickard MR, Mourtada-Maarabouni M, Williams GT (2011). Candidate tumour suppressor Fau regulates apoptosis in human cells: an essential role for Bcl-G. *Biochim Biophys Acta* **1812:** 1146-1153.

Pines J (2006). Mitosis: a matter of getting rid of the right protein at the right time. *Trends Cell Biol* **16:** 55-63.

Qi H, Dal Cin P, Hernandez JM, Garcia JL, Sciot R, Fletcher C *et al* (1996). Trisomies 8 and 20 in desmoid tumors. *Cancer Genet Cytogenet* **92:** 147-149.

Qing X, French BA, Oliva J, French SW (2011). Increased expression of FAT10 in colon benign, premalignant and malignant epithelial neoplasms. *Exp Mol Pathol* **90:** 51-54.

Raasi S, Schmidtke G, Groettrup M (2001). The ubiquitin-like protein FAT10 forms covalent conjugates and induces apoptosis. *J Biol Chem* **276:** 35334-35343.

Rabut G, Peter M (2008). Function and regulation of protein neddylation. 'Protein modifications: beyond the usual suspects' review series. *EMBO Rep* **9:** 969-976.

Rajput A, Dominguez San Martin I, Rose R, Beko A, Levea C, Sharratt E *et al* (2008). Characterization of HCT116 human colon cancer cells in an orthotopic model. *J Surg Res* **147:** 276-281.

Rani N, Aichem A, Schmidtke G, Kreft SG, Groettrup M (2012). FAT10 and NUB1L bind to the VWA domain of Rpn10 and Rpn1 to enable proteasome-mediated proteolysis. *Nat Commun* **3:** 749.

Rao CV, Yang YM, Swamy MV, Liu T, Fang Y, Mahmood R *et al* (2005). Colonic tumorigenesis in BubR1+/-ApcMin/+ compound mutant mice is linked to premature separation of sister chromatids and enhanced genomic instability. *Proc Natl Acad Sci U S A* **102:** 4365-4370.

Ren J, Kan A, Leong SH, Ooi LL, Jeang KT, Chong SS *et al* (2006). FAT10 plays a role in the regulation of chromosomal stability. *J Biol Chem* **281:** 11413-11421.

Ren J, Wang Y, Gao Y, Mehta SB, Lee CG (2011a). FAT10 mediates the effect of TNF-alpha in inducing chromosomal instability. *J Cell Sci* **124:** 3665-3675.

Ren J, Wang Y, Gao Y, Mehta SB, Lee CG (2011b). FAT10 mediates the effect of TNF-alpha in inducing chromosomal instability. *J Cell Sci* **124:** 3665-3675.

Rieder CL, Schultz A, Cole R, Sluder G (1994). Anaphase onset in vertebrate somatic cells is controlled by a checkpoint that monitors sister kinetochore attachment to the spindle. *J Cell Biol* **127:** 1301-1310.

Rubinstein AD, Eisenstein M, Ber Y, Bialik S, Kimchi A (2011). The autophagy protein Atg12 associates with antiapoptotic Bcl-2 family members to promote mitochondrial apoptosis. *Mol Cell* **44:** 698-709.

Rustgi AK (2007). The genetics of hereditary colon cancer. *Genes Dev* **21:** 2525-2538.

Ryan SD, Britigan EM, Zasadil LM, Witte K, Audhya A, Roopra A *et al* (2012). Up-regulation of the mitotic checkpoint component Mad1 causes chromosomal instability and resistance to microtubule poisons. *Proc Natl Acad Sci U S A* **109:** E2205-2214.

Saeki A, Tamura S, Ito N, Kiso S, Matsuda Y, Yabuuchi I *et al* (2002). Frequent impairment of the spindle assembly checkpoint in hepatocellular carcinoma. *Cancer* **94:** 2047-2054.

Sandler RS (1996). Epidemiology and risk factors for colorectal cancer. *Gastroenterol Clin North Am* **25:** 717-735.

Schmidtke G, Kalveram B, Weber E, Bochtler P, Lukasiak S, Hipp MS *et al* (2006). The UBA domains of NUB1L are required for binding but not for

accelerated degradation of the ubiquitin-like modifier FAT10. *J Biol Chem* **281:** 20045-20054.

Schuyler SC, Wu YF, Kuan VJ (2012). The Mad1-Mad2 balancing act - a damaged spindle checkpoint in chromosome instability and cancer. *J Cell Sci* **125:** 4197-4206.

Schvartzman JM, Sotillo R, Benezra R (2010). Mitotic chromosomal instability and cancer: mouse modelling of the human disease. *Nat Rev Cancer* **10:** 102-115.

Schvartzman JM, Duijf PH, Sotillo R, Coker C, Benezra R (2011). Mad2 is a critical mediator of the chromosome instability observed upon Rb and p53 pathway inhibition. *Cancer Cell* **19:** 701-714.

Shah JV, Botvinick E, Bonday Z, Furnari F, Berns M, Cleveland DW (2004). Dynamics of centromere and kinetochore proteins; implications for checkpoint signaling and silencing. *Curr Biol* **14:** 942-952.

Sotillo R, Hernando E, Diaz-Rodriguez E, Teruya-Feldstein J, Cordon-Cardo C, Lowe SW *et al* (2007). Mad2 overexpression promotes aneuploidy and tumorigenesis in mice. *Cancer Cell* **11:** 9-23.

Steeg PS (2003). Metastasis suppressors alter the signal transduction of cancer cells. *Nat Rev Cancer* **3:** 55-63.

Sudakin V, Chan GK, Yen TJ (2001). Checkpoint inhibition of the APC/C in HeLa cells is mediated by a complex of BUBR1, BUB3, CDC20, and MAD2. *J Cell Biol* **154:** 925-936.

Sullivan M, Morgan DO (2007). Finishing mitosis, one step at a time. *Nat Rev Mol Cell Biol* **8:** 894-903.

Sun Y (2006). E3 ubiquitin ligases as cancer targets and biomarkers. *Neoplasia* **8:** 645-654.

Szlosarek P, Charles KA, Balkwill FR (2006). Tumour necrosis factor-alpha as a tumour promoter. *Eur J Cancer* **42:** 745-750.

Tang Z, Bharadwaj R, Li B, Yu H (2001). Mad2-Independent inhibition of APCCdc20 by the mitotic checkpoint protein BubR1. *Dev Cell* **1:** 227-237.

Tang Z, Shu H, Oncel D, Chen S, Yu H (2004). Phosphorylation of Cdc20 by Bub1 provides a catalytic mechanism for APC/C inhibition by the spindle checkpoint. *Mol Cell* **16:** 387-397.

Taylor SS, Ha E, McKeon F (1998). The human homologue of Bub3 is required for kinetochore localization of Bub1 and a Mad3/Bub1-related protein kinase. *J Cell Biol* **142:** 1-11.

Taylor SS, Scott MI, Holland AJ (2004). The spindle checkpoint: a quality control mechanism which ensures accurate chromosome segregation. *Chromosome Res* **12:** 599-616.

Terzic J, Grivennikov S, Karin E, Karin M (2010). Inflammation and colon cancer. *Gastroenterology* **138:** 2101-2114 e2105.

Torres EM, Williams BR, Amon A (2008). Aneuploidy: cells losing their balance. *Genetics* **179:** 737-746.

Tu Y, Chen C, Pan J, Xu J, Zhou ZG, Wang CY (2012). The Ubiquitin Proteasome Pathway (UPP) in the regulation of cell cycle control and DNA damage repair and its implication in tumorigenesis. *Int J Clin Exp Pathol* **5:** 726-738.

Van der Veen AG, Schorpp K, Schlieker C, Buti L, Damon JR, Spooner E *et al* (2011). Role of the ubiquitin-like protein Urm1 as a noncanonical lysine-directed protein modifier. *Proc Natl Acad Sci U S A* **108:** 1763-1770.

van der Veen AG, Ploegh HL (2012). Ubiquitin-like proteins. *Annu Rev Biochem* **81:** 323-357.

Varetti G, Guida C, Santaguida S, Chiroli E, Musacchio A (2011). Homeostatic control of mitotic arrest. *Mol Cell* **44:** 710-720.

Wagenaar-Miller RA, Gorden L, Matrisian LM (2004). Matrix metalloproteinases in colorectal cancer: is it worth talking about? *Cancer Metastasis Rev* **23:** 119-135.

Wang CY, Yang P, Li M, Gong F (2009a). Characterization of a negative feedback network between SUMO4 expression and NFkappaB transcriptional activity. *Biochem Biophys Res Commun* **381:** 477-481.

Wang L, Yin F, Du Y, Du W, Chen B, Zhang Y *et al* (2009b). MAD2 as a key component of mitotic checkpoint: A probable prognostic factor for gastric cancer. *Am J Clin Pathol* **131:** 793-801.

Wang SI, Puc J, Li J, Bruce JN, Cairns P, Sidransky D *et al* (1997). Somatic mutations of PTEN in glioblastoma multiforme. *Cancer Res* **57:** 4183-4186.

Wang X, Jin DY, Ng RW, Feng H, Wong YC, Cheung AL *et al* (2002). Significance of MAD2 expression to mitotic checkpoint control in ovarian cancer cells. *Cancer Res* **62:** 1662-1668.

Weaver BA, Cleveland DW (2006). Does aneuploidy cause cancer? *Curr Opin Cell Biol* **18:** 658-667.

Weaver BA, Cleveland DW (2008). The aneuploidy paradox in cell growth and tumorigenesis. *Cancer Cell* **14:** 431-433.

Weaver BA, Silk AD, Cleveland DW (2008). Low rates of aneuploidy promote tumorigenesis while high rates of aneuploidy cause cell death and tumor suppression. *Cell Oncol* **30:** 453.

Weitzel DH, Vandre DD (2000). Differential spindle assembly checkpoint response in human lung adenocarcinoma cells. *Cell Tissue Res* **300:** 57-65.

Welchman RL, Gordon C, Mayer RJ (2005). Ubiquitin and ubiquitin-like proteins as multifunctional signals. *Nat Rev Mol Cell Biol* **6:** 599-609.

Westhorpe FG, Tighe A, Lara-Gonzalez P, Taylor SS (2011). p31comet-mediated extraction of Mad2 from the MCC promotes efficient mitotic exit. *J Cell Sci* **124:** 3905-3916.

Wilkinson KA, Henley JM (2010). Mechanisms, regulation and consequences of protein SUMOylation. *Biochem J* **428:** 133-145.

Wolfe F, Michaud K (2004). Heart failure in rheumatoid arthritis: rates, predictors, and the effect of anti-tumor necrosis factor therapy. *Am J Med* **116:** 305-311.

Wuthrich K (1990). Protein structure determination in solution by NMR spectroscopy. *J Biol Chem* **265:** 22059-22062.

Xirodimas DP, Sundqvist A, Nakamura A, Shen L, Botting C, Hay RT (2008). Ribosomal proteins are targets for the NEDD8 pathway. *EMBO Rep* **9:** 280-286.

Yan DW, Li DW, Yang YX, Xia J, Wang XL, Zhou CZ *et al* (2010). Ubiquitin D is correlated with colon cancer progression and predicts recurrence for stage II-III disease after curative surgery. *Br J Cancer* **103:** 961-969.

Yang CP, Liu L, Ikui AE, Horwitz SB (2010a). The interaction between mitotic checkpoint proteins, CENP-E and BubR1, is diminished in epothilone B-resistant A549 cells. *Cell Cycle* **9:** 1207-1213.

Yang M, Li B, Tomchick DR, Machius M, Rizo J, Yu H *et al* (2007). p31comet blocks Mad2 activation through structural mimicry. *Cell* **131:** 744-755.

Yang M, Li B, Liu CJ, Tomchick DR, Machius M, Rizo J *et al* (2008). Insights into mad2 regulation in the spindle checkpoint revealed by the crystal structure of the symmetric mad2 dimer. *PLoS Biol* **6:** e50.

Yang WL, Zhang X, Lin HK (2010b). Emerging role of Lys-63 ubiquitination in protein kinase and phosphatase activation and cancer development. *Oncogene* **29:** 4493-4503.

Yao X, Abrieu A, Zheng Y, Sullivan KF, Cleveland DW (2000). CENP-E forms a link between attachment of spindle microtubules to kinetochores and the mitotic checkpoint. *Nat Cell Biol* **2:** 484-491.

Yoon DS, Wersto RP, Zhou W, Chrest FJ, Garrett ES, Kwon TK *et al* (2002). Variable levels of chromosomal instability and mitotic spindle checkpoint defects in breast cancer. *Am J Pathol* **161:** 391-397.

Zhang DW, Jeang KT, Lee CG (2006). p53 negatively regulates the expression of FAT10, a gene upregulated in various cancers. *Oncogene* **25:** 2318-2327.

Zhao C, Denison C, Huibregtse JM, Gygi S, Krug RM (2005). Human ISG15 conjugation targets both IFN-induced and constitutively expressed proteins functioning in diverse cellular pathways. *Proc Natl Acad Sci U S A* **102:** 10200-10205.

Zhao X, Heng JI, Guardavaccaro D, Jiang R, Pagano M, Guillemot F *et al* (2008). The HECT-domain ubiquitin ligase Huwe1 controls neural differentiation and proliferation by destabilizing the N-Myc oncoprotein. *Nat Cell Biol* **10:** 643-653.

**ELSEVIER LICENSE**
**TERMS AND CONDITIONS**

Mar 27, 2013

This is a License Agreement between Steven Theng ("You") and Elsevier ("Elsevier") provided by Copyright Clearance Center ("CCC"). The license consists of your order details, the terms and conditions provided by Elsevier, and the payment terms and conditions.

**All payments must be made in full to CCC. For payment instructions, please see information listed at the bottom of this form.**

| | |
|---|---|
| Supplier | Elsevier Limited<br>The Boulevard,Langford Lane<br>Kidlington,Oxford,OX5 1GB,UK |
| Registered Company Number | 1982084 |
| Customer name | Steven Theng |
| Customer address | Strathmore Avenue Blk 59<br>Singapore, Singapore 142059 |
| License number | 3091810219286 |
| License date | Feb 18, 2013 |
| Licensed content publisher | Elsevier |
| Licensed content publication | Cell |
| Licensed content title | Hallmarks of Cancer: The Next Generation |
| Licensed content author | Douglas Hanahan,Robert A. Weinberg |
| Licensed content date | 4 March 2011 |
| Licensed content volume number | 144 |
| Licensed content issue | 5 |
| Number of pages | 29 |
| Start Page | 646 |
| End Page | 674 |
| Type of Use | reuse in a thesis/dissertation |
| Intended publisher of new work | other |
| Portion | figures/tables/illustrations |
| Number of figures/tables/illustrations | 1 |
| Format | both print and electronic |
| Are you the author of this Elsevier article? | No |
| Will you be translating? | No |
| Order reference number | |
| Title of your thesis/dissertation | Elucidation the role of FAT10 in tumorigenesis |
| Expected completion date | Apr 2013 |
| Estimated size (number of pages) | 140 |
| Elsevier VAT number | GB 494 6272 12 |
| Permissions price | 0.00 USD |
| VAT/Local Sales Tax | 0.0 USD / 0.0 GBP |
| Total | 0.00 USD |

**NATURE PUBLISHING GROUP LICENSE**
**TERMS AND CONDITIONS**

Mar 27, 2013

This is a License Agreement between Steven Theng ("You") and Nature Publishing Group ("Nature Publishing Group") provided by Copyright Clearance Center ("CCC"). The license consists of your order details, the terms and conditions provided by Nature Publishing Group, and the payment terms and conditions.

**All payments must be made in full to CCC. For payment instructions, please see information listed at the bottom of this form.**

| | |
|---|---|
| License Number | 3091801191090 |
| License date | Feb 18, 2013 |
| Licensed content publisher | Nature Publishing Group |
| Licensed content publication | Nature Reviews Cancer |
| Licensed content title | On the road to cancer: aneuploidy and the mitotic checkpoint |
| Licensed content author | Geert J. P. L. Kops , Beth A. A. Weaver and Don W. Cleveland |
| Licensed content date | Oct 1, 2005 |
| Volume number | 5 |
| Issue number | 10 |
| Type of Use | reuse in a thesis/dissertation |
| Requestor type | academic/educational |
| Format | print and electronic |
| Portion | figures/tables/illustrations |
| Number of figures/tables/illustrations | 1 |

| | |
|---|---|
| High-res required | no |
| Figures | Figure 2 of this particular papers. The mammalian mitotic checkpoint -signaling and silencing |
| Author of this NPG article | no |
| Your reference number | |
| Title of your thesis / dissertation | Elucidation the role of FAT10 in tumorigenesis |
| Expected completion date | Apr 2013 |
| Estimated size (number of pages) | 140 |
| Total | 0.00 USD |